

**RATE AND RELIABILITY OPTIMIZED MIMO CODING
SCHEMES AND LOW COMPLEXITY DETECTION**

A THESIS

Submitted by

BINDU P (PALAKKAL)

for the award of the degree

of

DOCTOR OF PHILOSOPHY



**DIVISION OF ELECTRONICS ENGINEERING
SCHOOL OF ENGINEERING
COCHIN UNIVERSITY OF SCIENCE AND TECHNOLOGY, KOCHI**

DECEMBER 2017



**SCHOOL OF ENGINEERING
COCHIN UNIVERSITY OF SCIENCE AND TECHNOLOGY
KOCHI, KERALA**

Dr. Jibukumar M. G.

Ph:+91 9497683331

Professor

email: jibukumar@cusat.ac.in

THESIS CERTIFICATE

This is to certify that the thesis entitled **RATE AND RELIABILITY OPTIMIZED MIMO CODING SCHEMES AND LOW COMPLEXITY DETECTION** submitted by **Bindu P (Palakkal)** to the Cochin University of Science and Technology, Kochi for the award of the degree of Doctor of Philosophy is a bonafide record of research work carried out by her under my supervision and guidance at the Division of Electronics, School of Engineering, Cochin University of Science and Technology. The contents of this thesis, in full or in parts, have not been submitted to any other University or Institute for the award of any degree or diploma.

I further certify that all the relevant corrections and modifications suggested by the audience during the pre-synopsis seminar and recommended by the Doctoral Committee have been incorporated in the thesis.

Kochi-682 022

Date:

Research Guide

Dr. Jibukumar M.G

DECLARATION

I hereby declare that the work presented in the thesis entitled **RATE AND RELIABILITY OPTIMIZED MIMO CODING SCHEMES AND LOW COMPLEXITY DETECTION** is based on the original research work carried out by me under the supervision and guidance of **Dr. Jibukumar M. G, Professor, Division of Electronics, School of Engineering, Cochin University of Science and Technology, Cochin-682 022** for the award of degree of Doctor of Philosophy with Cochin University of Science and Technology. I further declare that the contents of this thesis in full or in parts have not been submitted to any other University or Institute for the award any degree or diploma.

Kochi – 682 022
Date

Bindu P (Palakkal)

ACKNOWLEDGEMENTS

My prayers are for favours, and I am always blessed with opportunities. In this endeavour also, I realize, starting from the opportunity to work with an eminent guide, till the submission of this thesis, I am blessed a lot, with good health and wellbeing, and good support from many people.

My research guide Dr. Jibukumar. M. G, Professor, Division of Electronics, School of Engineering, Cochin University of Science and Technology, encouraged me continuously throughout the period of research. His involvement and patience in supervising the work is remarkable and any virtue in my technical writing is due entirely to him. I sincerely thank him for the support extended to me.

I would like to express my gratitude towards my doctoral committee member, Dr. Babita Roslind Jose and Dean (Faculty of Engineering) Dr. Sreejith. P. S for the valuable suggestions provided during my presentations, that has helped me in refining my results and presentations. I would also like to thank the faculty members of Division of Electronics, School of Engineering, for their support.

My fellow research scholars have always inspired me and shared their knowledge to get through the bottlenecks and I thank them for their valuable helps. I gratefully acknowledge the support from my colleagues and superiors, without which I could not have completed this work.

Irrespective of the sufferings and sacrifices they had during these years, my family members supported me throughout, and I owe them beyond words.

Bindu P (Palakkal)

ABSTRACT

Keywords : MIMO; spatial modulation (SM); transmit diversity; parity encoding; adaptive SM; Weylgroup encoding

Multiple input multiple output (MIMO) antenna communication is a breakthrough which has opened the doors to an exciting field of next generation wireless systems with many applications having various qualities of services (QoS) such as video, internet of things etc. at any time anywhere. The advantage offered by MIMO antenna systems is that it exploits the spatial domain along with the conventional time and / or frequency domain and hence provides an extra degree of freedom in design. Multipath fading, which is detrimental in single antenna systems, is effectively utilized by MIMO to enhance the performance or rate, at no cost of extra spectrum or power. The advantages offered by MIMO are at the cost of hard ware and design complexity. The design of channel coding schemes that are efficient in error handling and have affordable rate is a challenge. One of the other challenges is to reduce the complexity of decoding algorithm without degradation in bit error rate. Since the receiver complexity is a main concern in mobile/adhoc networks, detection algorithms are to be ingeniously designed so as to efficiently use the storage space and hardware available for computation. Importance is to be given for optimization of energy efficiency also, along with the performance and cost requirements. Designing MIMO systems to meet these conflicting needs is so challenging, and makes this research area rich and active since it's starting from 1990's.

In this thesis, we have presented some coding schemes that ensure acceptable rate and reliability in MIMO spatial multiplexing, spatial modulation and generalized spatial modulation systems. Also, link adaptation,

which is a powerful technique for ensuring rate and reliability, is employed in a generalized spatial modulation system and the performance is studied. The detection schemes proposed are less complex compared to the state of the art, for a reasonable number of transmit and receive antennas. Theoretical analyses are provided to evaluate the performance of proposed systems, and simulations are presented to support this. The performance of the proposed methods in terms of bit error rate and complexity is compared with the results in literature.

The limitations of the proposed methods and the intended extensions of the work in future are also presented in the thesis.

CONTENTS

| | |
|--|-------------|
| <i>Acknowledgements</i> | <i>i</i> |
| <i>Abstract</i> | <i>iii</i> |
| <i>List of tables</i> | <i>ix</i> |
| <i>List of figures</i> | <i>xi</i> |
| <i>Abbreviations</i> | <i>xiii</i> |
| <i>Notations</i> | <i>xv</i> |
| CHAPTER 1 INTRODUCTION | 1 |
| 1.1 Need for MIMO Systems | 1 |
| 1.2 Conventional MIMO Systems | 3 |
| 1.2.1 Spatial Multiplexing | 3 |
| 1.2.2 Spatial Diversity | 4 |
| 1.2.2.1 Receive Diversity | 5 |
| 1.2.2.2 Transmit Diversity and Space time coding | 5 |
| 1.2.3 Beam forming | 7 |
| 1.3 Energy Efficient MIMO Systems | 7 |
| 1.3.1 Spatial Modulation | 8 |
| 1.3.2 Generalised Spatial Modulation | 9 |
| 1.4 Massive MIMO Systems | 9 |
| 1.5 General MIMO Channel Model | 10 |
| 1.6 Motivation | 11 |
| 1.7 Objectives of this Work | 13 |
| 1.8 Work Done | 14 |
| 1.9 Organisation of the Thesis | 16 |
| CHAPTER 2 CODING AND DETECTION IN MIMO SYSTEMS - A REVIEW | 19 |
| 2.1 Spatial Multiplexing | 20 |
| 2.2 Spatial Modulation | 25 |
| 2.3 Generalised Spatial Modulation | 30 |
| 2.4 Adaptive Spatial Modulation | 33 |
| 2.5 Conclusions | 35 |

| | | |
|------------------|--|-----------|
| CHAPTER 3 | CODING FOR HIGH RELIABILITY IN SPATIAL MULTIPLEXING SYSTEM | 37 |
| 3.1 | Introduction | 37 |
| 3.2 | Probability of Block Error with QR Decomposition | 41 |
| 3.3 | Proposed Method of Coding and Detection | 43 |
| 3.3.1 | Encoding | 43 |
| 3.3.2 | Detection | 47 |
| 3.4 | Complexity Analysis | 49 |
| 3.5 | Simulation Results | 50 |
| 3.5.1 | Performance | 50 |
| 3.5.2 | Computational Complexity | 56 |
| 3.6 | Conclusions | 58 |
| CHAPTER 4 | A TRANSMIT DIVERSITY TECHNIQUE WITH HIGH RATE IN SPATIAL MODULATION SYSTEM | 59 |
| 4.1 | Introduction | 60 |
| 4.2 | Proposed Method for Diversity | 62 |
| 4.2.1 | Encoding | 63 |
| 4.2.2 | Detection | 72 |
| 4.3 | Complexity Analysis | 74 |
| 4.4 | Performance Analysis | 75 |
| 4.4.1 | BER Performance | 75 |
| 4.4.2 | Capacity Analysis | 76 |
| 4.5 | Simulation Results | 78 |
| 4.5.1 | Performance | 78 |
| 4.5.2 | Computational Complexity | 81 |
| 4.6 | Conclusions | 82 |
| CHAPTER 5 | A RATE CONFIGURABLE TRANSMIT DIVERSITY TECHNIQUE IN GENERALIZED SPATIAL MODULATION SYSTEM | 85 |
| 5.1 | Introduction | 86 |
| 5.2 | Proposed Method of Coding | 87 |
| 5.2.1 | Encoding | 88 |

| | | |
|-------------------------|--|------------|
| 5.2.2 | Decoding----- | 91 |
| 5.3 | Computational Complexity ----- | 99 |
| 5.4 | Simulation Results ----- | 102 |
| 5.4.1 | Performance ----- | 102 |
| 5.4.2 | Computational Complexity ----- | 106 |
| 5.5 | Conclusions ----- | 110 |
| CHAPTER 6 | RATE ADAPTATION IN GSM USING RCPC CODES ----- | 111 |
| 6.1 | Introduction ----- | 112 |
| 6.2 | Proposed RCPC Encoded GSM System ----- | 113 |
| 6.2.1 | RCPC Codes ----- | 113 |
| 6.2.2 | Adaptive GSM system ----- | 116 |
| 6.3 | Simulation Results ----- | 118 |
| 6.4 | Conclusions ----- | 122 |
| CHAPTER 7 | CONCLUSIONS----- | 123 |
| 7.1 | Thesis Contribution ----- | 123 |
| 7.1.1 | Spatial Multiplexing----- | 123 |
| 7.1.2 | Spatial Modulation ----- | 123 |
| 7.1.3 | Generalized Spatial Modulation----- | 124 |
| 7.1.4 | Rate Adaptation in GSM ----- | 124 |
| 7.2 | Drawbacks----- | 124 |
| 7.3 | Future Work----- | 125 |
| APPENDIX A | WEYL GROUP ----- | 127 |
| APPENDIX B | ALGORITHMS FOR THE SCHEMES----- | 129 |
| REFERENCES | ----- | 137 |
| LIST OF PAPERS | ----- | 149 |
| CURRICULUM VITAE | ----- | 151 |

LIST OF TABLES

| <i>Table</i> | <i>Title</i> | <i>Page No</i> |
|--------------|---|----------------|
| 3.1 | Mapping of parity information to x_4 | 45 |
| 3.2 | Comparison of computational complexity of QRD-P and QRD-M..... | 50 |
| 3.3 | Comparison of of effective spectral efficiency of QRD-P and QRD-M | 54 |
| 4.1 | Mapping of bit groups to Weyl Matrices | 64 |
| 4.2 | Antenna grouping and spectral efficiency (SE)..... | 65 |
| 4.3 | WET-SM encoding examples..... | 70 |
| 4.4 | Rate comparison of WET-SM with STBC-SM, SM and SM-CIOD..... | 71 |
| 4.5 | Computational complexity comparison of WET-SM, STBC-SM and SM-CIOD..... | 75 |
| 6.1 | Antenna selection in the adaptive GSM system | 117 |

LIST OF FIGURES

| <i>Figure</i> | <i>Title</i> | <i>Page No</i> |
|---------------|--|----------------|
| 1.1 | Spatial multiplexing system..... | 4 |
| 1.2 | Alamouti coding | 6 |
| 3.1 | Block diagram of QRD-P encoding | 43 |
| 3.2 | Mapping of x_4 in 16 QAM constellation..... | 45 |
| 3.3 | Search space with even parity | 46 |
| 3.4 | Tracing of nodes in QRD-P..... | 48 |
| 3.5 | BER Vs. SNR curves for QRD-P and QRD-M for $N_t = N_r = 4$, 16 QAM..... | 51 |
| 3.6 | BER Vs. SNR curves for QRD-P, coded QRD-M & 8QAM for $N_t = N_r = 4$ | 52 |
| 3.7 | SEeff Vs. SNR curves for QRD-P and QRD-M for $N_t = N_r = 4$, 16 QAM | 53 |
| 3.8 | BER Vs. SNR curves for QRD-P and QRD-M for $N_t = N_r = 8$, 16 QAM and $N_t = N_r = 4$, 64QAM | 55 |
| 3.9. | SEeff vs. SNR curves for QRD-P and QRD-M for $N_t = N_r = 8$, 16 QAM and $N_t = N_r = 4$, 64QAM | 56 |
| 3.10 | Number of flops vs. M for QRD-P and QRD-M, $N_t = N_r = 4$ | 57 |
| 3.11 | Number of nodes visited vs. M for QRD-P and QRD-M, $N_t = N_r = 4$ | 57 |
| 4.1 | Encoding and transmission in $N_t = 4$ WET-SM system | 67 |
| 4.2 | Theoretical and simulated BER Vs. SNR curves for WET-SM | 79 |
| 4.3 | BER Vs. SNR curves for WET-SM, STBC-SM and SM-CIOD | 80 |
| 4.4 | Capacity Vs. SNR curves for WET-SM, STBC-SM and SM-CIOD | 81 |
| 4.5 | Computational complexity comparison of WET-SM, STBC- SM and SM-CIOD | 82 |
| 5.1 | Block diagram of DESM system..... | 88 |
| 5.2 | Detection method of DESM..... | 93 |
| 5.3 | Algorithm for MGS QR decomposition..... | 101 |

| | | |
|-----|---|-----|
| 5.4 | BER vs. SNR curves for DESM, STBC-SM and GSM-ML for $N_t = N_r = 4, N_a = 3$ | 103 |
| 5.5 | BER vs. SNR curves of DESM and STBC-SM for $N_t = N_r = 6, N_a = 3$ | 105 |
| 5.6 | BER vs. SNR curves of DESM for $N_t = 4, 6, 10, N_r = 4, N_a = 3$ and for STBC-SM..... | 106 |
| 5.7 | Comparison of computational complexity of DESM, STBC- SM and GSM-QRD-M | 108 |
| | a) For fixed transmit antennas and constellation size..... | 108 |
| | b) For fixed transmit and active antennas | 108 |
| 5.8 | Comparison of rate of DESM and GSM | 109 |
| | (a) For fixed N_a | 109 |
| | (b) For fixed N_t | 109 |
| 6.1 | Example of RCPC encoding | 114 |
| 6.2 | GSM system with rate adaptation | 116 |
| 6.3 | BER Vs. SNR curves for puncturing Period $P = 3$ | 119 |
| 6.4 | Comparison of BER Vs. SNR for $P = 3$ and $P = 8$ | 120 |
| 6.5 | BER Vs. SNR curves for fixed 8bpcu rate..... | 121 |
| 6.6 | Throughput Vs. SNR curves for $P = 3$ and $P = 8$ | 122 |

ABBREVIATIONS

| | |
|----------|---|
| ARQ | Automatic Repeat Request |
| AWGN | Additive White Gaussian Noise |
| BLAST | Bell Laboratories layered space-time |
| BPSK | Binary Phase Shift Keying |
| BW | Band Width |
| CSI | Channel State Information |
| D-BLAST | Diagonal Bell Laboratories Layered Space-Time |
| DESM | Diversity Embedded Spatial Modulation |
| DoSM | Degree of Spatial Modulation |
| EGC | Equal Gain Combining |
| GSM | Generalised Spatial Modulation |
| H-BLAST | Horizontal Bell Laboratories Layered Space-Time |
| ICI | Inter Channel Interference |
| ISI | Intersymbol Interference |
| LLR | Log Likelihood Ratio |
| MIMO | Multiple-Input Multiple-Output |
| MISO | Multiple-Input Single-Output |
| ML | Maximum Likelihood |
| MMSE | Minimum Mean-Squared Error |
| MMSE-SIC | Minimum Mean-Squared Error with Successive Interference Cancellation |
| MRC | Maximum Ratio Combining |
| OFDM | Orthogonal Frequency Division Multiplexing |
| OSTBC | Orthogonal Space Time Block Code |
| PEP | Pairwise Error Probability |
| PSK | Phase Shift Keying |

| | |
|--------|---|
| QAM | Quadrature Amplitude Modulation |
| QoS | Quality of Service |
| QPSK | Quadrature Phase Shift Keying |
| QRD | QR Decomposition |
| QRD-M | QR Decomposition with M algorithm |
| QRD-P | QR Decomposition with Parity encoding |
| RA | Receive Antenna |
| RCPC | Rate Compatible Punctured Convolutional Code |
| RF | Radio Frequency |
| SC | Selection Combining |
| SD | Sphere Decoding |
| SIC | Successive Interference Cancellation |
| SISO | Single-Input Single-Output |
| SM | Spatial Modulation |
| SMX | Spatial Multiplexing |
| SNR | Signal to Noise Ratio |
| SSC | Switch and Stay Combining |
| SSK | Space Shift Keying |
| STBC | Space-Time Block Code |
| STTC | Space-Time Trellis Code |
| TA | Transmit Antenna |
| VBLAST | Vertical Bell Laboratories Layered Space-Time |
| WET-SM | Weyl Group Encoded Transmission in SM |
| ZF | Zero Forcing |
| ZF-IC | Zero Forcing with Interference Cancellation |
| bpcu | bits per channel use |
| iid | independent and identically distributed |

NOTATIONS

English Alphabets

| | |
|--------------|----------------------------------|
| R | The field of all real numbers |
| C | The field of all complex numbers |
| C | Constellation |
| \mathbf{z} | The vector \mathbf{z} |
| \mathbf{A} | The matrix \mathbf{A} |
| \mathbf{H} | MIMO channel matrix |
| \mathbf{x} | Transmitted signal vector |
| \mathbf{y} | Received signal vector |
| \mathbf{n} | AWGN |

Greek Symbols

| | |
|--------------|-----------------------------|
| σ_n^2 | Noise variance |
| ρ | Signal to noise power ratio |

Miscellaneous Symbols

| | |
|--------------------|--|
| $\arg \max_x f(x)$ | The value of x that maximizes the function $f(x)$ |
| $\arg \min_x f(x)$ | The value of x that minimizes the function $f(x)$ |
| e^x | Exponential of x |
| $\text{Im}(x)$ | The imaginary part of x |
| $\text{Re}(x)$ | The real part of x |
| $Q(x)$ | Q function of x |
| $H(X)$ | The entropy of random variable X |
| $H(Y/X)$ | The conditional entropy of random variable Y given random variable X |
| $I(X; Y)$ | The mutual information between random variables X and Y |
| $ x $ | The absolute value of the complex number x |

| | |
|---------------------------|---|
| x^* | The conjugate of a scalar or vector quantity x |
| $\ x\ $ | The norm of vector x |
| x^T | The transpose of vector x |
| x^H | The Hermitian (conjugate transpose) of vector x |
| A^T | The transpose of matrix A |
| A^H | The Hermitian (conjugate transpose) of matrix A |
| A^* | The conjugate of matrix A |
| A^{-1} | The inverse of matrix A |
| $\ A\ _F$ | The Frobenius norm of the matrix A |
| $\det(\mathbf{A})$ | The determinant of matrix A |
| $\text{tr}(\mathbf{A})$ | The trace of matrix A |
| \mathbf{I}_N | The $N \times N$ identity matrix |
| \mathbf{O}_N | The $N \times N$ all zero matrix |
| N_t | Number of transmit antennas |
| N_r | Number of receive antennas |
| h_{ij} | Channel coefficient between the j^{th} transmit and i^{th} receive antennas |
| $P(x)$ | Probability of x |
| \in | Element of |
| $\binom{n}{r}$ | Number of possible combinations in n , taken r at a time. |
| $\lfloor x \rfloor_{2^p}$ | Largest integer p such that $2^p < x$ |

Multiple input multiple output (MIMO) antenna communication is a promising technology for the next generation high speed wireless systems. The importance stems from the fact that the conventional frequency and time domains are saturated and MIMO additionally utilizes the spatial domain and yields a degree-of- freedom gain. This enables the MIMO technology to communicate at higher rates and/or reliability without any extra cost of spectrum or power. Since their invention in the mid-1990s, MIMO systems have been the focus of rich and active research in the area of wireless communications. Starting from the demand for high spectral efficiency, the research is now facing a paradigm shift to energy-efficient and sustainable technology. In this chapter, we give a brief introduction to the MIMO systems, our motivation to research and an overview of the work done.

1.1. NEED FOR MIMO SYSTEMS

There is more and more demand for reliable and high speed communication that supports many applications with various qualities of services (QoS) such as video, internet of things etc. at any time anywhere. Multipath fading, scarcity of available bandwidth, highly constrained transmit powers as well as hardware complexity and cost are hindering the achievement of such a wireless communication link. A simple approach to improve the bandwidth efficiency is to use higher order modulation schemes, with the drawback of poor reliability associated. Higher power is to be fed to the channels to combat this, which will normally be not possible due to the

regulatory issues and other constraints. On the other hand, reliability can be improved by providing the receiver with independently faded copies of the transmitted signal with the hope that at least one of these replicas will be received correctly. This most effective technique called diversity may be realized in terms of frequency, time, space, modulation etc. For example, delay diversity sends the same symbol delayed by a particular time after the first transmission (Wittneben, 1993). Channel coding may also be used to provide immunization against the impairments of the wireless channel. All these methods can be effected only with a cost of rate reduction in a single input single output (SISO) system.

MIMO systems are evolved as a solution to the above issue of tradeoffs among bandwidth, transmit power, rate and reliability while using single transmit and receive antenna. MIMO systems provide substantial increase in data rates without any increase in bandwidth or transmit power. At the same time, transmit and/or receive antenna diversity, also referred to as spatial diversity, can be implemented to combat the harmful effects of fading and provide high reliability without any rate reduction compared to a single antenna system. These benefits are the result of the capability of the MIMO systems to turn the multipath fading to a boon, which in the SISO system is most harmful. This is because, in rich scattering conditions, each signal received in a MIMO system is independently faded, which can then be combined in a proper way to minimize the error. The cost of these benefits is the complexity in transmitter as well as receiver circuits, which demands ingenious design.

Various diversity techniques can be combined to further improve the system performance in a wireless environment which gives more freedom to a communication engineer to achieve the required QoS. For example, combination of channel coding with spatial diversity can offer effective

solutions to the challenges faced in realizing reliable high-speed wireless communication links (Mietzner *et al.*, 2009). Therefore, coding over MIMO systems is fundamental to the realization of the promises offered by MIMO systems in terms of reliability and achievable rates.

As already mentioned, system complexity is one of the major issues while using multiple antennas, especially in the case of mobile handheld devices. Some issues are antenna selection and synchronization, power amplifier linearity and the complexity in implementing coding and decoding algorithms. Hardware complexity is somewhat affordable on the base station side, whereas it is to be kept as minimum as possible on the terminal side. These issues can be effectively tackled only with ingenious design of coding and decoding algorithms, which again emphasizes the importance of research in this field.

The following briefly explain different ways of exploiting multiple antennas at both the ends of the MIMO communication link, channel models and general detection methods. Detailed state of the art coding and detection schemes are given in literature review.

1.2. CONVENTIONAL MIMO SYSTEMS

1.2.1. Spatial Multiplexing

Spatial multiplexing (SMX) techniques simultaneously transmit independent information sequences, often called layers, over multiple antennas. Figure 1.1 illustrates the principle of SMX MIMO system. While this approach increases the transmission rate compared to a single-antenna system without requiring extra bandwidth or extra transmission power, the corresponding reliability is poor. Channel coding is often employed, in order to guarantee a

certain error performance. A well-known SMX scheme is the Bell-labs layered space-time architecture (BLAST) proposed by Foschini (1996).

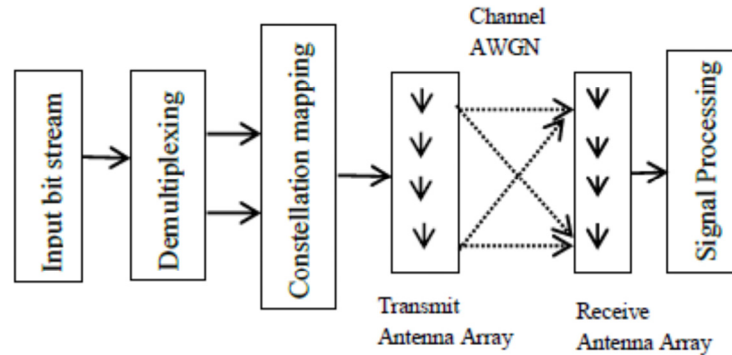


Fig. 1.1 Spatial multiplexing system

To recover the transmitted signal, linear as well as non-linear detectors can be utilized at the receiving end. Linear receivers like zero forcing (ZF), minimum mean square error (MMSE) are having low complexity but the error performance is poor. Successive interference cancellation (SIC) is a popular method of decoding, which can be combined with ZF or MMSE to improve the performance (Duman and Ghayeb, 2007). The maximum likelihood (ML), detection which performs an exhaustive search over all possible candidate vectors, gives optimum performance, but complexity is prohibitively high. Sphere decoding (SD) and QR decomposition with M algorithm (QRD-M) are used to reduce the search space in ML detection, with a performance trade off (Damen *et al.*, 2000; Kim and Yue, 2002).

1.2.2. Spatial Diversity

To improve the reliability of detection, multiple antennas should be used in such a way that diversity is achieved by transmitting and/or receiving redundant signals representing the same information. The transmission rate achieved in this case is comparable to that of SISO systems. As explained

below, appropriate combining methods are to be employed at the receiver to reap the diversity gain.

1.2.2.1 Receive Diversity

Receive diversity can be achieved by appropriately combining signals from more than one receive antennas. The optimal combining rule, called maximal ratio combining (MRC), linearly combines the received signals after co-phasing and weighting them with their respective channel gains. Thus the branches that have better channel gains, i.e., larger instantaneous signal-to-noise ratios (SNR), will be emphasized more than others. After the received signals are combined, the ML decision rule is applied. MRC implementation is complicated as it requires exact knowledge of the instantaneous channel gains. The alternative combining schemes are selection combining (SC), equal-gain combining (EGC) and switch-and-stay combining (SSC). In selection combining, the decision is made based on the received signal from the branch with the highest SNR. The implementation is simpler but the performance is inferior. In equal-gain combining, the signals of all branches are co-phased and summed together to form the equivalent channel output. In switch-and-stay combining, signal from a particular branch is considered for demodulation until the signal-to-noise ratio of that branch falls below a certain threshold, in which case another branch is selected. This combining algorithm is also called threshold combining due to the way it is implemented.

1.2.2.2 Transmit Diversity and Space time coding

Transmit diversity cannot be implemented merely by transmitting the same symbol through multiple antennas. Exploiting spatial diversity by multiple antennas at the transmitter requires that the signal be pre-processed or precoded before transmission. Space-time coding which is a two-dimensional

coding in time and space is an example. At the receiver, an appropriate combining of the redundant signals has to be performed. Optionally, multiple receive antennas can be used for receive diversity also, which will further improve the error performance. The advantage over conventional channel coding is that redundancy can be accommodated in the spatial domain, rather than in the time domain. Correspondingly, a diversity gain and a coding gain can be achieved without lowering the effective bit rate compared to single-antenna transmission. Two well-known spatial diversity techniques for systems with multiple transmit antennas are space time block codes (STBC, Alamouti, 1998) and space-time trellis codes (STTC, Tarokh *et al.*, 1998). Since Alamouti coding is utilized in this work, it is explained below.

- **Alamouti Coding**

In Alamouti coding (Figure 1.2), the input symbols are divided into groups of two symbols each and are transmitted simultaneously from the two antennas during a time slot. Let the signal transmitted from antenna 1 is x_1 and the signal transmitted from antenna 2 is x_2 during the first time slot. During the next symbol period, the signal transmitted from antenna 1 is $-x_2^*$ and the signal transmitted from antenna 2 is x_1^* . Let h_1 and h_2 respectively be

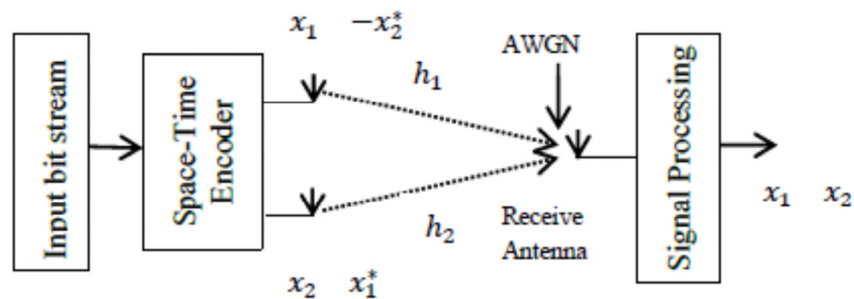


Fig.1.2 Alamouti coding

the channel gains from the first and second transmit antennas to the single receive antenna, that are assumed to be constant over two consecutive symbol periods. This peculiar way of transmission has the most attractive feature that it is possible to decode independently the two symbols that are transmitted simultaneously. This is due to the fact that the channel matrix is always orthogonal regardless of the channel coefficients. Orthogonal space time block codes (OSTBC) are an extension of this transmission scheme for more number of transmit antennas (Tarokh *et al.*, 1999).

1.2.3. Beamforming

Multiple-antenna techniques can also be utilized to improve the SNR at the receiver and to suppress co-channel interference by weighting the signal transmitted from different antennas by a proper factor. Transmit and receive beamforming can be performed to improve the SNR or to extend the coverage. A better beamforming gain can be achieved if the number of antennas in an array is large. However, the channel state information (CSI) is required for beamforming to achieve maximum SNR.

1.3. ENERGY EFFICIENT MIMO SYSTEMS

In practice, the above conventional MIMO systems need large number of power amplifiers, radio frequency (RF) chains, mixers, synthesizers, filters, etc., which substantially increase the circuit complexity and power dissipation at the transmitter side. Other disadvantages are the stringent synchronization requirements among the transmit antennas (TA) and the signal processing complexity at the receiver arising from the interference imposed by simultaneously transmitting many data streams. Energy efficiency is highly important for mobile hand held devices and it is to be optimized considering the factors such as interference to other co-channel users and environmental

impacts also. Therefore, recent research has focused on energy-efficient wireless communication techniques. Spatial modulation (SM) and generalized spatial modulation (GSM) are two MIMO techniques in this direction.

1.3.1. Spatial Modulation

In spatial modulation (SM), out of the available antennas, only one antenna is activated during a time slot. The information is conveyed through the active antenna index as well as through the symbol transmitted, which results in increased rate compared to a single antenna system (Mesleh *et al.*, 2008). There is no inter channel interference (ICI) and associated decoding complexity and it avoids antenna synchronization requirement. Other advantages are simpler transmitter design and better efficiency of power amplifiers. But these advantages are achieved at the cost of fast antenna switching requirement, large training overhead, sub optimum spectral efficiency compared to spatial multiplexing and lack of diversity gain.

In SM transmission, assuming there are N_t antennas at the transmitter, the information bit sequence is split into blocks of $\log_2(N_t K)$ bits, in which the antenna index part of $\log_2 N_t$ bits select the active antenna and constellation part of $\log_2 K$ bits select one of the K complex symbols of the signal constellation.

In SM, spatial constellation and signal constellation are not independent and in the optimal ML detection presented by Jeganathan *et al.* (2008), both the antenna and constellation indices are jointly estimated. The computational complexity is very high for the above due to the exhaustive search and it can be reduced with the two step suboptimal decoding (Xu, 2012), in which the antenna index and constellation point are detected separately.

1.3.2. Generalised Spatial Modulation

Generalised spatial modulation is a compromise between complexity and rate, in which more than one antenna will be activated at a time based on antenna selection pattern (Younis *et al.*, 2010). Many variations of this principle are reported in literature. In a GSM system with N_t transmit antennas, if N_a antennas are active at a time, the antenna selection requires $\log_2(N_c)$ bits where $N_c = \binom{N_t}{N_a}$. These N_a active antennas transmit symbols corresponding to each $\log_2 K$ bits at a time, where K is the size of the constellation.

The optimum detection rule is the ML criteria. In GSM, all possible candidate vectors within the constellation set K for all possible antenna combinations are to be considered to find the minimum distance metric. So, the complexity is very high and sub optimum detection methods with compromise in performance are available and will be pointed out in literature survey.

1.4. MASSIVE MIMO SYSTEMS

Massive MIMO is an emerging technology that uses antenna arrays with a few hundred antennas simultaneously serving many tens of terminals in the same time-frequency resource. Significantly improved spectral efficiency, improved channel response and simplified transceiver designs are the promises of this technology, which makes it suitable for next generation 5G wireless systems (Wang *et al.*, 2014; Akyildiz *et al.*, 2014). It is predicted that the 5G wireless system would be able to deliver as much as 1000 times of the capacity provided by today's mobile networks. In addition, 5G mobile system is expected to accommodate considerably larger number of wireless

connections to better support of existing and emerging applications. There would be no single technology that can meet the stringent QoS requirements of 5G, such as better delay, reliability, and higher spectral and energy efficiency. Therefore, a number of wireless technologies must be developed and jointly implemented (Gavrilovska *et al.*, 2016). So far, most of the research work related to massive MIMO has been purely theoretical, mostly because of its practical limitation regarding the hardware design and the huge and bulky antenna array dimensions. However, for very high carrier frequencies, i.e. in the millimeter wave band, the antenna array dimensions scale down significantly, providing practical and small scale designs (Le *et al.*, 2015). To put it briefly, massive MIMO is an enabler for the development of future broadband (fixed and mobile) networks, which will be energy-efficient, secure, and robust, and will use the spectrum efficiently.

1.5. GENERAL MIMO CHANNEL MODEL

Consider a MIMO system with N_t transmit antennas and N_r receiving antennas as in Figure 1.1. The received signal vector can be represented as given below

$$\mathbf{y} = \mathbf{H}\mathbf{x} + \mathbf{n} \quad (1.1)$$

where \mathbf{x} and \mathbf{y} are $N_t \times 1$ transmit and $N_r \times 1$ receive vector respectively, and \mathbf{H} stands for $N_r \times N_t$ channel matrix. The $(i,j)^{\text{th}}$ entry of \mathbf{H} indicates the fading coefficient between the j^{th} transmit and i^{th} receive antenna. General assumptions on MIMO channels are

- Linear, which implies that each received signal is the sum of scaled copies of the signals transmitted from all the transmit antennas, and AWGN.

- Flat-fading, or narrowband, i.e., there is no interference between symbols transmitted at different signaling intervals. In contrast, frequency-selective or wideband channels have inter symbol interference (ISI).
- Quasi-static or slow-fading, i.e., the channel response does not vary over one frame of communication. In practice, wireless channels vary with time because of the movement of transmitter, receiver or scatterers in the vicinity. According to the quasi-static assumption, the channel varies so slowly over one communication block that it can be treated as constant. Other possible channel models are the fast fading and block fading models. The fast fading model assumes that the channel varies independently from one signaling interval to the next. The block fading assumption is a compromise between the slow and fast extremes. Here, the channel is invariant in small blocks lasting a few signaling intervals, but varies independently from one block to the next.

Another important factor is the distribution of the random channel matrix \mathbf{H} , which are assumed to be iid. If the antennas are placed far enough apart, it is valid to assume that the coefficients h_{ij} are independent. Regarding fading, each h_{ij} is assumed to be a complex, zero-mean, circularly symmetric Gaussian random variable of unit variance, which is named as Rayleigh channel. Other possible channels are Ricean where a line of sight path is assumed or Nakagami in which instantaneous receive power is Gamma distributed (Duman and Ghrayeb, 2007; Tse and Viswanath, 2005).

1.6. MOTIVATION

Though spatial multiplexing provides high data rates, the decoding algorithms suffer from high complexity, variable throughput or poor

performance. The popular tree searching algorithms for decoding perform well in the high SNR regime, since the symbols detected first will be more reliable and the effect of error propagation will be less. But in the low SNR regime, the effect of error propagation will be prominent, which will affect the detection of higher layers and performance will be poorer. The lattice reduction aided detection requires transformation of the system before detection to obtain a better conditioned channel matrix. Channel coding schemes are often employed to achieve the desired bit error performance but results in rate reduction and coding-decoding complexity. Low complexity coding and detection in SMX systems with acceptable rate and error performance need further investigation.

Spatial multiplexing is preferred only when the rate is of prime importance as it is energy consuming and requires inter antenna synchronization and large number of receive antennas for low complexity detection. On the other hand, energy efficient systems like spatial modulation suffers from low transmission rates and lack of transmit diversity gain. High rate in SM is achievable with only large number of transmit antennas or higher modulation schemes, both of which results in performance degradation. Diversity in SM either requires more than one transmit antenna, complex coding or multiple time slots, and inherent advantages of the system is lost. Some of the systems reported achieves transmit diversity with single active antenna but are applicable to limited number of transmit antennas or require higher bandwidth (BW). SM Systems with transmit diversity and high rate without losing the advantage of single active antenna per time slot are to be developed considering the energy efficiency requirement of future mobile systems.

A trade off among the above two systems which offers acceptable rate and energy efficiency is the GSM system in which more than one transmit

antenna will be activated at each instance of time. This enables diversity and/or spectral /energy efficiency trade off, and removes the restriction in SM that the total number of antennas should be a power of two. The drawbacks of GSM are the detection complexity and large number of receive antennas required. Though transmit diversity is implemented by activating more than one antenna in systems like space time block coded spatial modulation (STBC-SM), but the multiplexing gain is lost (Basar *et al.*, 2011). Another system reported provides switching between spatial multiplexing and diversity (Heath and Paulraj, 2005). Considering that there will always be data that require high quality and data with a quality compromise possibility, amalgamation of both in GSM is a promising option for high rate and QoS requirements in emerging 5G systems.

1.7. OBJECTIVES OF THIS WORK

The objective of this work is to develop coding and decoding methods for MIMO systems that are having acceptable rate and error performance, with affordable computational complexity. Specifically,

- To develop low complexity coding and detection schemes that will improve the BER performance of spatial multiplexing systems, by means of reducing the probability of error propagation in tree search algorithms.
- To introduce transmit diversity in SM without sacrificing its inherent advantages of no ICI and synchronization requirements and without reducing the achievable rate.
- To incorporate diversity in GSM along with a multiplexing gain and to develop low complexity decoding method for the same.

- To design a rate configurable system, where there is an option for performance-rate trade off with the same number of active antennas, which is a good choice for next generation systems.

1.8. WORK DONE

Below we give an overview of the work done to develop rate and reliability optimized coding schemes for conventional as well as energy efficient MIMO systems.

- For spatially multiplexed MIMO systems, a method for reducing the computational complexity with the aid of parity information sent through one of the transmitted symbols is developed. The proposed tree search method utilizes QR decomposition of the channel matrix and only one candidate is kept at each level of tree decomposition, which reduces the computational complexity. The probability of error in the selection of the candidate to be retained at each level is kept to a minimum with the aid of parity information, which also reduces probability of error propagation. The BER performance of and complexity of the proposed system is compared with traditional QRD-M both for uncoded and coded systems.
- For energy efficient SM- MIMO, a transmit diversity scheme based on Weyl group encoding is introduced, where the information bits are encoded into matrices that belong to a coset of Weyl group first and the columns of these matrices are mapped onto the constellation as a second step. The advantage obtained here is that only one antenna will be active during a time slot, and single stream ML decoding is possible. This Weyl group encoded transmission in SM (WET-SM) achieves second order transmit diversity without any rate reduction or bandwidth

enhancement. The decoding complexity and BER performance is compared with other state of the art diversity schemes for SM.

- Next, we combined space time coding and spatial multiplexing with GSM to develop an energy efficient transmission method that is suitable for emerging large scale MIMO scenario. The proposed diversity embedded SM (DESM) provides required QoS for a high priority data and at the same time maintains a fair transmission rate by spatial multiplexing of a low priority data. Only limited feedback is required and the system can be configured for different diversity/non-diversity stream rates, as per the required QoS. As different from other schemes that utilize space time block codes for diversity, this does not impose any restriction on the number of active antennas. Utilizing some peculiarities of the channel matrix of the system, a QR decomposition based detection method that requires only four receiving antennas is shown to have good performance. The detection complexity of the proposed system is compared with some well-known GSM detection schemes, for reasonable number of transmit and active antennas. The effect of incorporating diversity on the rate of the system is also analysed.
- To further improve the performance of GSM, a link adaptation technique using code puncturing is applied. We considered a coded system that uses rate compatible punctured convolutional codes (RCPC) and analysed the performance. An antenna grouping method based on the CSI feedback from the receiver is used to adjust the transmission rate. The system is analysed with half rate convolutional mother code and for different puncturing lengths.

1.9. ORGANISATION OF THE THESIS

The rest of the thesis is organized into chapters as follows:

Chapter 2 gives a review of the coding and detection methods in spatial multiplexing, spatial modulation and generalised spatial modulation systems. Diversity schemes available for different MIMO systems and adaptation techniques are also presented. We have included most of the works that are relevant to our topic.

Chapter 3 proposes a method for performance improvement in spatial multiplexing systems. The method is based on QR decomposition of the channel matrix and the simple technique of parity information of the bit stream transmitted. Along with a performance improvement, it also reduces the complexity in detection. Simulation results are given to compare the performance of the proposed method with some detection methods in literature, in terms of BER and computational complexity.

Chapter 4 presents the Weyl group encoded transmission in SM, which increases the performance without rate reduction. Theoretical analysis of error performance and capacity is given to support the claims, and simulations are given to compare the theoretical and simulated values. The BER performance and complexity are compared with that of some diversity schemes in SM.

Chapter 5 presents a method to incorporate diversity and maintain fare transmission rate in GSM. A low complexity detection scheme that requires minimum number of receive antennas is also presented. The proposed system is shown to have very good error performance and the possibility to configure rate in various ways is also illustrated.

Chapter 6 analyses the performance of a GSM system in which link adaptation is done using RCPC codes. The system throughput and BER

performance are analyzed for various channel selection and puncturing schemes, using half rate convolutional code as the mother code.

Chapter 7 concludes the thesis with a brief discussion on the drawbacks of our methods and possible extension of our work in future.

Chapter

2

CODING AND DETECTION IN MIMO SYSTEMS - A REVIEW

In this chapter, we present a brief review of the works done so far by various researchers in the area of MIMO coding and detection, concentrating mainly in spatial multiplexing and spatial modulation. MIMO technology exploits the spatial domain along with the conventional time and/or frequency domain to turn multipath fading beneficial rather than destructive, and improve the performance or rate at no cost of extra spectrum (Mietzner *et al.*, 2009). But, meeting the conflicting requirements such as low bit error rate, low power consumption, low decoding complexity and high data rates is rather difficult and makes MIMO system design challenging. Spatial multiplexing (SMX) provides high data rates, but antenna synchronization requirements and signal processing complexity arises practical implementation problems (Paulraj and Kailath, 1992). Spatial modulation (SM), in which out of the available antennas, only a limited number is activated at a time is a low complexity solution to these problems achieved at the cost of rate reduction (Di Renzo *et al.*, 2014). A generalisation of the scheme, namely Generalised Spatial Modulation (GSM) provides an appealing compromise with energy efficiency and rate of transmission (Younis *et al.*, 2010). Channel conditions play an important role in MIMO system performance and to combat this, link adaptation in which transmission parameters are dynamically adjusted is applied in all the above systems and is crucial. We review the important coding schemes and detection algorithms in these areas that are related to our work. A comprehensive review is not intended, because of the large volume of works available.

The review is organized in the following manner. Starting from the evolution of MIMO with the spatial multiplexing system, developments such as spatial modulation and generalized spatial modulation are explored. Emphasis is given to low complexity decoding methods in these areas and reliability enhancement. Finally, link adaptation schemes are reviewed.

2.1 SPATIAL MULTIPLEXING

The spatial multiplexing system, first proposed in 1992 by Paulraj and Kailath, transmits multiple signals through all the available transmit antennas and hence offers high data rates. Following that, the Bell lab's layered space time architecture (BLAST) system is proposed by Foschini in 1996 that achieves bit rates approaching 90% of outage capacity. To ensure a certain error performance, channel coding is applied in BLAST in the following ways. In horizontal coding (H-BLAST), the channel coding is done separately for each data stream. In vertical coding (V-BLAST), the channel coding is performed first and then the stream is demultiplexed, modulated and transmitted through different antennas. A combination of these, called diagonal coding (D-BLAST) performs the encoding for each layer separately, but the antennas selected for sending the layers are changed in a modulo- M fashion (Foschini, 1996). It is theoretically proved that, with spatial multiplexing, the capacity of a MIMO system grows linearly with minimum of transmit and receive antennas (Foschini and Gans, 1998; Teletar, 1999). The first real time V-BLAST demonstrator was equipped with 8 transmit and 12 receive antennas and achieved high bit rates as envisaged theoretically (Golden *et al.*, 1999).

There are several detection algorithms for SMX systems that tradeoff performance and complexity. The maximum likelihood detection (MLD),

which performs an exhaustive search over all possible candidate vectors gives optimum performance, but complexity is prohibitively high (Van Nee *et al.*, 2000). Linear receivers like zero forcing (ZF) and minimum mean square error (MMSE) are having low complexity but the error performance is poor. Successive interference cancellation (SIC) is a popular method of detection in V-BLAST systems proposed by Wolniansky *et al.* (1998). SIC technique is sub-optimum in terms of the error probability and channel ordering based on SNR is usually adopted to improve the performance. ZF or MMSE method can be used as a nulling step first and then the layer with largest SNR is estimated, treating all other layers as interference. Then the influence of the detected layer is subtracted from the received signal and nulling is performed again, before detecting the second layer. This process is continued till all the layers are detected. An example of the scheme is that proposed by Liu and Liu (2008). The corresponding SIC detections are known as ZF-SIC and MMSE-SIC, respectively. To make the SIC detection less complicated, a more computationally efficient detection can be realized with the assistance of QR decomposition (Böhnke *et al.* (2003); Zhang *et al.* (2005)). The drawbacks of SIC are error propagation and that only partial diversity gain can be achieved. For these two reasons, the performance of SIC detection shows a significant gap from that of the ML detection. Recently, an improved SIC algorithm using multiple feedback is proposed by Mandloi *et al.* (2017), having near-optimal performance.

To alleviate the computational complexity of the conventional full search ML decoder while maintaining the optimal BER performance, the sphere decoding (SD) principle is applied. This is based on the algorithm for calculating vectors of short length in a lattice at a reduced complexity proposed first by Fincke and Pohst in 1985. Schnorr and Euchner (1994) proposed a

more efficient variation of the Fincke-Pohst SD algorithm based on the lattice basis reduction philosophy and represent a popular solution to the MIMO detection problem. Viterbo and Boutros (1999) applied the SD algorithm to the ML detection of multidimensional constellations transmitted over single-antenna. SD for MIMO has been proposed and analyzed by Damen *et al.* (2000), which is based on Fincke Pohst algorithm. By searching over only the lattice points lying inside a hypersphere centered at the received signal point, SD reduces the search space and consequently the required computational complexity. Chan and Lee (2002) modified the sphere decoding algorithm such that the performance is relatively insensitive to the initial choice of sphere radius. One of the drawbacks of these methods is that the application is restricted to real valued systems. Hochwald and Brink (2003) extended the sphere decoding algorithm to complex valued systems applying Cholsky factorization. Three types of SD are reported-the breadth first, depth first and best first. The Fincke Pohst algorithm is a depth first search. The breadth first signal decoder (Kang *et al.*, 2008) searches the closest lattice point based on a breadth-first search method, and is shown to exhibit a lower computational complexity than the depth first SD. Nonetheless, it seems that it does not provide sufficient complexity reduction when the size of signal constellation is large. Shen *et al.* (2010) presented a best first tree-searching approach that combines the features of classical depth-first and breadth-first approaches to achieve close to ML performance while minimizing the number of visited nodes.

The required computations in SD are highly dependent on the received SNR, and results in variable throughput. Addressing this issue, a fixed complexity SD has been proposed by Barbero and Thompson (2006). To achieve near ML performance, this requires iterative column ordering and extra

computations. Rachid and Daneshrad (2009) presented an iterative sphere decoding algorithm based on a constrained metric-first search. The search strategy minimizes the number of required iterations as well as the variation in the number of iterations. Further complexity reduction is achieved through the use of a simplified distance norm and sorted QR-decomposition.

A reduced complexity SD is proposed by Azzam and Ayanoglu (2007) in which decoding the real and imaginary parts of every jointly detected symbol is done independently of each other, using a new lattice representation. A probabilistic sphere decoding proposed by Shim and Kang (2008) reduces the complexity by adding a probabilistic noise constraint on top of the sphere constraint. At an early stage itself, branches unlikely to be survived are removed and a parameter called pruning probability allows tradeoff between the performance and complexity. A complexity improved sphere decoding method using PSK modulations is proposed by Castillo León *et al.* (2012). This method prevents the errors caused by QR decomposition by mapping the area of search by phase angle and is claimed to have low complexity and good performance. The results presented are only for two transmit and receive antennas and BPSK constellation. As a latest work, Jang *et al.* (2017) proposed circular sphere decoding (CSD) which is applicable to MIMO systems with arbitrary 2-D constellations.

A computationally inexpensive, fixed throughput algorithm is proposed by Wong *et al.* (2002), known as K-best tree search. It can be easily implemented in a pipeline manner, but to get ML performance, a high value of K is needed and hence complexity is higher. Guo and Nilsson (2006) presented a method to reduce the required value of K, but complex preprocessing such as matrix inversion is needed. An adaptive reduced complexity K-best decoding algorithm utilizing the winner path extension scheme is proposed by Shen and

Eltawil (2010) which requires a smaller K . The performance is comparable with SD but the throughput is variable.

Choi *et al.* (2010) proposed a low-complexity detection technique referred to as a reduced dimension maximum-likelihood search. The search space is restricted to a partitioned symbol space and the resulting performance loss is compensated by an algorithm which is an extension of sphere decoding. Also, re-computation of the metric for a set of weak symbols ignored earlier for each strong symbol candidate found during the first search is done.

A detection method using adaptive hybrid tree search is proposed by Lai *et al.* (2011) in which the search tree is expanded in the breadth first manner until a specified threshold is achieved and then the depth first search is employed. It utilizes the diversity of the higher layers as the tree is expanded and maintains detection performance at reduced complexity.

Another tree search method having fixed complexity is the QRD-M algorithm (Kim and Yue (2002); Kim and Iltis (2002)). M is the number of surviving branches selected based on the smallest accumulated squared Euclidean distance, which is the key parameter to determine the tradeoff between performance and complexity. With properly chosen M , QRD-M algorithm can achieve comparable performance to that of the ML detection with a complexity of the same order as that of the SIC.

An ill-conditioned channel matrix may result in significant degradation in the performance of MIMO detection. MMSE based QRD-M (MQRD-M) algorithm (Sun *et al.*, 2006) can effectively deal with this problem, but it is highly complex in computing QR factors of the augmented channel matrix. In addition, when the number of candidates is insufficient, the performance of the MQRDM and QRD-M algorithms degrade considerably.

Jeon *et al.* (2006) introduced an algorithm using partial decision feedback that reduces the complexity of conventional QRD-M. At each stage, a threshold is set based on the smallest accumulated metric and the survival branches are those which have accumulated metrics smaller than this threshold. It leads to reducing the number of branches to be searched at each stage.

Detert (2007) proposed a reduced complexity QRD-M algorithm based on diagonal loading preconditioning (DLP) to mitigate the impact of weak main diagonal elements of the channel matrix, and by pruning unnecessary branch computations. Another low complexity detection method is the adaptive parallel and iterative QRD-M algorithms proposed by Hui *et al.* (2012).

Kim *et al.* (2010) proposed an algorithm that attains ML performance with much less complexity based on the minimum mean square error (MMSE) criterion. The search space is reduced by excluding unreliable candidates utilizing a probability metric that evaluates the reliability with the normalized likelihood functions of each symbol candidate. A threshold parameter is introduced to tradeoff between complexity and performance. An efficient way of generating the log likelihood ratio (LLR) values which can be used for coded systems is also proposed. Kim *et al.* (2012) proposed an algorithm to alleviate the performance degradation due to an inaccurate LLR of QRD-M when the number of candidates is insufficient. This algorithm obtains soft information of MMSE equalization efficiently and the optimal weighted combining method used derives a more reliable clipping value from the soft information.

2.2 SPATIAL MODULATION

Though Spatial Multiplexing provides high data rates and signal processing complexity can be reduced using the various methods above, antenna synchronization requirements and the overall energy consumption

raises practical implementation problems. This has led the current MIMO research towards maximizing the energy efficiency. Spatial modulation (SM), in which out of the available antennas, only a limited number is activated at a time is a low complexity solution to this (Di Renzo *et al.*, 2014).

Spatial modulation was first proposed by Chau and Yu in 2001, known as space shift keying (SSK). It is a two antenna system in which one antenna is active all the time and the other one is activated depending on the information bit and achieves one bpcu rate. They also combine spatial information and 2-PSK modulation to achieve 2 bpcu rate. A multi-antenna modulation scheme is proposed by Haas *et al.* (2002) that activates only one transmit antenna out of the available antennas during each time slot and information bits equal to the number of transmit antennas are multiplexed orthogonally and transmitted. Two years later in 2004, Song *et al.* proposed a “channel hopping technique,” which is exactly known as SM MIMO today. This scheme transmits one of the two information streams using PSK/QAM and the second implicitly by activating a single transmit antenna. In 2005, Mesleh *et al.* independently proposed the above modulation scheme to develop an ICI-free multi-antenna modulation system. In 2006, the same authors further explored the scheme and used the terminology “spatial modulation” for the first time to identify this encoding mechanism. Yang and Jiao(2008) proposed a similar scheme namely information guided channel hopping (IGCH). The SSK concept originally proposed is generalized to arbitrary number of transmit antennas by Jeganathan *et al.* (2009). This encoding scheme, known today as SSK–MIMO, uses only the spatial-constellation diagram to transmit the information bits.

The SM/SSK encoding schemes require that the number of TAs is a power of two. The generalized SSK schemes remove this restriction, but activating more than one transmit antenna has the associated problems of

higher decoding complexity and increased power consumption in the RF chains, which are to be addressed. This problem is avoided in the non-integer based encoding mechanism proposed by Serafimovski *et al.* (2010), which relies on the application of modulus conversion to achieve fractional bit rates. The main drawback of this solution is the presence of an error propagation effect. This issue is solved by Yang and Aissa (2011) using a bit padding method. The idea is to map different bit lengths onto the indices of the TAs and then to use padding techniques for avoiding error propagation. This approach can be used for arbitrary numbers of TAs without error propagation.

The performance analysis of SM-MIMO by Handte *et al.* (2009) for transmission over various fading channel models has revealed that no transmit-diversity gains can be expected. So, new encoding methods are developed that offer the advantage of diversity along with low decoding complexity. Basar *et al.* (2011) combine the SM-MIMO and the Alamouti scheme to exploit the second-order diversity of the Alamouti code and multiplexing gain of SM. A pair of transmit antennas chosen from a spatial constellation diagram transmits the Alamouti code using two time slots. To ensure second order diversity and maximum coding gain, rotation angles are introduced and optimized. The scheme offers a normalized rate higher than one and ML optimum performance with single-stream decodability.

Sugiura *et al.* (2010a) introduced a transmit diversity scheme in which the information bits are spread using space-time matrices called dispersion matrices, which can be optimized for the desired performance. The rate limiting factor in this scheme is the number of dispersion matrices available, rather than the number of transmit antennas. The achievable transmit diversity is the minimum of the number of transmit antennas and the number of time slots.

Yang *et al.* (2011) proposed transmit-diversity schemes for SSK–MIMO with a single active TA per channel use. The encoding scheme utilizes N_s time slots and the achievable transmit-diversity order cannot be higher than $N_t - 1$ if the number of TAs is higher than two. For $N_s \leq N_t - 1$, transmit-diversity order equal to N_s is achieved if specific conditions and bit-to-antenna mapping functions are followed. If $N_t = 2$, a closed-loop scheme that provides second order transmit diversity is illustrated based on phase rotations.

Di Renzo and Haas (2011b; 2013) proposed a transmit-diversity scheme without rate reduction for SSK–MIMO and SM–MIMO communications that exploits the concept of time-orthogonal shaping filters. This TOSD–SSK–MIMO is capable of providing second-order transmit diversity, while using a single time-slot transmission and a single active antenna. The TOSD principle is generalized then by combining with OSTBCs for achieving transmit-diversity gains higher than two and for application to SM–MIMO communications. The adoption of time-orthogonal shaping filters facilitates ML-optimum single-stream decoding performance at a low complexity, but at the cost of increased bandwidth.

Rajashekar and Hari (2012b) designed an open-loop transmit-diversity scheme for SM–MIMO communications that has the beneficial property of providing transmit-diversity gains with the aid of a single active TA element. The proposal is based on the so-called complex interleaved orthogonal design (CIOD), which refers to a class of symbol-by-symbol decodable codes that offer full rate (one complex symbol per channel use) for MIMO systems having up to four TAs. The authors combine SM with CIOD and prove that the proposed scheme guarantees second order transmit diversity and the same rate as SM MIMO. This is achieved using a two-slot transmission scheme and by introducing phase rotations for the sake of guaranteeing full diversity.

Furthermore, the authors propose a low complexity decoding scheme. To achieve the same rate as SM, the required transmit antennas is increased by one and the scheme is not extended to more than four transmit antennas.

The original demodulation algorithm proposed for SM MIMO by Mesleh *et al.* (2008) is a two-step process that estimates the active antenna index and the transmitted symbol separately. It is suboptimal and is affected by high sensitivity to errors in demodulating antenna index. Jeganathan *et al.* (2008b) developed the ML-optimum demodulator for SM MIMO, and showed that some performance improvements can be expected compared to the suboptimal demodulator. But this joint decoding increases the complexity of detection. A signal vector based detection scheme having near ML performance is proposed by Wang *et al.* (2012a), that provides significant reduction in complexity especially for higher order constellation. Rajashekar and Hari (2012a) proposed an ML optimum demodulator for SM MIMO applicable to either square or rectangular lattice constellations such as QAM, whose complexity is independent of the size of the signal constellation diagram. Without searching through the signal constellation diagram, hard limiting is performed directly on the received signal and to further reduce the complexity of demodulating the spatial constellation diagram, SD is applied. Yu *et al.* (2012) proposed a low-complexity demodulator for SSK-MIMO systems based on the compressive sensing (CS) principle, which is especially suitable for large-scale MIMO with only a few active antennas. Younis *et al.* (2013) proposed two low-complexity demodulation schemes based on the SD principle, namely the Rx-SD and Tx-SD, which aim for reducing the search space of the number of RAs and TAs respectively. Via a proper choice of the parameters, it is shown that both demodulators provide a substantial reduction of the computational complexity, while retaining the same performance as ML-

optimum decoding. Xu *et al.* (2013) developed a decoding algorithm that allows separate decoding of the spatial and signal constellation diagrams, while taking into account their correlation. The authors proposed both hard and soft decision solutions, and showed that the optimal performance can still be retained, despite its low demodulation complexity.

2.3 GENERALISED SPATIAL MODULATION

Compared to the spatial multiplexing system, the above spatial modulation techniques have low rate. Jeganathan *et al.* (2008a) extended the SSK-MIMO principle by allowing more than one transmit antenna to be active in every channel use and by encoding the information bits onto various combinations of multiple active transmit antennas. For the same number of transmit antennas, the rate can be improved at the cost of performance loss and increased number of RF chains. This modulation scheme is referred to as GSSK now. Younis *et al.* (2010) combine the SM-MIMO and GSSK-MIMO concepts to further improve the achievable spectral efficiency. The proposed modulation scheme is termed as GSM-MIMO. The main idea is to modulate the information bits onto both the signal constellation diagram and combinations of multiple active TAs. The transmission is free from ICI but results in higher decoding complexity. Block mapping spatial modulation (BMSM) proposed by Qu *et al.* (2011) is another multi antenna activated system that maps the information bits to different combinations of transmit antenna indices and distinct constellation symbols for achieving high rates. Wang *et al.* (2012b) combined SM MIMO with spatial multiplexing for further increasing the rate at the cost of adding ICI and increasing the decoding complexity. The main idea of this MA-SM scheme is to allow the transmission of multiple symbols of the signal constellation diagram during the same channel use, and at the same time to encode some bits onto the indices of the active TAs.

These modified SM and SSK schemes such as GSSK, GSM, MASM etc. in which more than one transmit antenna will be activated at each instance of time enables diversity and/or spectral /energy efficiency trade off, and removes the restriction on the total number of antennas. The STBC-SM system (E. Basar *et al.*, 2011), pointed out in Section 2.2 is an example, which activates two antennas during a time slot and combines SM with space time block coding. Ntontin *et al.* (2013) proposed a diversity scheme suitable for the GSSK modulated MISO systems, denoted as adaptive GSSK (AGSSK) that achieves full transmit-diversity for fewer number of transmit antennas without reducing the achievable rate. For higher number of transmit antennas and rates, the performance of this scheme degrades due to smaller average minimum Euclidean distance. Time-orthogonal shaping filters are utilized to alleviate this, and transmit-diversity greater than the number of active antennas is achieved but requires higher bandwidth. Generalised space-time shift keying (G-STSK) scheme based on dispersion matrices in conjunction with PSK/QAM modulation is proposed by Sugiura *et al.*(2011b), in which activating a particular dispersion matrix provides an implicit means of conveying information bits and the system can be configured in various mimo modes such as SSK,STBC, BLAST etc.

Activating more antennas at the same time increases the receiver design complexity. In GSM, spatial and signal constellations are not independent and cannot be separately detected, without affecting performance. Along with this, decoding information from the entire possible antenna combinations require searching over a large signal space and optimum ML decoder is prohibitive. General linear decoders like ZF and MMSE for MIMO, which are having low complexity, lose this advantage when applied to GSM (Wang *et al.*, 2012b). Considering the above factors, linear as well as nonlinear decoders for GSM,

with varying performance and complexity are proposed. An ML group decodable receiver proposed by Cal-Braz *et al.* (2013) is particularly designed for 4 transmit and 2 active antennas and apply ML detection rule to partitions of received block. First, zero forcing equalization of received signal is performed and then partitioning is done by a linear transformation. However, ZF detection may cause noise amplification with additive white Gaussian noise and the performance will degrade. Xiao *et al.* (2014) proposed an ordered block MMSE (OB-MMSE) detection that sorts all the potential transmit antenna combinations (TAC) according to an ordering scheme and then apply conventional MMSE. Ordering plays an important role and there is high computational complexity in computing the weights for each TAC. An improved version of this scheme (Chen *et al.*, 2015) uses the concentrated ML distance metric (CEML) to generate better ordering results and an algorithm is developed to avoid redundant computations for reducing the complexity. The nonlinear detector developed for GSM by Cal-Braz and Sampaio- Neto (2014) is an extension of sphere decoding approach to SM, and the results presented for computational complexity are only for small number of transmit and receive antennas. Projection based detector presented by Wang *et al.*, (2012b) separate antenna set detection from symbol detection and Cal-Braz and Sampaio- Neto (2015) uses a projection filter bank that sorts all valid antenna combinations in terms of the projection magnitudes. For both, the complexity is high due to the projections required for each TAC. Layered message passing algorithm presented by Narasimhan and Chockalingam (2016) is having low complexity. All these detection schemes require either $N_r > N_t$ or the best results require that condition. Recently, a K-Best sphere decoding for soft detection of GSM considering the null space is proposed by Zheng *et al.* (2017) that keep the same complexity irrespective of SNR.

2.4 ADAPTIVE SPATIAL MODULATION

A method for achieving low bit-error rate (BER) and high spectral efficiency is by adjusting transmission parameters such as modulation order and coding scheme dynamically according to channel conditions, which is called link adaptation. Due to the existence of different spatial signalling techniques, the number of adaptation modes and the amount of feedback information required is high in MIMO systems and designing adaptation schemes is challenging. (Chae *et al.*, 2010).

MIMO systems that exploit time and frequency parameter changes for adaptation are well explored (Keller and Hanzo, 2000). Some of these schemes increase the throughput for a fixed error rate and the others reduce the error rate for a fixed transmission rate (Chae *et al.*, 2010). Throughput based techniques utilize robust modulation and coding schemes (MCS) when the channel condition is poor and as the channel quality improves, switches to higher order MCSs. Diversity based methods improve the error performance by selecting the MIMO transmission modes that offer higher robustness to fading. (Chae *et al.*, 2004; Heath and Paulraj, 2005; Forenza *et al.*, 2005). Another method of rate adaptation is code puncturing, if the system employs channel coding. This technique is applied in V-BLAST spatial multiplexing systems using RCPC codes and is shown to have better bandwidth efficiency without much degradation in performance (Sari *et al.*, 2009; 2010)

Only a few works have been reported in SM and GSM. Yang *et al.* (2011) proposed an adaptive SM scheme to achieve better system performance for a fixed data rate based on a modulation order selection criterion (MOSC). Furthermore, the spatial information conveying the mode of SM is utilized to reduce the complexity of the proposed algorithm.

Yang *et al.* (2012) developed link-adaptation schemes for spatial modulation systems based on the adaptive modulation (AM) and transmit mode switching (TMS) techniques. An optimal hybrid SM (OH-SM) scheme that jointly uses both AM and TMS techniques is first developed to efficiently utilize the channel resources. In OH-SM, the transmit mode is jointly adapted with modulation orders according to the channel condition. A suboptimal hybrid SM scheme, termed as concatenated SM(C-SM), is also proposed that exploits the multistage adaptation strategy to balance the trade-off between computational complexity and performance.

Mthethwa and Xu (2012) applied adaptive modulation to SM for maximizing the average throughput using the first-order statistics SNR and the average statistics SNR. Theoretical BER bounds are found for both the approaches and M-ary QAM switching levels are adaptively determined to meet the required BER and maximize the throughput.

Xiao *et al.* (2013) proposed a power scaling scheme, PS-SM, for improving the SM performance with limited feedback. The scheme is based on a scaling factor for weighting the modulated symbols of SM, to enlarge the minimal Euclidean distance and thus improve the system performance. The scheme is shown to outperform the conventional adaptive spatial modulation with the same feedback amount and similar computational complexity.

Ma *et al.* (2012) presented an adaptive joint mapping scheme for GSM namely AJM-GSM in which the input information bits are jointly mapped to a mapping table which indicates both the spatial constellation and the signal constellation. The mapping table is updated adaptively according to the channel state information, so that the performance of AJM-GSM is superior to GSM and SM.

2.5 CONCLUSIONS

The extensive literature review showed the current status of coding and detection in MIMO. The spatial multiplexing systems provide high data rates, but the detection schemes are either complex or suffer from performance degradation. Since the detection of a symbol depends on the previous symbols detected, the diversity present in detection of upper layers is advantageous only in the high SNR region, where the detection of lower layers is more reliable. So, when traded off for complexity, the performance loss is more profound in the low SNR region. The other disadvantages are variable throughput, degradation of the performance as channel condition number is high or complex preprocessing required.

Apart from ICI and antenna synchronization issues, SMX systems suffer from high energy consumption. Spatial modulation avoids these problems, but transmit diversity is an issue. The diversity schemes in SM require more than one antenna activation, more time slots of transmission or enhanced bandwidth. Rate reduction compared to SM is another disadvantage when diversity is introduced. GSM is a compromise with rate and energy efficiency, with an associated increase in detection complexity compared to SM. The available degree of freedom in GSM to provide rate and QoS tradeoff is not effectively utilized. Also, only a few works are reported in SM and GSM systems with link adaptation.

Based on these observations, we have developed some systems that are having fair data rates and reliability, which are explained in the following chapters.

Chapter

3

CODING FOR HIGH RELIABILITY IN SPATIAL MULTIPLEXING SYSTEM

Spatial multiplexing systems transmit independent information symbols through different antennas, using same frequency and time slot and results in higher transmission rate. At the receiver, the transmitted symbols are separated by employing an interference cancellation type of algorithm. The maximum likelihood detection, which performs an exhaustive search over all possible candidate vectors, gives optimum performance, but complexity is prohibitively high. Several suboptimal tree search algorithms based on QR decomposition are developed that reduce the search space, but with a performance degradation, especially in the low SNR region. Examples are sphere decoding proposed by Damen *et al.* (2003) and QRD-M algorithm proposed by Kim and Yue (2002). In this chapter, we propose a coding scheme and a tree search detection named as QRD-P (QR decomposition and parity aided detection), in which parity checking is introduced as a means of reducing the probability of error and computational complexity. The coding process encodes the parity information of other symbols in one symbol, which is utilized to increase the reliability of the candidate retained at each level of tree search, thereby reducing the probability of error propagation and improving the performance.

3.1 INTRODUCTION

Tree search algorithms based on QR decomposition of the channel matrix are utilized by many low complexity detection schemes. Consider the MIMO system model given in Section 1.5, with N_t transmit antennas and N_r

receiving antennas where $N_r \geq N_t$. The received signal is given by Equation (1.1), repeated below for convenience.

$$\mathbf{y} = \mathbf{H}\mathbf{x} + \mathbf{n} \quad (3.1)$$

where $\mathbf{x} = [x_1 \dots x_{N_t}]^T$ and $\mathbf{y} = [y_1 \dots y_{N_r}]^T$ are $N_t \times 1$ transmit and $N_r \times 1$ receive vector respectively. Each entry of \mathbf{x} belongs to a complex constellation C , size K of which depends on the modulation scheme. $\mathbf{n} = [n_1 \dots n_{N_r}]^T$ represents the complex AWGN vector whose covariance matrix is $\sigma_n^2 \mathbf{I}$, and \mathbf{H} stands for the $N_r \times N_t$ channel matrix. Assuming a quasi-static fading channel model, the fading coefficients are static within a frame of transmitted symbols and independent over frames (Duman and Ghayeb, 2007).

The maximum likelihood solution of Equation (3.1) is obtained by minimization of the metric $\|\mathbf{y} - \mathbf{H}\mathbf{x}\|^2$. With QR decomposition of the channel matrix, $\mathbf{H} = \mathbf{Q}\mathbf{R}$, where, \mathbf{Q} is an $N_r \times N_t$ unitary matrix and \mathbf{R} is an $N_r \times N_t$ upper triangular matrix.

Premultiplying Equation (3.1) by \mathbf{Q}^H gives

$$\mathbf{Q}^H \mathbf{y} = \mathbf{Q}^H \mathbf{Q} \mathbf{R} \mathbf{x} + \mathbf{Q}^H \mathbf{n} \quad (3.2)$$

Since \mathbf{Q} is unitary, $\mathbf{Q}^H \mathbf{Q} = \mathbf{I}$. So, Equation (3.2) can be reduced to

$$\tilde{\mathbf{y}} = \mathbf{R}\mathbf{x} + \tilde{\mathbf{n}} \quad (3.3)$$

where $\tilde{\mathbf{y}} = \mathbf{Q}^H \mathbf{y}$ and $\tilde{\mathbf{n}} = \mathbf{Q}^H \mathbf{n}$ are the transformed receive and noise vectors respectively, whose statistical properties are not altered as \mathbf{Q} is unitary. On expanding,

$$\begin{bmatrix} \tilde{y}_1 \\ \tilde{y}_2 \\ \vdots \\ \tilde{y}_{N_t} \end{bmatrix} = \begin{bmatrix} r_{11} & r_{12} & \dots & r_{1N_t} \\ 0 & r_{22} & \dots & r_{2N_t} \\ 0 & 0 & \dots & r_{kN_t} \\ 0 & 0 & \dots & r_{N_t N_t} \end{bmatrix} \begin{bmatrix} x_1 \\ x_2 \\ \vdots \\ x_{N_t} \end{bmatrix} + \begin{bmatrix} \tilde{n}_1 \\ \tilde{n}_2 \\ \vdots \\ \tilde{n}_{N_t} \end{bmatrix} \quad (3.4)$$

From Equations (3.3) and (3.4), the ML solution of Equation (3.1) is equivalent to the minimization of the metric

$$\|\tilde{\mathbf{y}} - \mathbf{R}\mathbf{x}\|^2 = \sum_{i=1}^{N_t} |\tilde{y}_i - \sum_{j=i}^{N_t} r_{ij} x_j|^2 \quad (3.5)$$

where \tilde{y}_i represents the i^{th} element of vector $\tilde{\mathbf{y}}$, r_{ij} denotes the $(i,j)^{\text{th}}$ element of the matrix \mathbf{R} , and x_j is the j^{th} element of vector \mathbf{x} . Equation (3.5) can be represented by a tree structure as follows.

$$\begin{aligned} \|\tilde{\mathbf{y}} - \mathbf{R}\mathbf{x}\|^2 = & \left| \tilde{y}_{N_t} - r_{N_t N_t} x_{N_t} \right|^2 + \left| \tilde{y}_{N_t-1} - r_{N_t-1 N_t-1} x_{N_t-1} - r_{N_t-1 N_t} x_{N_t} \right|^2 + \\ & \dots \dots \dots + \left| \tilde{y}_1 - r_{11} x_1 - r_{12} x_2 \dots \dots \dots - r_{1 N_t} x_{N_t} \right|^2 \end{aligned} \quad (3.6)$$

Each term in Equation (3.6) represent the branch metric at each level, and the path metric is the sum of the branch metrics. The metric calculation and detection starts by estimating x_{N_t} in the first term. There is no interference caused by any other x_i since the N_t^{th} row of \mathbf{R} contains only r_{N_t} , and the detection in the following levels depends on the symbols detected in the previous levels.

Sphere decoding and QRD-M are two well-known low complexity detection methods for spatial multiplexing systems, which use QR decomposition. SD reduces the search space in evaluating Equation (3.5) with the assumption that at least one candidate resides in the sphere represented by

$$\sum_{i=1}^{N_t} |\tilde{y}_i - \sum_{j=i}^{N_t} r_{ij} x_j|^2 \leq R^2 \quad (3.7)$$

where R denotes the initial radius of the sphere. During each step of tree search, valid candidates (lattice points) are found which satisfy Equation (3.7) and the search space is reduced by adjusting the radius, so that these newly discovered points lie on the surface of the sphere. As a result, the detection complexity can be reduced because the candidate search is restricted to the

lattice points found within the sphere. But due to the ambiguity in selecting the initial radius and varying values of radius at each level, the system suffers from variable throughput.

In QRD-M, the search complexity is reduced by keeping only a fraction of the entire branches at each level in Equation (3.6) which have the small accumulated metric values. In the first step, which estimates the N_t^{th} symbol x_{N_t} , the branch metric $|\tilde{y}_{N_t} - r_{N_t, N_t} x_{N_t}|$ is calculated with all possible candidates and M candidate symbols are selected with minimum values for the metric. In the following steps, ($i = N_t - 1, \dots, 1$), the candidates for x_j are obtained in QRD-M assuming the symbols $x_{N_t}, x_{N_t-1}, \dots, x_{j+1}$ are already detected in the previous steps and utilizing those M selected candidates.

However, the complexity of QRD-M is still high for higher modulation order and large number of antennas, due to the requirement of retaining M candidates at each level. This increase in computational complexity by the order of M at each level can be avoided if only one candidate can be retained at all levels. If the probability of error in selecting the candidate retained can be made minimum, the performance will not be affected and the computation at each level will be reduced. In the proposed QRD-P system, the candidate retained is selected based on the available parity information, which is having high reliability with the coding scheme employed. So, the probability of error and complexity of detection are reduced and performance is improved even in the low SNR region.

With the above background on tree searching, first we give a theoretical analysis of the dependence of block error probability on the detection error of successive symbols. Next we give our coding and detection method in QRD-P. Computational complexity of QRD-P is analysed and

simulations are presented to compare the BER performance and complexity of QRD-P with that of QRD-M.

3.2 PROBABILITY OF BLOCK ERROR WITH QR DECOMPOSITION

As given in Section 3.1, the solution of Equation (3.1) based on QR decomposition starts at first level by detecting x_{N_t} , which is free of any interference from other symbols as seen from the branch metric $|y_{N_t} - r_{N_t N_t} x_{N_t}|^2$ in Equation (3.6). In the second level, detection of x_{N_t-1} is performed with the known values of x_{N_t} . The process continues up to the last level and at each level, the symbol decision depends on all the previous symbols detected. So, erroneous detection of a symbol in the earlier stages increases the probability of error in the subsequent stages. The error probability in detecting a block of symbols utilizing QR decomposition can be determined as follows.

If x_k^c denotes the event that k^{th} symbol is detected correctly and x_k^e that of error, the probability of correctly detecting a block of N_t symbols is given by

$$\begin{aligned}
 P_c(N_t) &= P(x_1^c, x_2^c, \dots, \dots, x_{N_t}^c) \\
 &= \prod_{k=1}^{N_t} P(x_k^c | x_{k+1}^c, \dots, \dots, x_{N_t}^c) \\
 &= \prod_{k=1}^{N_t} \{1 - P(x_k^e | x_{k+1}^c, \dots, \dots, x_{N_t}^c)\} \tag{3.8}
 \end{aligned}$$

The probability that k^{th} symbol is in error, given all symbols $x_{k+1} \dots \dots \dots x_{N_t}$ are detected correctly is

$$P(x_k^e | x_{k+1}^c, \dots, \dots, x_{N_t}^c) = P_e(k) = Q\left(\frac{R_k}{\sigma}\right) \tag{3.9}$$

where $Q(\cdot)$ denotes the Q function of the argument and R_k is the k^{th} diagonal entry in the \mathbf{R} factor of QR decomposition of \mathbf{H} matrix (Zhang *et al.*, 2005). Substituting in Equation (3.8),

$$P_c(N_t) = \prod_{k=1}^{N_t} \left(1 - Q\left(\frac{R_k}{\sigma}\right)\right) \quad (3.10)$$

To illustrate how the block error probability depends on the detection error of successive symbols, we consider a system with $N_t = N_r = 4$, so that \mathbf{R} is a 4 x 4 upper triangular matrix and from Equation (3.9),

$$P_e(4) = Q\left(\frac{r_{44}}{\sigma}\right) \quad (3.11)$$

$$P_e(3) = P(x_3^e | x_4^c) = Q\left(\frac{r_{33}}{\sigma}\right) \quad (3.12)$$

The probability of correct detection of a block of two symbols x_4, x_3 is

$$P_c(2) = \left(1 - Q\left(\frac{r_{33}}{\sigma}\right)\right) \left(1 - Q\left(\frac{r_{44}}{\sigma}\right)\right) \quad (3.13)$$

By neglecting the product term, the probability of error in detecting a block of x_4, x_3 is

$$P_{eb}(2) = 1 - P_c(2) \approx Q\left(\frac{r_{33}}{\sigma}\right) + Q\left(\frac{r_{44}}{\sigma}\right), \quad (3.14)$$

From Equations (3.12) and (3.14), it is clear that in detecting the block x_4, x_3 the probability of error is less if x_4 is detected correctly. Similarly, in detecting a block of three symbols x_4, x_3, x_2 , the probability of error if x_4 and x_3 are detected correctly is

$$P_e(2) = P(x_2^e | x_4^c, x_3^c) = Q\left(\frac{r_{22}}{\sigma}\right) \quad (3.15)$$

whereas if there is an error in detecting x_3 or x_4

$$P_{eb}(3) \approx Q\left(\frac{r_{22}}{\sigma}\right) + Q\left(\frac{r_{33}}{\sigma}\right) + Q\left(\frac{r_{44}}{\sigma}\right) \quad (3.16)$$

which is higher. In the last level of detection,

$$P_e(1) = P(x_1^e \mid x_4^c, x_3^c, x_2^c) = Q\left(\frac{r_{11}}{\sigma}\right) \quad (3.17)$$

$$P_{eb}(4) \approx Q\left(\frac{r_{11}}{\sigma}\right) + Q\left(\frac{r_{22}}{\sigma}\right) + Q\left(\frac{r_{33}}{\sigma}\right) + Q\left(\frac{r_{44}}{\sigma}\right) \quad (3.18)$$

From Equations (3.17) and (3.18), we can see that ensuring the correct detection of first three symbols detected will minimize the block detection error. The proposed QRD-P is an efficient way of ensuring correct detection of first three symbols, without any additional computation, as explained below.

3.3 PROPOSED METHOD OF CODING AND DETECTION

3.3.1 Encoding

Parity of the transmitted bit sequence can be effectively utilized for reducing the detection error as well as complexity. For example, consider a system with $N_t = N_r = 4$ where the transmitted signal vector is represented as $\mathbf{x} = [x_1 \ x_2 \ x_3 \ x_4]^T$. Assuming 16 QAM constellation, x_i represent a symbol in it and 16 bits are transmitted simultaneously through 4 transmit antennas. Among this, x_1 , x_2 and x_3 represents the information bits and x_4 is dedicated for parity information. The encoding process is shown in Figure 3.1.

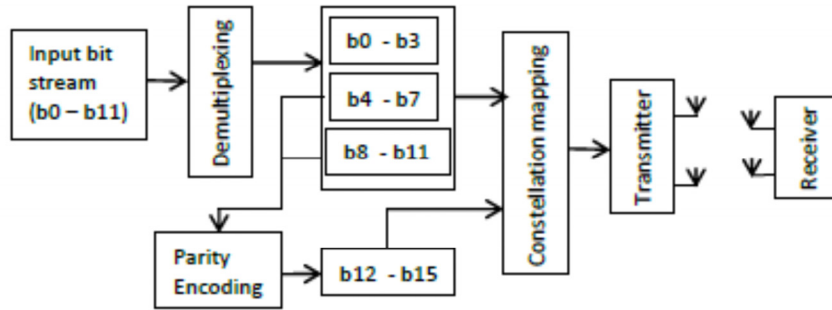


Fig. 3.1 Block diagram of QRD-P encoding

For encoding, the information bit sequence is divided into blocks of 12 bits and each block is again divided into sub blocks of 4 bits and mapped to constellation points as x_1 , x_2 and x_3 . The parity information of the above data is encoded as x_4 , considering the following matters.

The first factor to be considered is the selection of the symbols, the parity information of which is to be encoded in x_4 so as to minimize the block error. Encoding the parity of all the three data blocks corresponding to x_1 , x_2 and x_3 requires three bits and correspondingly there are eight possible constellation points for x_4 . For reducing the probability of error in detecting x_4 , the parity encoding is limited to two blocks, so that there are only four possible constellation points, and these two blocks are selected as follows. As already explained, the probability of error in detecting x_1 in the last level is reduced by the correct detection of x_4 , x_3 , and x_2 , which is also evident from Equations (3.17) and (3.18). So, it is obvious that x_2 and x_3 are the two symbols whose error is to be minimized using the parity information.

The second factor is that, x_4 is the first symbol which is detected independently of the other symbols that are sent simultaneously. Since it carries the parity information that is to be used for reducing the probability of error in the detection of x_3 and x_2 in the next levels, the correct detection of x_4 is essential. So, the selection of symbols in the constellation to represent x_4 is very important.

Assuming that the same 16 QAM constellation is used for parity and information symbols, to encode the four possible values of parity of x_2 and x_3 , 00, 01 10 and 11, four constellation points are to be selected from the 16 available points. Since the probability of error in detection is inversely proportional to the minimum distance between the candidate points, the most distant four points on the corners in the 16 QAM constellation, marked as red

crossed circles in Figure 3.2 are used to represent x_4 . Note that the Euclidean distance between these points is $6\sqrt{E_s}/\sqrt{10}$ where E_s is the average symbol energy, which is three times the distance between adjacent points, and probability of error in the detection of x_4 is reduced proportionally (Proakis, 2008). The parity information of x_2 and x_3 obtained from the second and third sub blocks of input sequence, represented by $b_4 - b_7$ and $b_8 - b_{11}$ in Figure 3.1 are mapped into these points, as shown in Table 3.1.

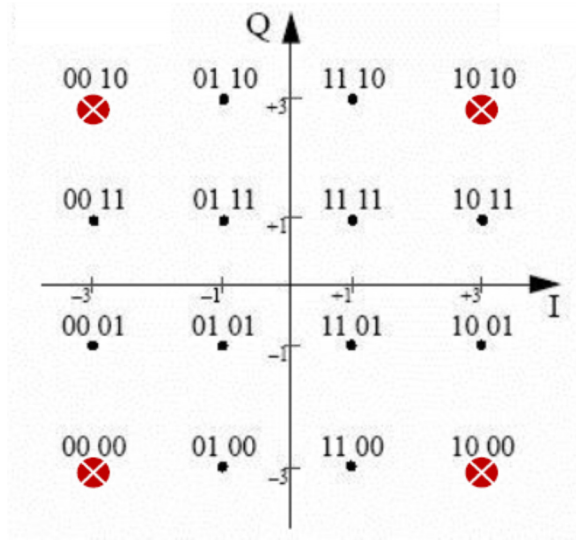


Fig.3.2. Mapping of x_4 in 16 QAM constellation

Table 3.1 Mapping of parity information to x_4

| Parity bits | First two bits of x_4 | Representation of parity bits in x_4 | x_4 |
|-------------|-------------------------|--|-------|
| 00 | 00 | Not inverted | 0000 |
| 10 | 00 | Not inverted | 0010 |
| 01 | 10 | inverted | 1010 |
| 11 | 10 | inverted | 1000 |

The parity information is also utilized to reduce the search space of x_3 and x_4 . For example, consider the even parity condition. As shown in Figure 3.3, points that satisfy even parity are only eight, marked as blue crossed circles. So, instead of searching all over the 16 points of constellation to estimate x_2 or x_3 , only these eight points are to be considered, which reduces the required comparisons and hence the complexity. The distance between adjacent constellation points is $2\sqrt{E_s}/\sqrt{10}$, whereas the distance between valid points that satisfy parity condition (blue crossed circles) is increased to $\sqrt{8E_s}/\sqrt{10}$, so that error probability is reduced proportionally.

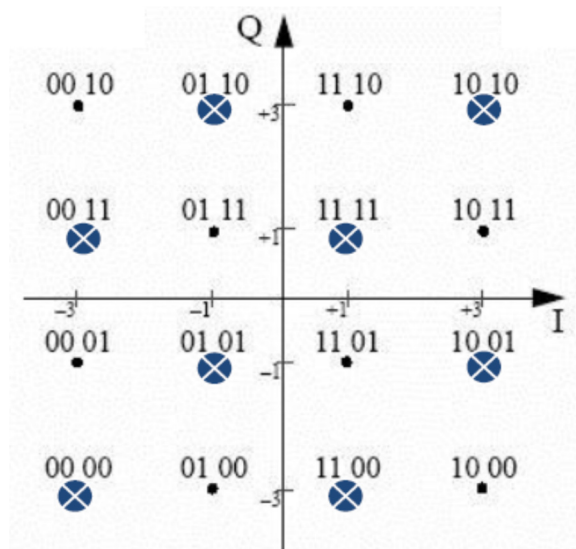


Fig.3.3 Search space with even parity

The reduction in spectral efficiency due to a symbol utilized for sending parity information is affordable, considering the large reduction in computational complexity, as will be explained in section 3.4. Considering the improvement in bit error rate performance achieved by this simple coding also, the spectral efficiency reduction is affordable.

3.3.2 Detection

Here, the detection process in QRD-P formulated for minimizing the metric in Equation (3.6) is explained. With $N_t = N_r = 4$, Equation (3.6) can be rewritten as follows.

$$\|\tilde{\mathbf{y}} - \mathbf{R}\mathbf{x}\|^2 = |y_4 - r_{44}x_4|^2 + |y_3 - r_{33}x_3 - r_{34}x_4|^2 + |y_2 - r_{22}x_2 - r_{23}x_3 - r_{24}x_4|^2 + |y_1 - r_{11}x_1 - r_{12}x_2 - r_{13}x_3 - r_{14}x_4|^2 \quad (3.19)$$

The branch and path metrics are calculated as follows.

Step1: In the first level of detection, the metric, say $f_1(x_4) = |y_4 - r_{44}x_4|^2$ is calculated to estimate x_4 . As can be seen, this detection of x_4 is independent of the interference from the symbols transmitted from other antennas and hence can be done independently. In QRD-P, this metric is to be calculated only for the four possible candidates of x_4 and here itself there is a computational reduction. The candidate that corresponds to the minimum metric is selected as the sent symbol. From this, the parity information of the symbols x_2 and x_3 are extracted.

Step2: The second metric, $f_2(x_3, x_4) = |y_3 - r_{33}x_3 - r_{34}x_4|^2$ is calculated with the fixed value of x_4 and with only eight possible candidates for x_3 , which satisfy the parity condition. The value of x_3 which corresponds to the minimum metric is retained.

Step3: The same process as in step2 is repeated for fixing the value for x_2 from the metric, $f_3(x_2, x_3, x_4) = |y_2 - r_{22}x_2 - r_{23}x_3 - r_{24}x_4|^2$, from the fixed values of x_4 and x_3 .

Step4: From the metric,

$$f_4(x_1, x_2, x_3, x_4) = |y_1 - r_{11}x_1 - r_{12}x_2 - r_{13}x_3 - r_{14}x_4|^2,$$

x_1 is calculated having obtained the values of x_4, x_3 , and x_2 . Here all 16 possible candidates are considered since no parity information is available. The process is illustrated in Figure 3.4.

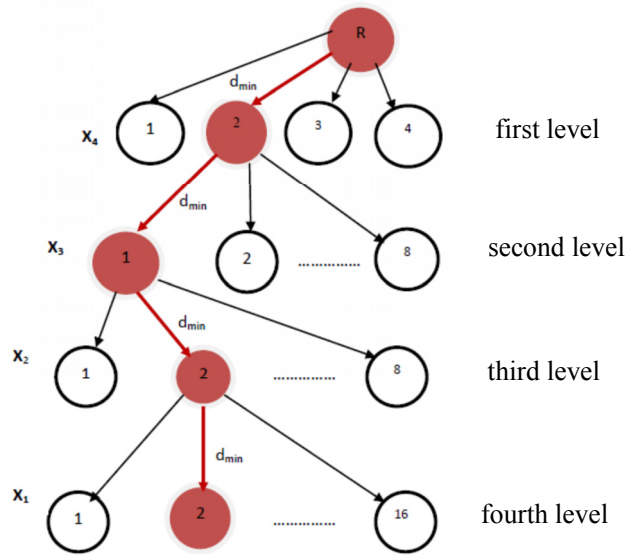


Fig. 3.4. Tracing of nodes in QRD-P

R is the root node and there are four child nodes in the first level of detection, representing the four possible values of x_4 . The node with minimum branch metric $d_{\min} = \min f_1(x_4)$ given in step1 is selected as x_4 , shown as the red shaded node2 in first level. In the second level which detects x_3 , there are 8 child nodes 1, 2.....8 to be considered for calculating the branch metric that satisfy the parity condition obtained from x_4 . The branch metrics given in step2 are calculated with these nodes for x_3 and the only one node retained in the first level for x_4 . The node that corresponds to the minimum metric, shown as shaded node1 in the second level, is fixed as the correct symbol for x_3 . Similarly in the third level, the eight child nodes with correct parity and single nodes retained for x_4 in the first level and for x_3 in

the second level are considered for calculating the branch metrics. The node retained for x_2 in this level is 2, and with the fixed nodes in the previous three levels, the fourth level calculates the minimum path metric considering all the sixteen nodes and the selected node 2 for x_1 completes the path selected finally.

3.4 COMPLEXITY ANALYSIS

In this section the computational complexity of QRD-P is compared with that of QRD-M. The complexity is computed in terms of the number of real additions and multiplications required for computing the metric. However, the computations required for matrix transposing and QR decomposition are excluded since they are the same for both methods.

In QRD-P, the number of real multiplications is given by $4\left\{4\sum_{i=1}^{N_t-1} i + \frac{K}{2}N_t + P\right\} + 2\left(\frac{K}{2}N_t + P\right)$, where P is the number of points in the constellation representing the symbol with parity information. For example, in the illustration in Section 3.3, $P = 4$. Here the first term accounts for the metric calculations and the second term for the norm square operations in Equation (3.6). This result directly follows from Equation (3.6) considering that only one candidate that satisfies parity condition is retained at each level as explained in Section 3.3. Number of additions required is only $2P + K\sum_{i=2}^{N_t} i$ since the path metric summation is only with single candidates retained at each level.

In QRD-M, real multiplications needed is given by $4\left\{\left(\sum_{i=1}^{N_t-1} i + K(N_t - 1)\right)M + K\right\} + 2(MK + K(N_t - 1))$, with the first and second term having the same interpretation as above, and M is the number of candidates retained at each level. The summation of terms in the path metric calculation requires $2K\left(1 + M\sum_{i=1}^{N_t} i\right)$ additions (Kim *et al.*, 2010).

A comparison of the computations required for detection with 16 QAM constellation is shown in Table 3.2. From the table it can be seen that compared to QRD-M, with $M = 4$, there is a reduction of 74% in the number of multiplications and a reduction of 88% in the number of additions. It is also clear that for QRD-M, the required additions and multiplications are approximately doubled when M is doubled (see the columns for QRD-M in Table 3.2), whereas QRD-P requires fixed number of additions and multiplications as it retains only one candidate at each level.

Table 3.2 Comparison of computational complexity of QRD-P and QRD-M

| Detection scheme | QRDM | | | QRD-P |
|------------------|------|-----|------|-------|
| | M=1 | M=2 | M=4 | |
| Addition | 352 | 672 | 1312 | 152 |
| Multiplication | 392 | 704 | 1328 | 344 |

3.5 SIMULATION RESULTS

In this section, simulation results are presented to compare the performance of QRD-P and QRD-M. The simulations are carried out considering MIMO systems with $N_t = N_r = 4$, $N_t = N_r = 8$, 16 QAM and 64 QAM constellations, where flat fading Rayleigh channels are assumed. Also, different transmit and receive antennas are assumed uncorrelated. For QRD-M, the parameter M is set to 1, 2, and 4.

3.5.1 Performance

The bit error rates for QRD-P and QRD-M, for a range of SNR values are shown in Figure 3.5. As can be seen, even at low values of SNR, QRD-P shows an SNR gain of 5dB for same bit error rate, compared to QRD-M, $M = 1$, where

the number of computations are approximately the same. With $M = 4$, where there is a large difference in computations, proposed method shows a gain of 3dB.

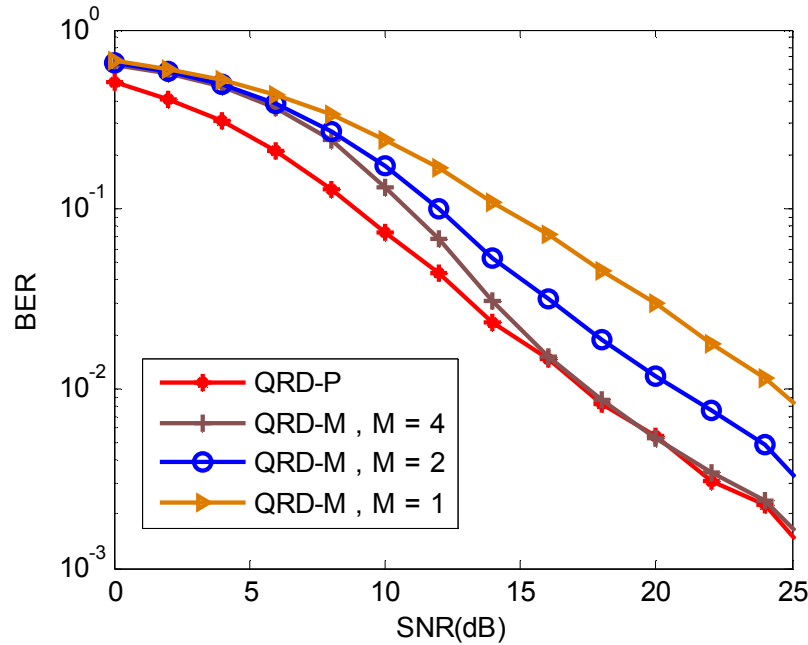


Fig. 3.5 BER Vs. SNR curves for QRD-P and QRD-M for $N_t = N_r = 4$, 16 QAM

Again, to illustrate the strength of QRD-P, we compare the performance with a coded system that employs QRD-M. For this, a simple (7, 4) linear block code is used, where hard decision approach can be applied as such. It is clear from Figure 3.6 that at moderate SNR of 10 dB, QRD-P shows 3dB improvement compared to QRD-M, $M = 1$, which is having the same complexity of detection. Figure 3.6 also shows the performance of QRD-M with 8QAM modulation, which is having the same information rate of 12 bits per time slot as QRD-P. Compared with this scheme also, QRD-P performance is better.

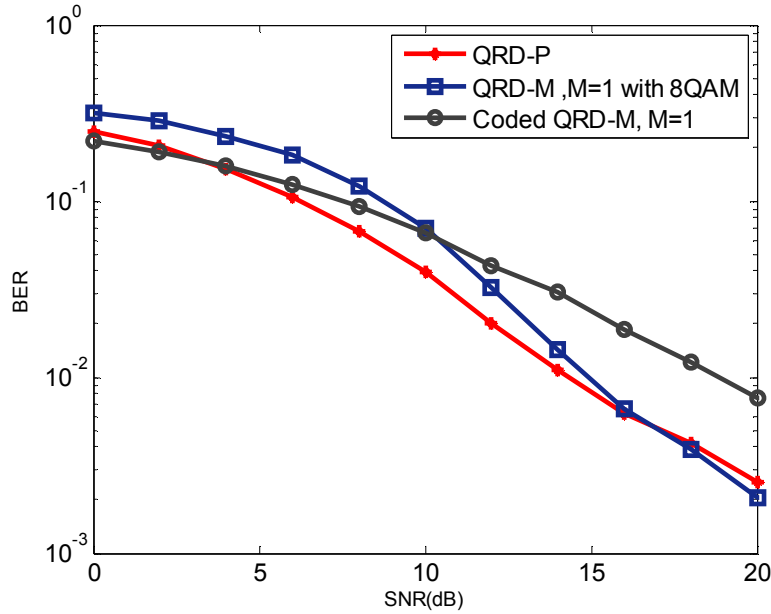


Fig.3.6 BER Vs. SNR curves for QRD-P, coded QRD-M & 8QAM for $N_t = N_r = 4$

Since only three symbols are carrying information out of the four symbols transmitted, the apparent data rate, which is the data rate considering only information bits is low for QRD-P. If the effective data rate, which is the percentage of correctly received information bits is considered, it is high for QRD-P. To establish this, we define a term called effective spectral efficiency (SE_{eff}) at a particular SNR and for a fixed block of bits as follows.

$$SE_{\text{eff}} = \frac{\text{Number of bits received correctly}}{\text{Effective number of bits transmitted.}}$$

where effective number of bits is the number of information bits transmitted in that particular block of bits. In QRD-M, all the four symbols transmitted carries information, and so there is no difference between the actual bits transmitted and the effective bits. But for QRD-P system illustrated here, the effective bits are only 75% of the actual bits transmitted. Even though the

effective bits are less in QRD-P, most of them are received correctly and information transfer is better. This aspect is considered in defining SE_{eff} and so it is a term introduced as measure of the actual performance of the system. The effective spectral efficiency vs. SNR curves for QRD-P and QRD-M are given in Figure 3.7. It shows that effective spectral efficiency of QRD-P is better even at low values of SNR. At SNR = 10dB, 90% spectral efficiency is achieved by QRD-P, whereas QRD-M, $M = 1$ attains the same efficiency at SNR = 15. M has to be increased to 4 to attain same efficiency at SNR = 10dB, and for lower values of SNR, even with $M = 4$, the efficiency is less. It can be seen that compared to coded systems also, QRD-P has a better effective spectral efficiency.

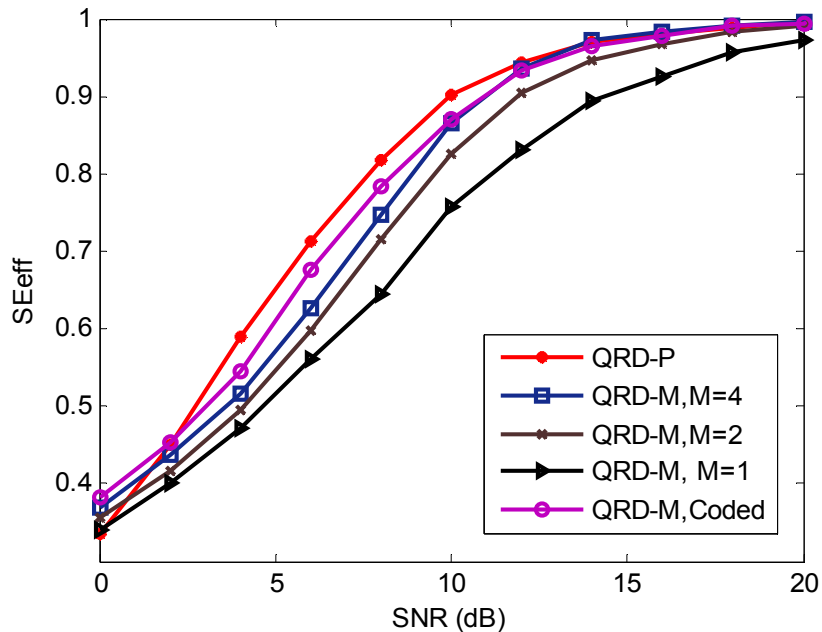


Fig. 3.7. SE_{eff} vs. SNR curves for QRD-P and QRD-M for $N_t = N_r = 4$, 16 QAM

The comparison of effective spectral efficiency for the proposed method and QRD-M in numerical form is provided in Table 3.3. At 5dB, there is a large difference in spectral efficiency even though $M = 4$ is used for QRD-M. Even the coded QRD-M shows the same spectral efficiency only at 15 dB SNR. Note that the bit error rates derived from table 3.3 for QRD-M exactly match with the results shown in Figures 3.5 and 3.6. For QRD-P, the change is due to the consideration of errors in the information bits only for calculating the effective spectral efficiency.

Table 3.3 Comparison of effective spectral efficiency of QRD-P and QRD-M

| SNR = 5 dB | | | | |
|-----------------------------|----------------|-------------------|-------------------|--------------------|
| A block of 1000 bits | QRD-P | QRD-M, M=1 | QRD-M, M=4 | Coded QRD-M |
| Effective bits | 750 | 1000 | 1000 | 570 |
| Bits received correctly | 470 (62.7%) | 500 (50%) | 550 (55%) | 336 (58.9%) |
| SNR = 10 dB | | | | |
| Bits received correctly | 675 (90%) | 700 (70%) | 850 (85%) | 485 (85%) |
| SNR = 15 dB | | | | |
| Bits received correctly | 743 (99%) | 900 (90%) | 990 (99%) | 565 (99.1%) |

The performance of the system as we increase the transmit antennas or the constellation size is illustrated next. Figure 3.8 shows the BER performance of QRD-P and QRD-M for a system with $N_t = N_r = 8$, 16QAM modulation. For QRD-M, a moderate value of $M = 2$ is assumed. The BER performance shows 3dB Improvement for almost all values of SNR. Figure 3.8 also compares the performance as we increase the constellation size to 64QAM, in a system with $N_t = N_r = 4$. Here also, performance of QRD-P is better than QRD-M, but the SNR gain is somewhat lower compared to the system of eight transmit antennas.

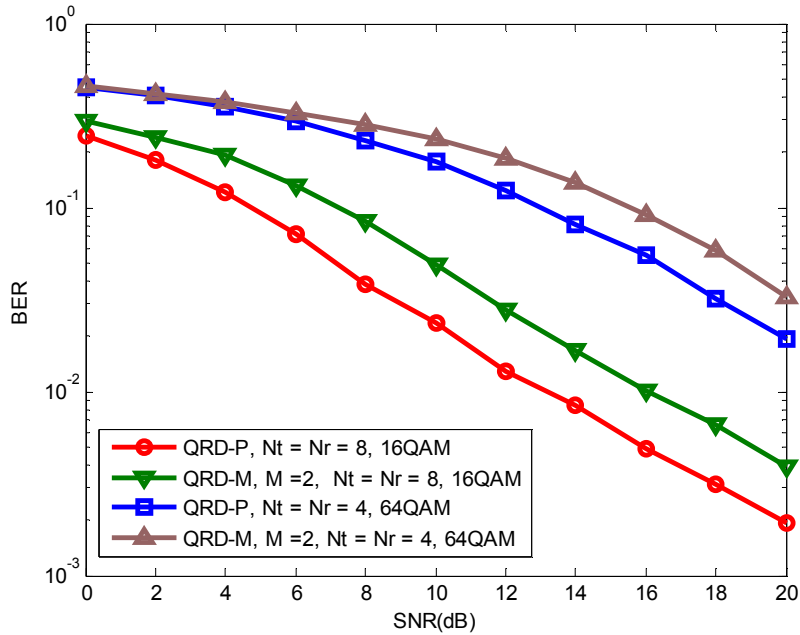


Fig.3.8 BER Vs. SNR curves for QRD-P and QRD-M for $N_t = N_r = 8$, 16QAM and $N_t = N_r = 4$, 64QAM

In QRD-P, in the $N_t = N_r = 8$ antenna system, two out of the eight transmit antennas are utilized for sending parity information of the four symbols transmitted through other antennas. As in the previous system of four transmit antennas, the information rate is reduced to 75%. As explained before, to compare the actual performance, the effective spectral efficiency of the above systems is plotted in Figure 3.9. As can be seen, the performance of QRD-P for $N_t = N_r = 8$ antenna system is better. For higher modulation order of 64 QAM in $N_t = N_r = 4$ antenna system, the effective spectral efficiency better than QRD-M only at high SNR region. This indicates that QRD-P performs better as the number of transmit antennas are higher, rather than for higher constellation sizes.

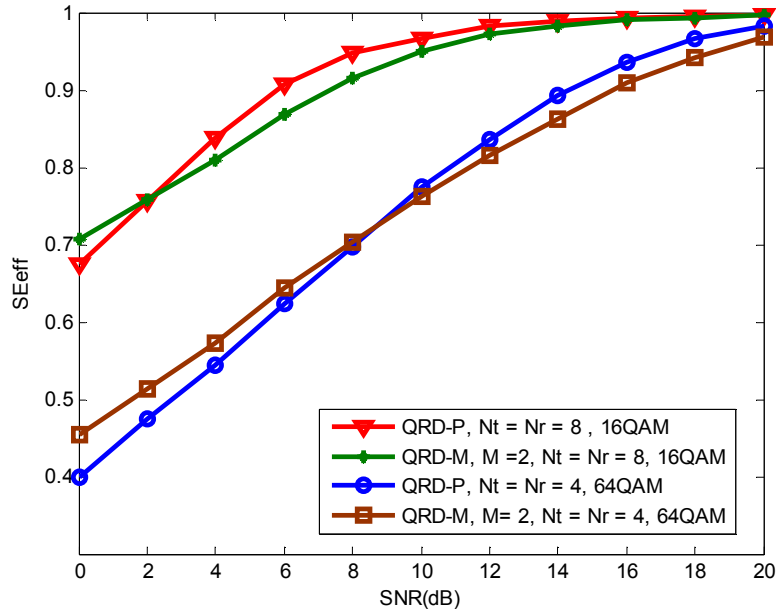


Fig. 3.9. SEff vs. SNR curves for QRD-P and QRD-M for $N_t = N_r = 8, 16\text{QAM}$ and $N_t = N_r = 4, 64\text{QAM}$

3.5.2 Computational Complexity

For comparing the computational complexity, the average number of flops which is machine independent, is plotted against M , in Figure 3.10. For QRD-M, the number of flops is higher and varies as M is varied. In QRD-P, the computational complexity is independent of the value of M , since only one symbol is retained at each level of detection. The overhead due to parity encoding is in bit level and is negligible. Another factor compared is the number of nodes visited as M is varied, which depends on the constellation size. For large constellation size and high values of M , it can be seen from Figure 3.11 that huge number of nodes are visited in QRD-M, which in turn increases the computation required. In QRD-P, nodes visited are independent of M and only a small increase is there due to increase in constellation size.

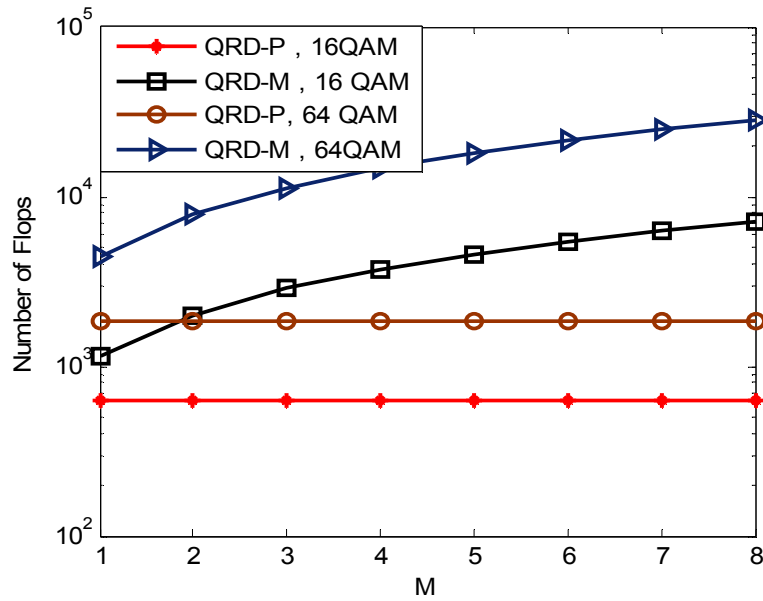


Fig. 3.10. Number of flops vs. M for QRD-P and QRD-M, $N_t = N_r = 4$

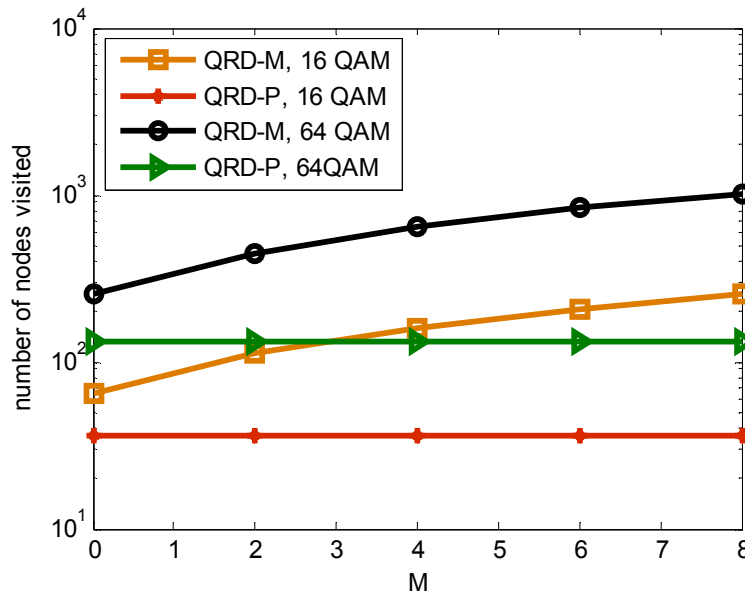


Fig. 3.11. Number of nodes visited vs. M for QRD-P and QRD-M, $N_t = N_r = 4$

3.6 CONCLUSIONS

This chapter proposed a coding scheme named as QRD-P that improves the BER performance of SMX-MIMO detection with the aid of parity information sent through one of the transmitted symbols. With the added advantage of low complexity detection, QRD-P shows better performance in terms of BER and effective spectral efficiency even at low values of SNR, compared to the traditional QRD-M method. This is due to retaining only one reliable candidate at each level, utilizing the redundancy introduced by the parity information. The cost of the lower computational complexity is the information bit rate, which is reduced to three fourth of the standard SMX-MIMO, even though the data rate is the same. But, it is seen that the effective spectral efficiency, which is a measure of the percentage of correctly received bits to the sent information bits is better even at low values of SNR.

As the number of transmit antennas increases, either more symbols are to be utilized for encoding the parity information or more points in the constellation are to be used to represent the parity encoded symbol. In the first case, the effective data rate will be reduced whereas the second solution will increase the computational complexity slightly. This drawback is compensated with the improved performance even at low values of SNR.

4 A TRANSMIT DIVERSITY TECHNIQUE WITH HIGH RATE IN SPATIAL MODULATION SYSTEM

Spatial multiplexing offers high transmission rates, but impose practical implementation problems of antenna synchronization and signal processing complexity. The multiple RF chains along with the power amplifiers at the transmitter make the system unattractive due to low energy efficiency. A low complexity solution to these problems is the so called spatial modulation. In SM, out of the available antennas, only one antenna is activated at a time and hence there is no ICI and associated decoding complexity. SM can convey information through the active antenna index as well as through the symbol transmitted and results in increased rate compared to a single antenna system, without increase in energy consumption (Mesleah *et al.*, 2006; Di Renzo, *et al.*, 2014). Since only one antenna is active during a time slot, the spectral efficiency compared to spatial multiplexing is less and transmit diversity gains cannot be provided. Another restriction in SM is that the total number of transmit antennas has to be a power of two. Literature survey revealed that the existing transmit diversity techniques in SM either activates more than one transmit antenna and the inherent advantages of SM are lost, or requires more number of time slots and results in rate reduction. The single antenna activated solutions to transmit diversity need higher bandwidth or complex optimization of parameters (Di Renzo *et al.*, 2014). In this chapter, we introduce a single antenna activated scheme in SM named as WET-SM (Weyl group encoded transmission in SM), that offers second order transmit diversity without any

rate reduction. The other advantages of WET-SM are that it is suitable for any number of transmit antennas and the computational complexity increases only linearly with the number of antennas.

4.1 INTRODUCTION

The SM transmission is as follows. Assuming there are N_t antennas at the transmitter, the information bit sequence is split into blocks of $\log_2(N_t K)$ bits, in which the antenna index part of $\log_2 N_t$ bits select the active antenna and constellation part of $\log_2 K$ bits select one of the K complex symbols of the signal constellation. The transmitted signal vector in SM is

$$\mathbf{x} = [0 \ 0 \ 0 \ \dots \ x_q \ \dots \ 0]^T$$

\uparrow
 t^{th} position

where $x_q \in \mathcal{C}$ the complex constellation of size K . So, the signal vector in SM has $N_t - 1$ zero entries and only one non zero entry corresponding to the active antenna at t^{th} position.

As per this system model and as shown by Handte *et al.* (2009), it is clear that no transmit diversity can be achieved in SM since only one antenna is activated during each time slot. Some encoding techniques utilize more than one transmit antenna and/or more than one time slot to achieve diversity. STBC-SM (Basar *et al.*, 2011) and SM-CIOD (Rajashekar and Hari, 2012) are two such schemes that offer diversity and still maintain low complexity single stream decodability.

The STBC-SM combines SM with space time block coding, so that both antenna index and STBC carry information and diversity is achieved. With Alamouti scheme as the mother STBC, two antennas and two RF chains will be

active during each time slot. The spatial constellation diagram selects these two antenna combinations from the total N_t antennas available. The possible antenna activation patterns with the corresponding symbols transmitted are arranged as code books, such that each codebook is composed of antenna combinations that are never used in another codebook. This is to ensure diversity and maximize coding gain distance by providing different rotation angles to codebooks. The rate of the code is $\frac{1}{2} \log_2 c + \log_2 K$ where c is the degree of spatial modulation (DoSM) given by $c = \left[\binom{N_t}{2} \right]_{2^p}$, p a positive integer, and K is the constellation size. The decoding complexity of the system increases linearly with DoSM, which is very high as the number of antennas increases. The system also requires synchronization of two antennas.

Second order diversity with a single active antenna per time slot is achieved by the CIOD based scheme. In this scheme, $\tilde{s}_1 = s_{1I} + js_{2Q}$ and $\tilde{s}_2 = s_{2I} + js_{1Q}$ are the symbols transmitted, where \tilde{s}_1 and \tilde{s}_2 are obtained by swapping the imaginary parts of s_1 and s_2 . During the first timeslot, \tilde{s}_1 is transmitted through the first antenna and the second antenna is kept inactive, and \tilde{s}_2 is transmitted through the second antenna during the second time slot while the first antenna is inactive. The two antennas are selected from the total antennas in the same way as STBC-SM, with DoSM given by $c = \left[\binom{N_t}{2} \right]_{2^p}$. With N_t antennas and DoSM N_t over two channel uses, the rate achieved is $\frac{1}{2} (\log_2 N_t + \log_2 K^2)$ bpcu. With DoSM N_t over one channel use, rate is $\log_2(N_t \cdot K)$ bpcu, but $N_t + 1$ antennas are required. Here also, to achieve diversity and maximize coding gain, rotation angles are provided to the constellation and code books. The ML search complexity of the scheme is high compared with the standard SM and the performance depends on DoSM.

Here, we propose a transmit diversity technique in SM with only one active antenna during a time slot based on a bits to matrix conversion method. The information bits are not directly mapped to constellation points as in the existing systems, but they are first encoded into matrices that belong to Weyl group (MacWilliams and Sloane, 1977; Arab *et al.*, 2011). Then the columns of these matrices are mapped to the constellation as a second step. The advantage obtained is that due to the peculiarity of Weyl Group matrix, a single antenna will be active during a time slot and at the same time diversity is achieved.

Weyl group is a Unitary Matrix group. The multiplicative Weyl Group G_w is generated by two matrices, $\frac{1}{\sqrt{2}} \begin{bmatrix} 1 & 1 \\ 1 & -1 \end{bmatrix}$ and $\begin{bmatrix} 1 & 0 \\ 0 & i \end{bmatrix}$. As these matrices are unitary, all the matrices generated by them are also unitary. The group is divided into 12 cosets and each coset contains 16 invertible matrices. The first coset, which is a sub group of Weyl group is given by

$$C_0 = \left\{ \alpha \begin{bmatrix} 1 & 0 \\ 0 & +1 \end{bmatrix}, \alpha \begin{bmatrix} 0 & 1 \\ +1 & 0 \end{bmatrix} \right\} \quad (4.1)$$

with $\alpha \in \{+1, -1, +i, -i\}$. (see appendix for details)

Blocks of 4 bits are mapped to the 16 matrices in this coset on a one to one basis. In the next section, based on the above, we propose a transmit diversity technique that has the single stream decodability with only one active antenna during a time slot.

4.2 PROPOSED METHOD FOR DIVERSITY

Here we assume that there are two information streams, a high priority stream that need diversity based on the required QoS (stream1) and a low priority stream for increasing the rate (stream2). The encoding process is different for the low and high priority data. High priority information bits are

not directly mapped to constellation points but they are encoded into matrices that belong to Weyl group first. The matrices thus obtained along with the low priority data determines the transmission symbols during the two time slots. The antenna selection is done using the bits of low priority data. In the following sections, we explain the encoding process in detail.

4.2.1 Encoding

The encoding in the proposed WET-SM is based on bits to matrix conversion and antenna grouping. The bits to Weyl Group matrix conversion is done so as to encode the information in such a way that diversity is achieved and at the same time rate of transmission is not reduced. This is made possible by utilizing the following features of Weyl Group matrices, that are easily observable from the rows of Table 4.1, obtained by expanding Equation (4.1).

1. The first column of these matrices can be grouped into two as given below, bit group B_ϕ and bit group B_ψ , elements of which are the negatives of the elements of B_ϕ .

$$\begin{aligned}
 B_\phi &= \left\{ \begin{bmatrix} 1 \\ 0 \end{bmatrix} \begin{bmatrix} 0 \\ 1 \end{bmatrix} \begin{bmatrix} i \\ 0 \end{bmatrix} \begin{bmatrix} 0 \\ i \end{bmatrix} \right\} \\
 B_\psi &= \left\{ \begin{bmatrix} -1 \\ 0 \end{bmatrix} \begin{bmatrix} 0 \\ -1 \end{bmatrix} \begin{bmatrix} -i \\ 0 \end{bmatrix} \begin{bmatrix} 0 \\ -i \end{bmatrix} \right\}
 \end{aligned} \tag{4.2}$$

2. The matrices can be grouped as follows, based on the second column. In the first matrix $\begin{bmatrix} 1 & 0 \\ 0 & 1 \end{bmatrix}$, the second column is just the inverted form of first column. All the eight matrices that fall in this category are grouped as B_ξ and the others where the second column is negative of the inverted form of the first column are grouped as B_η , an example being the matrix $\begin{bmatrix} 1 & 0 \\ 0 & -1 \end{bmatrix}$.

Table 4.1 Mapping of bit groups to Weyl Matrices

| Information bits | 0000 | 0001 | 0010 | 0011 |
|------------------|--|---|--|---|
| Matrix | $\begin{bmatrix} 1 & 0 \\ 0 & 1 \end{bmatrix}$ | $\begin{bmatrix} 1 & 0 \\ 0 & -1 \end{bmatrix}$ | $\begin{bmatrix} 0 & 1 \\ 1 & 0 \end{bmatrix}$ | $\begin{bmatrix} 0 & 1 \\ -1 & 0 \end{bmatrix}$ |
| Information bits | 0100 | 0101 | 0110 | 0111 |
| Matrix | $\begin{bmatrix} -1 & 0 \\ 0 & -1 \end{bmatrix}$ | $\begin{bmatrix} -1 & 0 \\ 0 & 1 \end{bmatrix}$ | $\begin{bmatrix} 0 & -1 \\ -1 & 0 \end{bmatrix}$ | $\begin{bmatrix} 0 & -1 \\ 1 & 0 \end{bmatrix}$ |
| Information bits | 1000 | 1001 | 1010 | 1011 |
| Matrix | $\begin{bmatrix} i & 0 \\ 0 & i \end{bmatrix}$ | $\begin{bmatrix} i & 0 \\ 0 & -i \end{bmatrix}$ | $\begin{bmatrix} 0 & i \\ i & 0 \end{bmatrix}$ | $\begin{bmatrix} 0 & i \\ -i & 0 \end{bmatrix}$ |
| Information bits | 1100 | 1101 | 1110 | 1111 |
| Matrix | $\begin{bmatrix} -i & 0 \\ 0 & -i \end{bmatrix}$ | $\begin{bmatrix} -i & 0 \\ 0 & i \end{bmatrix}$ | $\begin{bmatrix} 0 & -i \\ -i & 0 \end{bmatrix}$ | $\begin{bmatrix} 0 & -i \\ i & 0 \end{bmatrix}$ |

The spatial constellation diagram of SM is used to represent the group information. With this, the transmission from a specific antenna represents a particular group and hence only four symbols are required to represent the eight elements in Equation (4.2). Also, the matrix group information is conveyed in WET-SM in an implicit manner so that it will not reduce the rate, as will be explained.

Matrix mapping is done using a look up table, whereby each four bits of stream1, ie. high priority data, are mapped on a one to one basis to a matrix that belongs to the first coset of Weyl Group. An example of mapping is shown in Table 4.1. The transmission of this encoded data will be explained after introducing the second step of our method, which is antenna grouping.

The antennas are grouped as A_ϕ and A_ψ so as to make the codebooks noninterfering and reduce the computational complexity. The minimum number of antennas in a group should be two, so that $N_t \geq 4$. In a group of two antennas, each antenna represents different information so that the two antennas selected should not be part of another group. Then, if the group selected in the first time slot is avoided in the second time slot, computation required while decoding is

reduced. Table 4.2 illustrates the grouping and the spectral efficiency (SE) resulting from antenna selection. The group selection bits select a set of two antennas from any of the group and the antenna selection bits select one antenna from that group. Spectral efficiency due to antenna selection is the average of the group selection bits and antenna selection bits. To see the advantage of grouping, consider the 16 antenna WET-SM system in which the antenna group (1, 2) is selected in the first time slot. If all the other antennas (3-16) are considered for the second time slot, maximum number of bits that can be communicated is 3 ($\lfloor 14 \rfloor_{2^p}$, p a positive integer).

Table 4.2. Antenna grouping and spectral efficiency (SE)

| No. of antennas | Grouping | | Group selection | Antenna selection | SE in WET-SM (bpcu) | SE in STBC-SM (bpcu) |
|-----------------|-------------------------|--------------------------------|-----------------|-------------------|---------------------|----------------------|
| | A_ϕ | A_ψ | No. of bits | No. of bits | | |
| 4 | (1,2) | (3,4) | 1 | 1 | 1 | 1 |
| *6 | (1,2) | (3,4) (5,6) | 1 | 2 | 1.5 | 1.5 |
| 8 | (1,2) (3,4) | (5,6) (7,8) | 2 | 2 | 2 | 2 |
| 16 | (1,2) (3,4) (5,6) (7,8) | (9,10) (11,12) (13,14) (15,16) | 3 | 3 | 3 | 3 |

* Here, antennas 5 & 6 can be grouped with any antenna elements used in the second time slot. If the number of antenna elements are not a power of two, grouping can be done like this.

In the antenna selection process employed in WET-SM, only the antennas in A_ψ , ie. (9-16) are used in the second time slot, which will communicate same number of bits ($\lfloor 8 \rfloor_{2^p} = 3$), which shows that there is no reduction in spectral efficiency (SE) due to antenna selection with the grouping strategy employed in WET-SM. At the same time, since the number of antennas to be considered for decoding in the second time slot is less, a significant reduction in decoding complexity results. The last two columns of Table 4.2 also show that the spectral

efficiency of WET-SM is the same as that of STBC-SM, for the given number of transmit antennas.

The details of encoding and transmission in WET-SM are illustrated in Figure 4.1. The process is illustrated with an example of four transmit antenna system, with QPSK modulation. As shown in Figure 4.1, each four bits of the high priority data which need diversity, (stream1) are first converted to matrices and according to the first column of these matrices, they are grouped as B_ϕ or B_ψ . The transmission starts in the first time slot T1 by selecting the antenna group by the first bit of stream 2. The Weyl group matrix corresponding to the four bits of stream 1 is formed and if the first column belongs to B_ϕ , it is mapped to one of the four symbols of QPSK and sent through antenna 1 of the group selected. If the first column belongs to B_ψ , it is sent through antenna 2 of the group selected after constellation mapping. Constellation rotation will be applied before sending, as will be explained in the codebook construction. The information regarding the second column of the matrix, whether it is just the inverted form of column1 or the negative of the inverted form of column1, is not directly sent but is implicitly conveyed by selecting a particular constellation rotation during the transmission in the second time slot.

During the second time slot, the second antenna group (the group that is not used in the first time slot) is selected. The antenna in that group is selected according to the second bit of bit stream2. If it is zero, the first antenna is selected and otherwise the second. The next two bits are mapped to the constellation as follows. If the implicit information to be conveyed is that the second column of the matrix is just the inverted form of column1 (matrix belongs to B_ξ), the two bits are mapped to four symbols of QPSK, with a

constellation rotation of a specific angle. If the matrix belongs to B_η , ie. the second column of the matrix is negative of the inverted form of column1, the two bits are mapped to the four symbols of QPSK with a constellation rotation of another specific angle. That means the elements of B_ξ and B_η will be mapped to separate subsets of codebook.

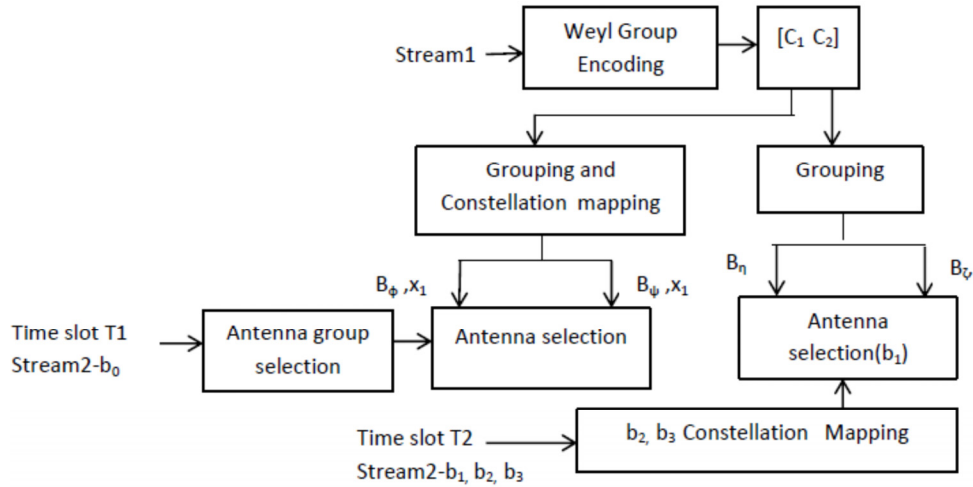


Fig. 4.1. Encoding and transmission in $N_t = 4$ WET-SM system

The code book construction is as follows, with rows indicating the time slot and the columns indicating the active antenna.

$$X_\alpha = \{X_{11}, X_{12}\} = \left\{ \begin{pmatrix} x_1 & 0 \\ 0 & 0 \end{pmatrix}, \begin{pmatrix} 0 & x_1 \\ 0 & 0 \end{pmatrix} \right\} \quad (4.3)$$

$$X_\beta = \{X_{21}, X_{22}\} = \left\{ \begin{pmatrix} 0 & 0 \\ x_2 & 0 \end{pmatrix}, \begin{pmatrix} 0 & 0 \\ 0 & x_2 \end{pmatrix} \right\} \quad (4.4)$$

where x_1 and x_2 are elements of rotated constellations which ensures diversity of order two, ie. $x_1 = x_i$, $x_2 = e^{j\theta} x_i$; x_i being the QPSK symbol. The codebook X_k is formed by combining one matrix X_{1i} from X_α and another

matrix X_{2j} from X_β . The codebooks formed like this will be interfering and will not satisfy the rank criteria for maximum diversity gain (Cho *et al.*, 2010), given by

$$v = \min \text{rank}_{p \neq q} \left\{ (X_p - X_q)(X_p - X_q)^H \right\} \quad (4.5)$$

where X_p and X_q are two different code word matrices. To avoid this scenario and to ensure diversity, the complete code book construction, with non-interfering code words grouped together is as follows. Note that X_1 , X_3 and X_2 , X_4 contains the same codewords with a different rotation angle, which is used to convey the information regarding the second column of the matrix.

$$X_1 = \left\{ \begin{pmatrix} x_1 & 0 & 0 & 0 \\ 0 & 0 & x_2 & 0 \\ 0 & 0 & x_1 & 0 \\ x_2 & 0 & 0 & 0 \end{pmatrix}, \begin{pmatrix} 0 & x_1 & 0 & 0 \\ 0 & 0 & 0 & x_2 \\ 0 & 0 & 0 & x_1 \\ 0 & x_2 & 0 & 0 \end{pmatrix} \right\} e^{j\theta_1} \quad (4.6)$$

$$X_2 = \left\{ \begin{pmatrix} x_1 & 0 & 0 & 0 \\ 0 & 0 & 0 & x_2 \\ 0 & 0 & x_1 & 0 \\ 0 & x_2 & 0 & 0 \end{pmatrix}, \begin{pmatrix} 0 & x_1 & 0 & 0 \\ 0 & 0 & x_2 & 0 \\ 0 & 0 & 0 & x_1 \\ x_2 & 0 & 0 & 0 \end{pmatrix} \right\} e^{j\theta_2} \quad (4.7)$$

$$X_3 = \left\{ \begin{pmatrix} x_1 & 0 & 0 & 0 \\ 0 & 0 & x_2 & 0 \\ 0 & 0 & x_1 & 0 \\ x_2 & 0 & 0 & 0 \end{pmatrix}, \begin{pmatrix} 0 & x_1 & 0 & 0 \\ 0 & 0 & 0 & x_2 \\ 0 & 0 & 0 & x_1 \\ 0 & x_2 & 0 & 0 \end{pmatrix} \right\} e^{j\theta_3} \quad (4.8)$$

$$X_4 = \left\{ \begin{pmatrix} x_1 & 0 & 0 & 0 \\ 0 & 0 & 0 & x_2 \\ 0 & 0 & x_1 & 0 \\ 0 & x_2 & 0 & 0 \end{pmatrix}, \begin{pmatrix} 0 & x_1 & 0 & 0 \\ 0 & 0 & x_2 & 0 \\ 0 & 0 & 0 & x_1 \\ x_2 & 0 & 0 & 0 \end{pmatrix} \right\} e^{j\theta_4} \quad (4.9)$$

where $\theta_1, \theta_2, \theta_3, \theta_4$ are the rotation angles provided to ensure that all the codebooks have become non-interfering. For any two different code word matrices, it can be verified using Equation (4.5) that the difference matrix is not

rank deficient and offers full diversity. The coding gain distance (CGD) for different error conditions are given below, in which x_k and \tilde{x}_k represent the possible transmitted and estimated symbols during time slots $k = 1, 2$.

- 1) When the transmitted matrix and the estimated matrix belong to the same codebook.

$$\text{CGD}_1 = |x_1 - \tilde{x}_1|^2 |x_2 - \tilde{x}_2|^2 \quad (4.10)$$

- 2) When they belong to the same codebook group

$$\text{CGD}_2 = |x_1|^2 |x_2|^2 + |\tilde{x}_1|^2 |\tilde{x}_2|^2 - 2\text{Re}(x_1 x_2 \tilde{x}_1^* \tilde{x}_2^*) \quad (4.11)$$

- 3) When they belong to different codebook group, in general

$$\text{CGD}_3 = A_1 A_2 ; \text{ where}$$

$$A_1 = k_1 - 2\text{Re}(x_1 \tilde{x}_1^* e^{j(\theta_k - \theta_l)})$$

$$A_2 = k_2 - 2\text{Re}(x_2 \tilde{x}_2^* e^{j(\theta_k - \theta_l)}) \quad (4.12)$$

$k_i = |x_i|^2 + |\tilde{x}_i|^2$, and $\text{Re}(\cdot)$ represents real part of its argument. The coding gain can be maximized by optimizing θ for different constellations (Xian and Liu, 2005). The optimum values for QPSK modulation as found by computer simulations are $e^{j\theta_1} = 1 + j0$; $e^{j\theta_2} = 0.9808 + j0.1950$; $e^{j\theta_3} = 0.4976 + j0.8674$; $e^{j\theta_4} = 0.8090 + j0.5878$. Two examples of coding are given in Table 4.3.

In example.1 of Table 4.3, since the first bit of stream2 is '1', the antenna group selected is A_ψ in the first time slot T1. The matrix corresponding to bit stream1 as obtained from Table 4.1 is $\begin{bmatrix} -1 & 0 \\ 0 & -1 \end{bmatrix}$. Since the first column of this, $\begin{bmatrix} -1 \\ 0 \end{bmatrix}$, belongs to B_ψ , antenna 2 of the group selected is used for sending the corresponding QPSK symbol. The other antenna group, ie. A_ϕ is selected for the second time slot. The antenna selected in that group is 1 since

the second bit of stream2 is '0'. The QPSK symbol corresponding to next two bits of stream2 is sent through this antenna. The code word thus formed, $\begin{pmatrix} 0 & 0 & 0 & x_1 \\ x_2 & 0 & 0 & 0 \end{pmatrix}$ belongs to X_2 and X_4 . The rotation angle is selected based on the information of the second column of the matrix. Here, since the second column of the matrix is just the inverted form of first column, θ_2 is selected. This can be compared with the rotation angle θ_4 selected in the second example, where the second column of the matrix is negative of the inverted form of the first column.

Table 4.3. WET-SM encoding examples

| | Example 1 | | Example 2 | |
|------------------------|--|---------------------|--|---------------------|
| | Bit Stream1 0100 | Bit Stream2 1010 | Bit Stream1 1001 | Bit Stream2 0101 |
| Time slot | T1 | T2 | T1 | T2 |
| Selected antenna group | A_ψ | A_ϕ | A_ϕ | A_ψ |
| Matrix | $\begin{bmatrix} -1 & 0 \\ 0 & -1 \end{bmatrix}$ | | $\begin{bmatrix} i & 0 \\ 0 & -i \end{bmatrix}$ | |
| Antenna in the group | 2 | 1 | 1 | 2 |
| Transmitted Matrix | $\begin{pmatrix} 0 & 0 & 0 & x_1 \\ x_2 & 0 & 0 & 0 \end{pmatrix} e^{j\theta_2}$ | | $\begin{pmatrix} x_1 & 0 & 0 & 0 \\ 0 & 0 & 0 & x_2 \end{pmatrix} e^{j\theta_4}$ | |

From the above examples, it can be seen that only one antenna will be active during each time slot and at the same time diversity of order two is achieved for stream1 since two channel responses are involved in determining the four bits of stream1.

The rate achievable in WET-SM is given by $\frac{1}{2}(\log_2[N_1]_{2^p} + \log_2[N_2]_{2^p} + \log_2 W + \log_2 K)$ where N_1 and N_2 are the number of antennas in group 1 and 2 respectively, W is the number of matrices in the Weyl group coset and K is the size of the constellation. The following Table 4.4 shows the rate enhancement in WET-SM compared to STBC-SM and SM-CIOD. The constellation assumed is QPSK and 8QAM. For both the cases, the rate

achieved by WET-SM is high compared to the STBC-SM and SM-CIOD. The rate is the same as that achieved by SM for antennas which are a power of two and in the other case, for example in the 12 antenna system, the rate is high compared to SM also.

Table 4.4. Rate comparison of WET-SM with STBC-SM, SM and SM-CIOD

| Number of antennas | Rate (bpcu) | | | | | | | |
|--------------------|-------------|------|---------|------|---------|------|------|------|
| | WET-SM | | STBC-SM | | SM-CIOD | | SM | |
| | QPSK | 8QAM | QPSK | 8QAM | QPSK | 8QAM | QPSK | 8QAM |
| 4 | 4 | 5 | 3 | 4 | 3 | 4 | 4 | 5 |
| 8 | 5 | 6 | 4 | 5 | 3.5 | 4.5 | 5 | 6 |
| 12 | 5.5 | 6.5 | 5 | 6 | - | - | 5 | 6 |
| 16 | 6 | 7 | 5 | 6 | 4 | 5 | 6 | 7 |

The scheme can be extended to any number of antenna elements with the grouping strategy given in Table 4.2. But, the constellation used depends on the bits encoded at a time in bitstream1. For encoding bits more than 4 and to use higher constellations, we can use Kronecker products of Weyl group matrices, which require more time slots. Alternatively, we can use a bit padding method that requires only two time slots as follows. For using 8QAM constellation, we can take blocks of 5 bits at a time, matrix encode the last four bits and prefix the first bit before constellation mapping. For example, consider that the bits to be transmitted are 01100. The matrix encoding of 1100 as seen from Table 4.1 is $\begin{bmatrix} -i & 0 \\ 0 & -i \end{bmatrix}$. The 8QAM symbol corresponding to first column of the matrix is obtained by prefixing '0', which is the first bit of the bit stream to be transmitted. The group information and antenna selection can then be done exactly as before. For the second time slot, in order to get diversity for the prefixed '0' also, the 8QAM conversion of the last two bits of stream 2 is to be done by prefixing '0' itself. This will result in reduced rate.

4.2.2 Detection

We assume the system model given in section 1.5 with N_t transmit antennas and N_r receiving antennas, perfect CSI at the receiver and a flat fading channel with quasi static path gains for the two time slots of transmission. The received signal can be expressed as

$$\mathbf{y} = \mathbf{H}\mathbf{x} + \mathbf{n} \quad (4.13)$$

where $\mathbf{y} = [y_1 \dots y_{N_r}]^T$ is the $N_r \times 1$ receive vector and $\mathbf{n} = [n_1 \dots n_{N_r}]^T$ represents the complex AWGN vector whose covariance matrix is $\sigma_n^2 \mathbf{I}$, and \mathbf{H} stands for the $N_r \times N_t$ channel matrix. As given in section 4.1, $\mathbf{x} = [0 \ 0 \ \dots \ x_q \ \dots \ 0]^T$ is the modulated transmit vector in SM, where x_q belongs to a complex constellation C of size K , depending on the modulation scheme selected.

The detection schemes in SM can be classified as optimal and suboptimal. The spatial constellation and signal constellation are not independent and in the optimal ML detection, (Jeganathan *et al.*, 2008), both the antenna and constellation indices are jointly estimated. The joint detection rule for single receive antenna is as follows.

$$(\hat{x}_l, \hat{h}_m) = \arg \min_{m,l} \|y - h_m x_l\|^2 \quad (4.14)$$

where x_l indicates the l^{th} constellation symbol and h_m the m^{th} antenna coefficient in the channel matrix and \hat{x}_l, \hat{h}_m represents the estimated values of the same. For applying this principle to WET-SM, consider the received signal in time slots T1 and T2

$$y_t = h_{m_t} x_{l_t} + n_t \quad ; t = 1,2 \quad (4.15)$$

where the subscript ' t ' indicates the time slot. In evaluating the antenna index

\hat{m}_1 and the transmitted symbol \hat{x}_{l_1} for time slot T1, the whole N_t antennas and the whole symbol points resulting from constellation rotation are to be considered. But, since the same group of antennas will not be utilized for the second time slot of transmission, and the constellation points should be in the same codebook, the decisions in the second time slot are done with the following constraint on index m_2 (assuming equal number of antennas in each group). $1 \leq m_2 \leq \frac{N_t}{2}$ or $\frac{N_t}{2} \leq m_2 \leq N_t$ according to the antenna group estimated in time slot T1, and the constellation symbol $\hat{x}_{l_2} \in X_k$, the code book estimated in T1.

The computational complexity is comparatively high for the above due to the exhaustive search and it can be reduced with the two step suboptimal decoding (Xu, 2012) given below, in which the antenna index and constellation point are detected separately.

Find the equalized symbols for each antenna and for each time period,

$$\begin{aligned} \tilde{x}_{e_1} &= \frac{h_m^\dagger y_1}{|h_m|^2} \text{ and } \tilde{x}_{e_2} = \frac{h_m^\dagger y_2}{|h_m|^2}. \text{ Then choose} \\ \hat{x}_{l_1} &= x_{l_1}, \hat{h}_{m_1} = h_{m_1} \text{ and } \hat{x}_{l_2} = x_{l_2}, \hat{h}_{m_2} = h_{m_2} \text{ such that} \\ (\hat{x}_{l_1}, \hat{h}_{m_1}) &= \arg \min d^2(x_{l_1}, \tilde{x}_{e_1}), \\ (\hat{x}_{l_2}, \hat{h}_{m_2}) &= \arg \min d^2(x_{l_2}, \tilde{x}_{e_2}) \end{aligned} \quad (4.16)$$

Here in WET-SM, the computations are to be done considering that $x_{l_1}, x_{l_2} \in X_k$, the same constellation group and the antennas $h_{m_1}, h_{m_2} \in A_k$, the same antenna group. From the antenna index and constellation index $(\hat{x}_{l_1}, \hat{h}_{m_1})$ estimated in the first time slot, we can find the first column of the code matrix. From \hat{x}_{l_2} , the symbol information for second time slot as well as the information regarding the second column of the matrix is deduced, and \hat{h}_{m_2} gives the second bit of bit stream2. The error in the estimation of the

second column of the matrix is minimal since it depends only on the constellation group of the estimated symbol in the second time slot and not on the exact symbol. Based on the look up table, inverse mapping is done then to convert the matrix into the original bit sequence.

4.3 COMPLEXITY ANALYSIS

First consider the computational complexity of optimum ML decoding rule in which the estimates for symbol and antenna index are found from Equation (4.14). In estimating the antenna index \hat{m}_1 for time slot T1, the whole N_t antennas are to be considered, and the constellation points are $4K$, due to constellation rotation. So, for the first time slot, The ML decoding complexity of this method in terms of the complex multiplications is $4N_tK$. For the second time slot, this will be $\binom{N_t}{2}(K)$, since the same group of antennas will not be utilized for the second time slot transmission, and the constellation points should be in the same codebook. This is less compared to the decoding complexity of STBC-SM, which is $2cK$ where c is the number of ways in which antenna selection is possible, given by $c = \left[\binom{N_t}{2} \right]_{2^p}$, p a positive integer and $c \geq N_t$. For SM-CIOD, low DoSM scheme is assumed, for which the minimum complexity of detection is $2N_tK$ where all the interleaved symbols are to be considered. In WET-SM, complexity can again be reduced if the suboptimal method as given by Equation (4.16) is employed. Here the complex multiplications are only for calculating the equalized symbols and is only $2N_t$. A comparison of the computational complexity (number of complex multiplications) of WET-SM with STBC-SM and SM-CIOD is given in Table 4.5. The comparison is made with number of antennas as a parameter, since complexity is more dependent on that. The constellation chosen is 8QAM for STBC-SM and SM-CIOD and QPSK for WET-SM, so as

to have the same rate of transmission. As the number of antennas increases, WET-SM is much better in complexity and in the forthcoming large scale MIMO scenario, this is beneficial.

Table 4.5 Computational complexity comparison of WET-SM, STBC-SM and SM-CIOD

| No. of Transmit Antennas (N_t) | SE (bpcu) | Computational Complexity | | |
|------------------------------------|-----------|--------------------------|---------|---------------------------|
| | | STBC-SM | SM-CIOD | Proposed WET-SM (Optimal) |
| 4 | 4 | 64 | 160 | 72 |
| 8 | 5 | 256 | 320 | 144 |
| 16 | 6 | 1024 | 640 | 288 |

4.4 PERFORMANC ANALYSIS

The performance of WET-SM is analysed in this section in terms of the upper bound on the BER probability and capacity behaviour.

4.4.1 BER Performance

The bit error rate of the system which transmits m bits over two consecutive symbol intervals is upper bounded by the union bound (Duman and Ghrayeb, 2007)

$$P_b \leq \frac{1}{2^m} \sum_{i=1}^{2^m} \sum_{j=1}^{2^m} \frac{P(X_i - X_j)n_{i,j}}{m} \quad (4.17)$$

Where $P(X_i - X_j)$ is the pairwise error probability that the matrix X_j is decided when the matrix X_i is transmitted and $n_{i,j}$ is the number of bits in error between the matrices X_i and X_j .

$$P(X_i - X_j) \leq \prod_{i=1}^{N_t} \left(\frac{1}{1 + \frac{E_x}{4N_0} \lambda_i} \right)^{N_r} \quad (4.18)$$

Where λ_i s are the eigen values of $(X_i - X_j)(X_i - X_j)^H$, E_x the symbol

energy and N_0 the noise power spectral density. For the proposed WET-SM, the number of bits in error in $X_i - X_j$ is calculated as follows.

$n_{i,j} = n_1 + n_2 + n_3$, where

$n_1 = \frac{1}{2} \left[\text{Ones} \left\{ (X_i)^1 - (X_j)^1 \right\} \right]$, where $\text{Ones}\{A\}$ represents the number of ones in matrix A and $(A)^1$ represents the operation of replacing all nonzero elements in A with 1. This gives the error bits in antenna selection.

$$n_2 = 1 ; \text{if } \text{par}_k \left\{ \text{XOR} \left((X_{i1})^1, (X_{j1})^1 \right) \right\} = 1, \text{ else } n_2 = 0 ,$$

where A_{i1} represents the first row of A_i , $\text{par}_k(A)$ represents the parity of k elements of A taken at a time where k is the number of antennas in a group and XOR represents the logical XOR operation. This gives the error bits in antenna group selection.

$\max(n_3) = 2$, which is the error bits due to the erroneous implicit information

The above theoretical error rate is compared with the actual error rate obtained for various modulation schemes in the simulation section.

4.4.2 Capacity Analysis

The capacity behavior of an $N_t \times N_r$ WET-SM system is analyzed here. Since the capacity is different for the two time slots of transmission for the proposed method, the capacity for each time slot (C1 and C2) is calculated and the average is taken. As can be seen from the system model presented in section 4.2.2, there are two independent input signal spaces, one being the transmitted symbol space X and the other the antenna index/channel signal space X_{ch} . The output signal space is Y . The mutual information between the input and output signal spaces is given by

$$I(X, X_{ch}; Y) = I(X; Y|X_{ch}) + I(X_{ch}; Y) \quad (4.19)$$

Since the selection of the antenna group and, within the group, the antenna selection are purely random, the capacity contribution of the second term in (4.19) for time slot T_1 is

$$C_{11} = \max_{p(x)} I(X_{ch}; Y) = \frac{1}{N_t} \sum_{i=1}^{N_t} \log_2(1 + \rho h_i^H h_i) \quad (4.20)$$

where ρ is the average received SNR (Biglieri *et al.*, 2007). Since $x \in X$ is iid complex Gaussian random variable with pdf given by

$$p(x) = \frac{1}{\pi \sigma_x^2} \exp\left(-\frac{|x|^2}{\sigma_x^2}\right) \quad (4.21)$$

the pdf of the received signal for a given selection of the transmit antenna is

$$p(y|x_{ch} = i) = \frac{1}{\pi \sigma_i^2} \exp\left(-\frac{|y|^2}{\sigma_i^2}\right) \quad (4.22)$$

where $\sigma_i^2 = (h_i^H h_i) \sigma_x^2 + \sigma_N^2$; ($i = 1, 2, \dots, N_t$). The average pdf of the received signal is

$$p(y) = \frac{1}{N_t} \sum_{i=1}^{N_t} \frac{1}{\pi \sigma_i^2} \exp\left(-\frac{|y|^2}{\sigma_i^2}\right) \quad (4.23)$$

and the capacity of the first term in (4.19) for T_1 is given by

$$C_{12} = \max_{p(x)} I(X; Y|X_{ch}) = \frac{1}{N_t} \sum_{i=1}^{N_t} \left[\int_{\mathcal{Y}} p(y|x_{ch}=i) \log_2 \left(\frac{p(y|x_{ch}=i)}{p(y)} \right) dy \right] \quad (4.24)$$

So, the capacity for the first time slot is $C_1 = C_{11} + C_{12}$. For the second time slot, only half number of antennas are involved (assuming equal number of antennas in each group), and the capacity contribution of the second term in (4.19) for time slot T_2 is calculated with only half the number of antennas.

$$C_{21} = \frac{1}{N_t/2} \sum_{j=1, j \neq i}^{N_t/2} \log_2(1 + \rho h_j^H h_j) \quad (4.25)$$

Similarly, the capacity due to the first term in (4.19) for T_2 is

$$C_{22} = \frac{1}{N_{t/2}} \sum_{j=1}^{N_{t/2}} \left[\int_{\mathcal{Y}} p(y|x_{ch=i}) \log_2 \left(\frac{p(y|x_{ch=i})}{p(y)} \right) dy \right] \quad (4.26)$$

Since the signal in the second time slot conveys information about the bit stream1 also, there is a capacity contribution due to this implicit information, which is given by

$$C_{23} = \frac{1}{N_{t/2}} \sum_{j=1}^{N_{t/2}} \left[\int_{\mathcal{Y}} p(y|x_{ch=i}) \log_2 \left(\frac{p(y|x_{ch=i})}{p(y)} \right) dy \right] \quad (4.27)$$

So, the capacity for the second time slot is $C_2 = C_{21} + C_{22} + C_{23}$. The total capacity per time slot is given by the average of C_1 and C_2 . Due to the third term in C_2 , there is a capacity increase in this method without increasing the number of antennas or the constellation size.

4.5 SIMULATION RESULTS

In this section, we present simulation results and compare the performance of the proposed method with STBC and CIOD based transmit diversity schemes in SM-MIMO. We assume perfect CSI at the receiver and a flat Rayleigh fading channel with quasi static path gains for the two time slots of transmission and AWGN. The theoretical upper bound is compared with the actual simulation results of the proposed system. The bit error rate, capacity and computational complexity of the system are compared with that of STBC-SM and SM-CIOD.

4.5.1 Performance

The theoretical upper bound on BER is calculated in section 4.4.1 and the same is compared with simulation in Figure 4.2. The comparison is done for $N_t = 4$ and $N_r = 1$, with QPSK and 8-PSK constellations. The difference

between analytical results and simulation studies is negligible for almost all values of SNR. This validates the theoretical analysis given in Section 4.4.1

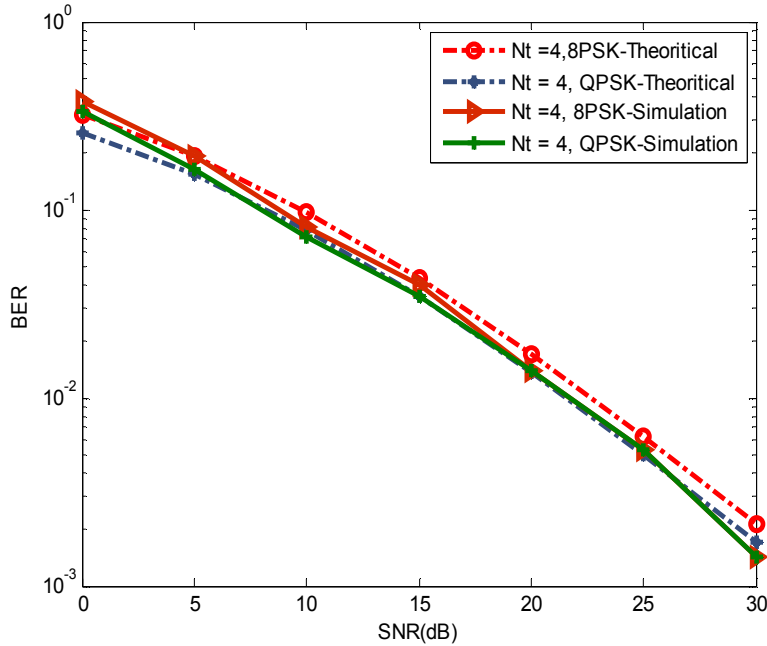


Fig. 4.2 Theoretical and simulated BER Vs. SNR curves for WET-SM

Next we compare the BER performance of the proposed WET-SM system with the standard SM, and diversity schemes STBC-SM and SM-CIOD, in Figure 4.3. As explained, the simulation is done with four transmit antennas and QPSK constellation for both the data streams, which is suitable for the 4 bit mapping in WET-SM system. With these conditions, the rate achieved by WET-SM is 4bps/Hz and for the same rate, STBC-SM and SM-CIOD uses 8 QAM. For SM, to achieve the same rate, QPSK constellation is enough.

It can be seen from the $N_r = 1$ curves of SM and WET-SM that the bit error rate of WET-SM is much better compared to the performance of SM, which is having no diversity. Even at an error rate of 10^{-2} , the SNR gain is around 5dB. WET-SM, $N_r = 1$ achieves the performance of SM-CIOD with

$N_r = 2$. With two receive antennas, the SNR gain compared with SM-CIOD is more than 5dB for high error rates, and the difference increases as the error rate lowers. Compared with the two antenna activated STBC-SM, $N_r = 2$, the performance is better at low SNR values, and is almost the same at higher values of SNR.

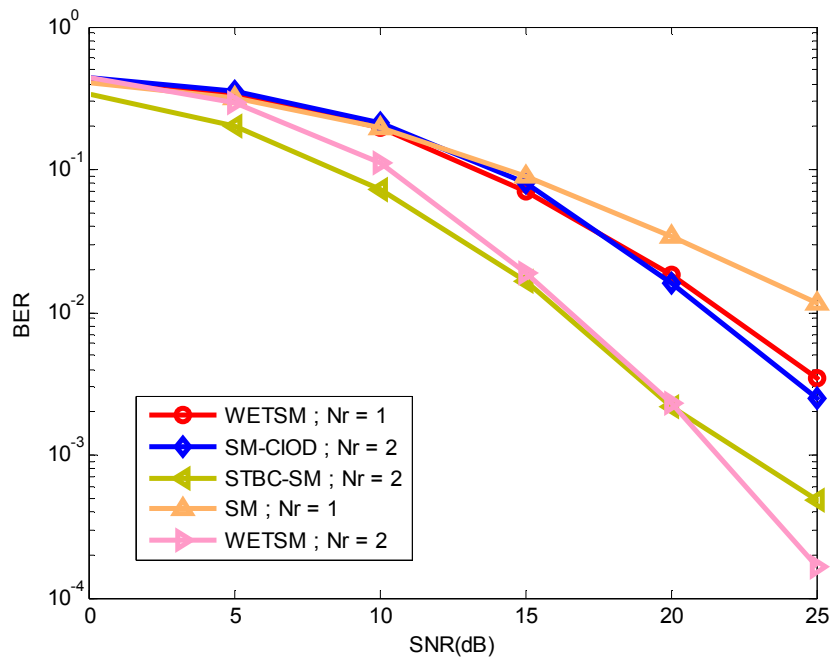


Fig. 4.3. BER Vs. SNR curves for WET-SM, STBC-SM and SM-CIOD

Figure 4.4 is based on the capacity analysis presented in Section 4.4.2, where the average capacity for the two time slots is plotted assuming $N_t = 4$. Since there is no antenna selection in the second time slot in STBC-SM, its capacity is less. Due to the information conveyed by the antenna selection in T2, WET-SM and SM-CIOD have higher capacity. Since there is information conveyed by the data stream2 about data stream1, the capacity of the WET-SM

is much higher. The difference in capacity achieved by WET-SM compared to the other two schemes increases as SNR increases.

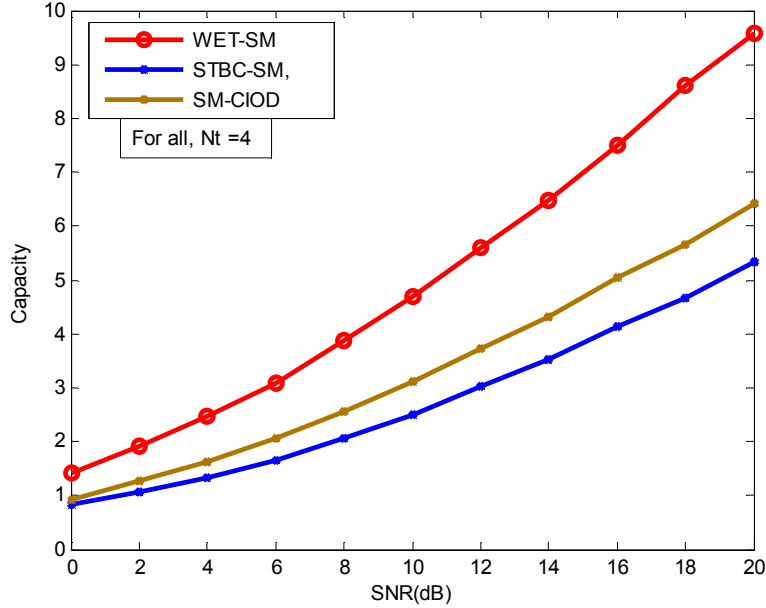


Fig. 4.4. Capacity Vs. SNR curves for WET-SM, STBC-SM and SM-CIOD

4.5.2 Computational Complexity

The large computational complexity as the number of antennas increases is the main drawback of the systems that have ML decodability. For the proposed WET-SM, this increase is very less. As explained in Section 4.3, the ML decoding complexity of the proposed WET-SM method in terms of the complex multiplications is $4N_tK + \left(\frac{N_t}{2}\right)(K)$ where N_t is the number of transmit antennas and K is the constellation size. The two terms correspond to the first and second time slots respectively. This is less compared to the decoding complexity of STBC-SM, which is $2cK$, where $c \geq N_t$. The simulation assumes QPSK for WET-SM and 8QAM for STBC-SM and SM-CIOD, which provides the same transmission rate for all the schemes. As the

number of antennas increases, there is a large increase in computations for STBC-SM compared to WET-SM, and SM-CIOD also shows high values, as is clear from Figure 4.5

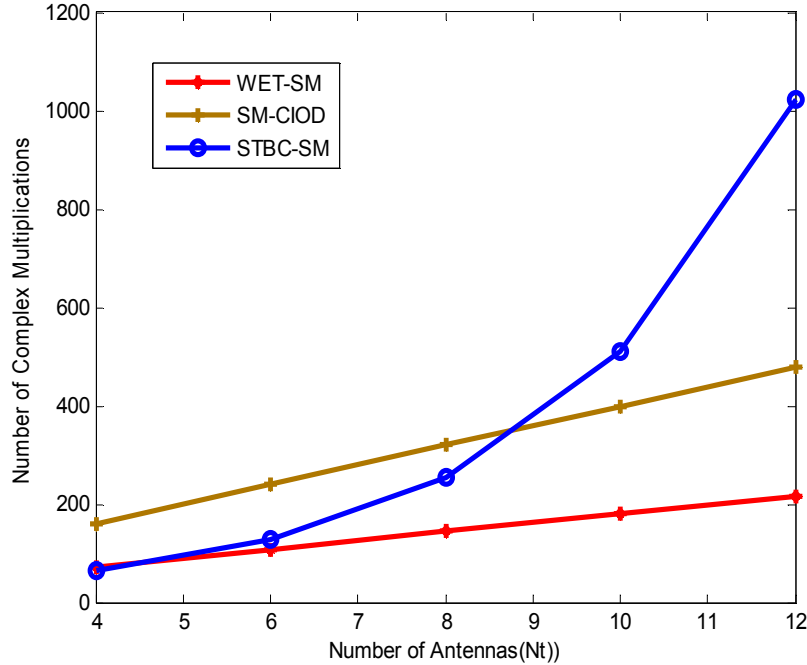


Fig. 4.5. Computational complexity comparison of WET-SM, STBC-SM and SM-CIOD

4.6 CONCLUSIONS

In this chapter, we proposed a single antenna activated transmission method for transmit diversity in spatial modulation based on Weyl group encoding. The method, named as WET-SM achieves second order transmit diversity and a higher rate that depends on the number of transmit antennas, the number of matrices in the Weyl group coset and the size of the constellation. For example, the method is capable of transmitting 4bpcu in one

time slot, whereas with the same number of transmit antennas and constellation size, the rate is only 3bpcu for SM-STBC and CIOD based schemes. WET-SM is shown to be capable of achieving better performance compared to standard SM scheme, STBC-SM and CIOD based schemes, considering the active antenna elements and required computations. The precoding required is the disadvantage, but it offers the simplicity of single stream ML decoding. The increase in computational complexity as the number of antenna elements is increased is found to be very less. Therefore, the proposed WET-SM system, with its feasibility to adaptive transmission is a good choice for effective transmit diversity in SM, especially in large scale MIMO. The system can be extended for encoding more number of bits at a time, utilizing the Kronecker product of the Weyl group matrices.

Chapter

5 A RATE CONFIGURABLE TRANSMIT DIVERSITY TECHNIQUE IN GENERALIZED SPATIAL MODULATION SYSTEM

Spatial modulation alleviates the inherent problems of conventional MIMO such as inter antenna synchronisation requirement and inter channel interference by activating only one antenna at each time instant. (Mesleh *et al.*, 2008). Even though the antenna index as well as the PSK/QAM symbol transmitted conveys information, the rate compared to spatial multiplexing is less. There is no possibility for implementing transmit diversity and/or spectral /energy efficiency trade off and the total number of antennas is restricted to a power of two. GSM is a scheme proposed by Younis *et al.* (2011), which removes these restrictions by activating more than one transmit antenna during each time slot. Incorporating transmit diversity is possible in GSM, but the distinctive methods employed for decoding diversity schemes necessitates separation of the diversity layer from the other during detection and increases the detection complexity. Another problem in GSM is the receiver design complexity, due to the requirement of jointly decoding spatial constellation and signal constellation and the large number of possible antenna combinations that are to be considered for this. Most of the decoders reported has the restriction that the number of receiving antennas (N_r) has to be at least the same as the total number of transmit antennas (N_t), and the detection complexity increases proportionally. Considering these issues of diversity, detection complexity and the restriction on the number of receive antennas, we

propose a method to incorporate diversity in GSM. The proposed method named as diversity embedded SM (DESM) provides diversity and a fair transmission rate without imposing any restriction on the number of active antennas. The low complexity detection method proposed performs well with only four receive antennas and negligible feedback overhead.

5.1 INTRODUCTION

We consider a GSM MIMO system with N_t transmit antennas in which only N_a antennas are active at a time and N_r receiving antennas, represented by (N_t, N_a, N_r) . A high value of N_a will provide high multiplexing gain but increased complexity of decoding and performance loss due to ICI impose a practical limitation on N_a . Receiving antennas required depends on the detection method employed.

The encoding of information bit sequence in GSM is as follows. The input bits are split into blocks of $\log_2(N_c K^{N_a})$ prior to transmission where N_c is the number of valid active antenna combinations given by $\left[\binom{N_t}{N_a} \right]_{2^p}$, and K is the size of the constellation. In each block, $\log_2(N_c)$ bits are used to select the N_a active antennas. Remaining $N_a \log_2 K$ bits of the block are mapped to N_a constellation symbols by taking $\log_2 K$ bits at a time and sent through N_a active antennas. For example, in a (6, 3, 4) GSM system, three antennas will be active during each time slot which can be selected from the 6 available antennas in $N_c = \left[\binom{6}{3} \right]_{2^p} = 16$ ways and hence the antenna selection bits are $\log_2(16) = 4$. Assuming a constellation size of $K = 4$, the information bit sequence is split into blocks of $\log_2(16 \times 4^3) = 10$ bits. The first four bits are used for selecting the three active antennas and the next 6 bits are mapped to QPSK constellation symbols taking two bits at a time and sent through these

selected antennas. The structure of the transmitted complex vector \mathbf{x} with N_t elements is as follows.

$$\mathbf{x} = [0 \ 0 \dots x_1 \ 0 \ 0 \dots x_2 \ 0 \ 0 \dots x_{N_a} \ 0 \ 0 \dots]^T$$

$\uparrow \qquad \qquad \uparrow \qquad \qquad \uparrow$

active antenna positions

where $x_1, x_2, \dots, x_{N_a} \in \mathcal{C}$ represents the complex scalar PSK/QAM modulated symbol in the constellation chosen. Thus the transmit signal vector \mathbf{x} in GSM has $N_t - N_a$ zero entries and N_a non zero entry corresponding to the active antennas.

Since more than one antennas are active during a time slot, transmit diversity can be implemented in GSM. For example, as explained in Section 4.1, STBC-SM (Basar *et al.*, 2010) achieves diversity by transmitting STBCs through the antennas selected using spatial constellation diagram, but all the active antennas are used for STBC transmission and suffer from low multiplexing gain and resulting rate loss. In the next section, we explain the proposed DESM system that combines space time coding and spatial multiplexing in GSM to achieve reasonable rate, reliability and energy efficiency.

5.2 PROPOSED METHOD OF CODING

Consider a GSM system represented by (N_t, N_a, N_r) model in Section 5.1. In the proposed DESM system, the data to be transmitted consists of a high priority data stream for which a specific quality of service is to be ensured and a low priority data stream. The proposed DESM ensures the specific QoS for the high priority data stream using transmit diversity and by spatial multiplexing the low priority data along with this, a fair data rate is maintained. In a general scenario, it is not necessary that the same constellation should be used for high and low priority data (all sub channels), but here we presume the same constellation of size K .

5.2.1 Encoding

Figure 5.1 illustrates encoding in the DESM system. The high priority data stream is encoded using the Alamouti scheme, assuming second order transmit diversity is enough for ensuring high reliability/ required QoS. For transmitting this high priority data, which we call the diversity stream, two best channels are selected based on the CSI feedback. As mentioned, feeding back the antenna indices of two channels introduces very low feedback overhead and at the same time improves the performance of the system. If x_1 and x_2 are the constellation symbols corresponding to consecutive $\log_2 K$ bits of the high priority data, during the first time slot, x_1 and x_2 are sent through these fixed antennas, and during the second time slot, $-x_2^*$ and x_1^* are sent as in Alamouti scheme.

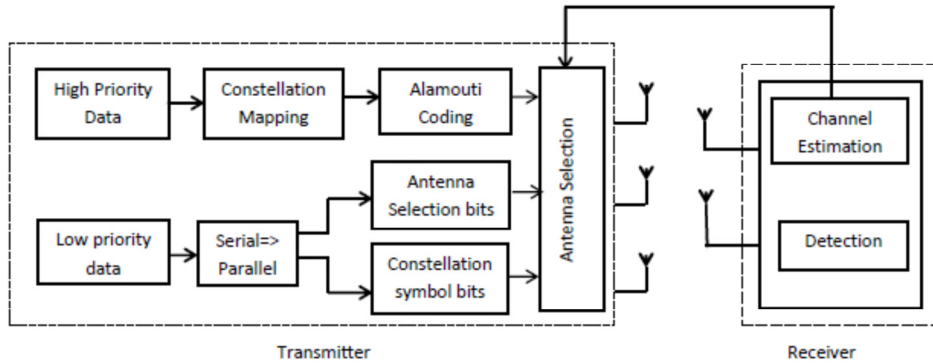


Fig. 5.1. Block diagram of DESM system

The low priority data, called the non-diversity stream, is sent along with this Alamouti coded data in a spatial multiplexing manner to increase the overall rate. Since two antennas are prefixed for high priority data, only $N'_a = N_a - 2$ antennas are available for this, which are to be selected from $N'_t = N_t - 2$ antennas randomly during a time slot. So, the antenna selection

bits are $L_1 = \log_2 N'_c$, where $N'_c = \left\lfloor \binom{N'_t}{N'_a} \right\rfloor_{2^p}$. With a constellation size of K , $L_2 = N'_a \log_2 K$ bits can be sent through these N'_a antennas during a time slot. So, the low priority data is split into blocks of $L_1 + L_2$ bits and during each time slot, L_1 bits select antennas for sending the symbols corresponding to next L_2 bits, simultaneously through the Alamouti coded data. This low priority data sent during each time slot ensures a high rate in DESM.

The DESM system achieves second order transmit diversity for the Alamouti coded high priority data irrespective of the spatial multiplexing employed. Let \mathbf{d} and \mathbf{n} denote the message vectors composed of symbols transmitted from diversity stream layer D and non-diversity stream layer N respectively. In the code words formed as $X_k = X_d + X_n$, symbols from layer D achieves a transmit diversity order v as given below, irrespective of the symbols transmitted from layer N (Diggavi *et al.*, 2008)

$$v = \min_{\substack{d_1 \neq d_2 \in D \\ n_1, n_2 \in N}} \text{rank} \left\{ (X_p - X_q)(X_p - X_q)^H \right\} \quad (5.1)$$

where X_p and X_q are two different code words.

To find the diversity order of DESM, we assume a three antenna activated system so that only one antenna is selected during each time slot to send the non-diversity stream, but the result can be extended to more number of antennas. As the non-fixed antenna selection is independent during each time slot and the diversity stream detection is performed with the received signals during two consecutive time slots (as will be illustrated in Section 5.2.2), the possible codebooks can be represented as follows.

$$X_1 = \begin{pmatrix} x_1 & x_2 & \mathbf{0} & x_3 & \mathbf{0} \\ -x_2^* & x_1^* & \mathbf{0} & x_4 & \mathbf{0} \end{pmatrix} \quad (5.2)$$

$$X_2 = \begin{pmatrix} x_1 & x_2 & \mathbf{0} & x_3 & \mathbf{0} \\ -x_2^* & x_1^* & x_4 & \mathbf{0} & \mathbf{0} \end{pmatrix} \quad (5.3)$$

where x_1 and x_2 represent the Alamouti coded symbols and x_3 and x_4 are the spatial multiplexing data sent along with this during first and second time slots respectively. The symbols x_3 and x_4 sent during the two consecutive time slots can be through the same antenna as given in codebook1 and through different antennas as shown in codebook2. The boldface $\mathbf{0}$ represents the row vector of inactive antennas.

In the case of diversity stream, the difference in code words is due to difference in symbols only, since the antennas are fixed. But, in the case of low priority data, since the antenna index and the symbols convey information, the difference in code words can be due to both. So, the difference matrix in general is

$$\begin{aligned} X_D = (X_p - X_q) &= \begin{pmatrix} x_1 - \hat{x}_1 & x_2 - \hat{x}_2 & x_3 & \mathbf{0} & -\hat{x}_3 & \mathbf{0} \\ -x_2^* + \hat{x}_2^* & x_1^* - \hat{x}_1^* & \mathbf{0} & x_4 & \mathbf{0} & -\hat{x}_4 \end{pmatrix} \\ &= \begin{pmatrix} e_1 & e_2 & e_3 & \mathbf{0} & e_3' & \mathbf{0} \\ -e_2^* & e_1^* & \mathbf{0} & e_4 & \mathbf{0} & e_4' \end{pmatrix} \end{aligned} \quad (5.4)$$

where $e_k, e_k' = x_k - \hat{x}_k$ in general and for $x_k \in X_n$, it can also be x_k or $-\hat{x}_k$.

$$X_D X_D^H = \begin{bmatrix} |e_1|^2 + |e_2|^2 + |e_3|^2 + |e_3'|^2 & 0 \\ 0 & |e_2|^2 + |e_1|^2 + |e_4|^2 + |e_4'|^2 \end{bmatrix} \quad (5.5)$$

As per Equation (5.1), e_1 and e_2 cannot be zero simultaneously, and hence for any value of e_3, e_4, e_3' , and e_4' , the determinant of the above matrix is of degree two and hence second order diversity is achieved. The same can be proved for special cases of difference due to antenna index or due to symbol error.

The rate achieved by DESM is $(\log_2 K + \log_2 N'_c + N'_a \log_2 K)$ bpcu where as that of STBC-SM is $\frac{1}{2} \log_2 c + \log_2 K$, where $c = \left[\binom{N_t}{2} \right]_{2^p}$ (Basar *et al.*, 2011). Though c is higher compared to $N'_c = \left[\binom{N'_t}{N'_a} \right]_{2^p}$, the rate achieved by DESM is much higher due to the $N'_a \log_2 K$ factor. Since only STBC codes are transmitted in STBC-SM, there is a restriction on the number of active antennas whereas in DESM, we have relaxation in the antenna constraint, i.e. any number greater than two and less than N_t is allowed in DESM. Compared to GSM, which is having a rate of $\log_2 N_c + N_a \log_2 K$ bpcu, rate of DESM is lower since $N'_c < N_c$, and $N'_a < N_a$. As will be shown in simulation section, the percentage reduction, compared to the rate of transmission is affordable. Also, the BER performance of DESM is much better compared to both STBC-SM and GSM due to the fact that two fixed antennas are used for diversity stream transmission. Another advantage of DESM is that the system can be configured in various ways, as will be illustrated in simulation results.

5.2.2 Decoding

The received signal is given by $\mathbf{y} = \mathbf{H}\mathbf{x} + \mathbf{n}$, where \mathbf{y} and \mathbf{n} are the $N_r \times 1$ receive and AWGN vectors respectively. \mathbf{H} is the $N_r \times N_t$ channel matrix, the entries of which are iid complex Gaussian random variables with zero mean and variance σ_n^2 . The transmitted signal vector \mathbf{x} has the structure given Section 5.1, with N_a non zero entry corresponding to the active antennas and $N_t - N_a$ zero entries corresponding to idle antennas. We assume Rayleigh channel under block fading condition, so that the channel remains constant for the two time slots of transmission of diversity stream. We assume perfect CSI at the receiver and partial CSIT, with a limited feedback

channel that transmits the indices of the two antennas with best fading characteristics.

The proposed detection method is based on QR decomposition of the \mathbf{H} matrix. The low priority data is detected first, and its interference is cancelled from the received signal and then the high priority data is detected. The active antenna selection method explained in Section 5.2.1 makes it possible to arrange the \mathbf{H} matrix of this system in such a way that the resulting Q and R factors reduce the computational complexity much. In a DESM system with N_t transmit antennas N_r receive antennas and N_a active antennas, if $N_t \geq N_r + N_a - 2$, a condition that is easy to fulfill, the computational complexity of DESM is very less compared to the other GSM detection methods in literature. This detection method requires only four receive antennas to achieve good BER performance whereas most of the detection schemes require $N_r = N_t$. Moreover, receive diversity can be utilized for low priority data detection, even though it is the first layer detected, which is not possible in conventional SIC methods. The high priority data detection is made free from any interference of the low priority data without affecting the orthogonality of the \mathbf{H} matrix. These aspects of DESM detection are explained in detail in the following paragraphs.

As already explained in Chapters 3 and 4, the optimum detection is the maximum likelihood criteria. In GSM, all possible candidate vectors within the constellation set K and all possible antenna combinations are to be considered to find the minimum distance metric as per the ML rule $\hat{\mathbf{x}} = \arg.\min_{\mathbf{x} \in K} \|\mathbf{y} - \mathbf{H}\mathbf{x}\|^2$. The principle of QR decomposition already explained in Section 3.1 changes estimation criteria to

$$\hat{\mathbf{x}} = \arg.\min_{\mathbf{x} \in C} \|\tilde{\mathbf{y}} - \mathbf{R}\mathbf{x}\|^2 \quad (5.6)$$

$\tilde{\mathbf{y}} = \mathbf{Q}^H \mathbf{y}$ is the transformed receive vector. The summation term of Equation (5.6) can be re-written in a recursive form as follows.

$$\|\tilde{\mathbf{y}} - \mathbf{R}\mathbf{x}\|^2 = \sum_{i=1}^{N_t} |\tilde{y}_i - \sum_{j=i}^{N_t} r_{ij} x_j|^2 \quad (5.7)$$

where \tilde{y}_i represents the i^{th} element of vector $\tilde{\mathbf{y}}$, r_{ij} denotes the $(i,j)^{\text{th}}$ element of the matrix \mathbf{R} , and x_j is the j^{th} element of vector \mathbf{x} . Equation (5.7) can be represented by a tree structure with $N_t + 1$ levels, and each node in the tree contains K child nodes. Therefore the ML solution can be acquired by finding the path with smallest path metric in the tree constructed by Equation (5.7). Figure 5.2 shows the detection process in DESM, based on the above principle.

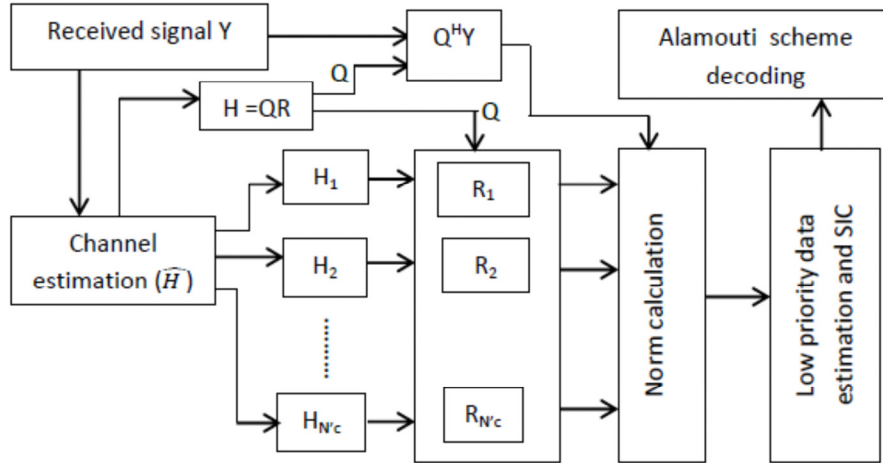


Fig. 5.2. Detection method of DESM

The complete detection requires received signals in two consecutive time slots due to the Alamouti coding used. During each time slot, the antenna indices of low priority data stream, along with the symbols is detected first. Then the interference of this data is cancelled from the received signal to form the detection matrix of high priority data. As stated in Section 5.2.1, most

favorable channels are utilized for sending the Alamouti code and the receiver with full CSI arranges the \mathbf{H} matrix according to the descending order of the column norms, as given below.

$$\mathbf{H} = [\mathbf{h}_1 \ \mathbf{h}_2 \ \mathbf{h}_3 \ \dots \ \mathbf{h}_{N_t}] \quad (5.8)$$

where \mathbf{h}_k , $k = 1, 2, \dots, N_t$ denote the $N_r \times 1$ channel vectors and $\|\mathbf{h}_1\| > \|\mathbf{h}_2\| > \|\mathbf{h}_3\| \dots > \|\mathbf{h}_{N_t}\|$. The following arbitrary \mathbf{H} matrices given by

$$\mathbf{H}_k = [\mathbf{h}_1 \ \mathbf{h}_2 \ \mathbf{0}_{N_r \times N_i} \ \mathbf{h}_{C_k}] \quad (5.9)$$

are formed then, where $N_i = N_t - N_a$ is the number of idle channels and \mathbf{h}_{C_k} is the $N_r \times N'_a$ matrix formed by k^{th} permitted combination of non-fixed antenna responses. For example, with $N_t = 6$ and $N_a = 4$, the number of permitted antenna combinations is $N'_c = \left[\binom{N_t}{N'_a} \right]_{2^p} = 4$ and let it be (3,4), (5,6), (3,5) and (4,6). Then,

$$\mathbf{H}_1 = [\mathbf{h}_1 \ \mathbf{h}_2 \ \mathbf{0} \ \mathbf{0} \ \mathbf{h}_3 \ \mathbf{h}_4]$$

$$\mathbf{H}_2 = [\mathbf{h}_1 \ \mathbf{h}_2 \ \mathbf{0} \ \mathbf{0} \ \mathbf{h}_5 \ \mathbf{h}_6]$$

$$\mathbf{H}_3 = [\mathbf{h}_1 \ \mathbf{h}_2 \ \mathbf{0} \ \mathbf{0} \ \mathbf{h}_3 \ \mathbf{h}_5]$$

$$\mathbf{H}_4 = [\mathbf{h}_1 \ \mathbf{h}_2 \ \mathbf{0} \ \mathbf{0} \ \mathbf{h}_4 \ \mathbf{h}_6]$$

QR decomposition of these matrices are formed then, whereby we get,

$$\mathbf{H}_k = \mathbf{Q}_k \mathbf{R}_k \quad (5.10)$$

The all zero columns of the \mathbf{H}_k s are retained in QR decomposition because if the number of columns $\geq N_r + N_a - 2$, the QR decomposition will have the peculiarity that all the \mathbf{Q}_k will be the same and the \mathbf{R}_k s differ only in the last $N_a - 2$ columns. This factor reduces the computational overhead in forming N'_c QR decompositions. If $N_t > N_r + N_a - 2$, then we

have to retain only $N_r + N_a - 2$ columns in \mathbf{H}_k s to make \mathbf{Q}_k the same, and extra all zero columns are omitted.

By exploiting the above feature, the computation required in solving Equation (5.6) is minimized as follows. Since the antenna indices of the low priority data are unknown, to solve the Equation (5.6), we have to pre-multiply the received signal \mathbf{y} with N'_c possible values of \mathbf{Q}_k^H to find the \mathbf{H}_k that gives the minimum metric. This will be a computational overhead in general, but in the DESM system, $\mathbf{Q}_1 = \mathbf{Q}_2 = \dots = \mathbf{Q}_k = \mathbf{Q}$, and hence this computation is to be performed only once, giving

$$\tilde{\mathbf{y}} = \mathbf{Q}^H \mathbf{y} = \mathbf{Q}^H \mathbf{Q} \mathbf{R}_k \mathbf{x}_k + \tilde{\mathbf{n}} \quad (5.11)$$

where $k = 1, 2, \dots, N'_c$, and $\tilde{\mathbf{n}} = \mathbf{Q}^H \mathbf{n}$

In all the QR decompositions, $\mathbf{Q}^H \mathbf{Q} = \mathbf{I}$ and the above equation reduces to

$$\tilde{\mathbf{y}} = \mathbf{R}_k \mathbf{x}_k + \tilde{\mathbf{n}} \quad (5.12)$$

where $\mathbf{R}_k = \begin{bmatrix} r_1 & r_2 & \mathbf{0} & \mathbf{0} & \dots & r_{k_1} & r_{k_{N_a-2}} \end{bmatrix}$.

\mathbf{H}_k is not a square matrix always because in DESM we can have $N_r < N_t$ and some all zero columns are deleted from \mathbf{H} to form \mathbf{H}_k . So, \mathbf{R}_k is not a truly upper triangular matrix. The last $N_a - 2$ columns will have full non zero entries and the remaining \mathbf{R}' is an $N_r \times N_r$ upper triangular matrix with $N_r - 2$ all zero columns. $\mathbf{x}_k = \begin{bmatrix} x_1 & x_2 & 0 & 0 & \dots & x_{k_1} & \dots & x_{k_{N_a-2}} \end{bmatrix}^T$ is the modulated signal vector of length $N_r + N_a - 2$ in which x_1 and x_2 represent the high priority data sent with Alamouti coding and $x_{k_1} \dots x_{k_{N_a-2}}$ represent the low priority data sent along with this. It is clear from the above structure of \mathbf{R}_k that $x_{k_1} \dots x_{k_{N_a-2}}$ will not have any interference from x_1 and x_2 .

Considering the above structure of \mathbf{R}_k , the detection metric in Equation (5.7) can be modified as $\sum_{i=1}^{N_r} |\tilde{y}_i - \sum_{j=i}^{N_o} r_{ij} x_j|^2$ where $N_o = N_r + N_a - 2$ is the optimum number of columns retained. This is a tree structure with N_r levels, and as in normal QR based detection, the solution starts from the last level with $i = N_r$. But, in DESM, in general, (for $N_t > N_r$) the last two levels starts with $j = N_r + 1$. The two levels with $i = N_r$ and $N_r - 1$ are free from interference of x_1 and x_2 and is used here for detecting all low priority data symbols $x_{k_1} \dots \dots x_{k_{N_a-2}}$ using ML rule. For the above example, with $N_r = 4$, the last (fourth) level solution is from $\|y_4 - r_{45}x_3 - r_{46}x_4\|^2$ and the third level, given by $\|y_3 - r_{35}x_3 - r_{36}x_4\|^2$ is also utilized for increased reliability. The same process is repeated for all the \mathbf{R}_k s, the minimum metric is found, and the corresponding \mathbf{R}_k and \mathbf{x}_k gives active antenna index \hat{h}_k and symbols sent.

Compared to the sphere decoding method in GSM (Cal-Braz and Sampaio- Neto, 2014), null symbol is avoided since only valid antenna combinations are used. Computation overhead in calculating the ML metric corresponding to all the \mathbf{R}_k s is very less since only $N_a - 2$ columns of the \mathbf{R}_k s are different. ML detection here makes pre-calculation and storing of $r_{ij} x_j$ s for a frame duration and only the summation and squaring operation is to be performed every time slot, whereas it is not possible in sphere decoding and QRD-M (Kim and Yue, 2002). A more detailed explanation is given in Section 5.3.

After computing $N_a - 2$ valid antennas and the corresponding symbols, the interference due to these terms are cancelled from \mathbf{y} to form the matrix corresponding to the Alamouti code.

$$\tilde{\mathbf{y}} = [\mathbf{h}_1 \quad \mathbf{h}_2] \begin{bmatrix} x_1 \\ x_2 \end{bmatrix} + [\tilde{\mathbf{n}}] \quad (5.13)$$

Multiplying the above equation with $[\mathbf{h}_1 \quad \mathbf{h}_2]^H$ on both sides,

$$\begin{bmatrix} \check{y}_1 \\ \check{y}_2 \end{bmatrix} = (|\mathbf{h}_1|^2 + |\mathbf{h}_2|^2) \begin{bmatrix} x_1 \\ x_2 \end{bmatrix} + \begin{bmatrix} \check{n}_1 \\ \check{n}_2 \end{bmatrix} \quad (5.14)$$

This makes the detection of x_1 and x_2 independent and ML solution can be found (Alamouti,1998).

The following examples illustrate two typical cases. One is a small antenna system with $N_a = 3$ and $N_t = 4$, used in indoor communication and the other is for downlink in mobile scenario, where the base station is equipped with large number of transmit antennas. For small systems, the condition $N_t \geq N_r + N_a - 2$ is not satisfied and hence \mathbf{Q}_k s will be different. The second example shows how the detection is done with minimum columns of \mathbf{R} , when there are a large number of transmit antennas.

1) $N_t = N_r = 4, N_a = 3$

$$\mathbf{H}_1 = [\mathbf{h}_1 \ \mathbf{h}_2 \ \mathbf{0} \ \mathbf{h}_4] ; \mathbf{H}_2 = [\mathbf{h}_1 \ \mathbf{h}_2 \ \mathbf{0} \ \mathbf{h}_3]$$

where $\mathbf{h}_1, \mathbf{h}_2, \mathbf{h}_3$ and \mathbf{h}_4 are 4×1 vectors.

$$\mathbf{H}_k = \mathbf{Q}_k \mathbf{R}_k ; k = 1, 2$$

Here $\mathbf{Q}_1 \neq \mathbf{Q}_2$ since the condition $N_t > N_r + N_a - 2$ is not satisfied. This will not impose much computational complexity since only two \mathbf{Q}_k s are to be found and the computations are for two antenna combinations.

$$\mathbf{y} = \mathbf{H}_1 \mathbf{x}_1 = \mathbf{Q}_1 \mathbf{R}_1 \mathbf{x}_1 \text{ where } \mathbf{x}_1 = [x_1 \ x_2 \ 0 \ x_4]^T, x_k \in \mathcal{C} \quad (5.15)$$

$$\check{\mathbf{y}}_1 = \mathbf{Q}_1^H \mathbf{y} = \mathbf{Q}_1^H \mathbf{Q}_1 \mathbf{R}_1 \mathbf{x}_1 + \mathbf{Q}_1^H \mathbf{n} = \mathbf{R}_1 \mathbf{x}_1 + \check{\mathbf{n}}_1 \quad (5.16)$$

$$ie \begin{bmatrix} \check{y}_1^1 \\ \check{y}_2^1 \\ \check{y}_3^1 \\ \check{y}_4^1 \end{bmatrix} = \begin{bmatrix} r_{11} & r_{12} & 0 & r_{14}^{(1)} \\ 0 & r_{22} & 0 & r_{24}^{(1)} \\ 0 & 0 & 0 & r_{34}^{(1)} \\ 0 & 0 & 0 & r_{44}^{(1)} \end{bmatrix} \begin{bmatrix} x_1 \\ x_2 \\ 0 \\ x_4 \end{bmatrix} + \begin{bmatrix} \check{n}_1^1 \\ \check{n}_2^1 \\ \check{n}_3^1 \\ \check{n}_4^1 \end{bmatrix} \quad (5.17)$$

Note that the third column of \mathbf{H}_1 is a zero vector, retaining of which ensures the last two rows of \mathbf{R}_1 are independent of x_1 and x_2 . Hence the metric calculation for this condition with all possible values of x_4 is as follows

$$d_1 = \min \left(\left\| \tilde{y}_4^1 - r_{44}^{(1)} x_4 \right\|^2 + \left\| \tilde{y}_3^1 - r_{34}^{(1)} x_4 \right\|^2 \right) \quad (5.18)$$

This norm is calculated with two stage norms and hence will have better reliability. This feature is available only if $N_r \geq 4$. Similarly,

$$\tilde{\mathbf{y}}_2 = \mathbf{Q}_2^H \mathbf{y} = \mathbf{Q}_2^H \mathbf{Q}_2 \mathbf{R}_2 \mathbf{x}_2 + \mathbf{Q}_2^H \mathbf{n}_2 = \mathbf{R}_2 \mathbf{x}_2 + \tilde{\mathbf{n}}_2 \quad (5.19)$$

where $\mathbf{x}_2 = [x_1 \ x_2 \ 0 \ x_3]^T$, $x_k \in \mathcal{C}$. Note that the first two columns of \mathbf{R}_1 and \mathbf{R}_2 are the same and the fourth column is $[r_{14}^{(2)} \ r_{24}^{(2)} \ r_{34}^{(2)} \ r_{44}^{(2)}]^T$. If $\tilde{\mathbf{y}}_2 = \mathbf{Q}_2^H \mathbf{y} = [\tilde{y}_1^2 \ \tilde{y}_2^2 \ \tilde{y}_3^2 \ \tilde{y}_4^2]^T$, the metric with all possible values of x_3 is taken as

$$d_2 = \min \left(\left\| \tilde{y}_4^2 - r_{44}^{(2)} x_3 \right\|^2 + \left\| \tilde{y}_3^2 - r_{34}^{(2)} x_3 \right\|^2 \right) \quad (5.20)$$

$$\text{So, } \langle \hat{R}_k, \hat{x}_k \rangle = \arg \min_{R_k, x_k} (d_1, d_2)$$

From \hat{R}_k , the antenna index \hat{h}_k is available.

$$2) N_t = 6, N_r = 4, N_a = 4$$

$\mathbf{H}_k = [\mathbf{h}_1 \ \mathbf{h}_2 \ \mathbf{0} \ \mathbf{0} \ \mathbf{h}_i \ \mathbf{h}_j]$, where $i \neq j$ and $\mathbf{H}_k, k = 1:4$ corresponds to k^{th} permitted combination of \mathbf{h}_i and \mathbf{h}_j where $i, j = 3:6$. $\mathbf{h}_1, \mathbf{h}_2, \dots, \mathbf{h}_6$ are 4×1 vectors

$$\mathbf{y} = \mathbf{H}_k \mathbf{x}_k \text{ where } \mathbf{x}_k = [x_1 \ x_2 \ 0 \ 0 \ x_i \ x_j]^T, \ x_k \in \mathcal{C}$$

$$\mathbf{H}_k = \mathbf{Q}_k \mathbf{R}_k \text{ where } \mathbf{Q}_1 = \mathbf{Q}_2 = \mathbf{Q}_3 = \mathbf{Q}_4 = \mathbf{Q}$$

$$\tilde{\mathbf{y}} = \mathbf{Q}^H \mathbf{y} = \mathbf{Q}^H \mathbf{Q} \mathbf{R}_k \mathbf{x}_k + \mathbf{Q}^H \mathbf{n} = \mathbf{R}_k \mathbf{x}_k + \tilde{\mathbf{n}}$$

For $k = 1$, take $i = 3$ and $j = 4$. Then,

$$\begin{bmatrix} \tilde{y}_1 \\ \tilde{y}_2 \\ \tilde{y}_3 \\ \tilde{y}_4 \end{bmatrix} = \begin{bmatrix} r_{11} & r_{12} & 0 & 0 & r_{15}^{(1)} & r_{16}^{(1)} \\ 0 & r_{22} & 0 & 0 & r_{25}^{(1)} & r_{26}^{(1)} \\ 0 & 0 & 0 & 0 & r_{35}^{(1)} & r_{36}^{(1)} \\ 0 & 0 & 0 & 0 & r_{45}^{(1)} & r_{46}^{(1)} \end{bmatrix} \begin{bmatrix} x_1 \\ x_2 \\ 0 \\ x_3 \\ x_4 \end{bmatrix} + \begin{bmatrix} \tilde{n}_1 \\ \tilde{n}_2 \\ \tilde{n}_3 \\ \tilde{n}_4 \end{bmatrix} \quad (5.21)$$

Note that the third and fourth columns of \mathbf{H}_k are zero vectors. Here, retaining these will ensure that the number of columns in $\mathbf{H}_k = N_r + N_a - 2$ and hence \mathbf{Q} is the same for all the QR decompositions and the last two rows of \mathbf{R}_k are independent of x_1 and x_2 . For higher values of N_t , more columns of \mathbf{H} will be zero vector, but only two columns need to be retained, which will reduce the computation in calculating $N_t - N_r$ columns and the corresponding multiplication in finding $\mathbf{Q}^H \mathbf{y}$. The combined distance metric for x_3 and x_4 is taken as follows

$$d_1 = \min \left(\left\| \tilde{y}_4 - r_{45}^{(1)} x_3 - r_{46}^{(1)} x_4 \right\|^2 + \left\| \tilde{y}_3 - r_{35}^{(1)} x_3 - r_{36}^{(1)} x_4 \right\|^2 \right) \quad (5.22)$$

Note that if more number of receive antennas are used, the metric available from more rows of Equation (5.22) can also be added to this to have improved performance, which then will be a trade off with complexity and receive diversity. For all four possible $\mathbf{R}_k \mathbf{x}_k$ combinations, distance metrics are calculated and the antenna index and transmitted symbols are given by

$$\langle \hat{R}_k, \hat{x}_k \rangle = \arg \min_{R_k, x_k} (d_1, d_2, d_3, d_4) \quad (5.23)$$

The computational complexity of this method is analyzed in the next section.

5.3 COMPUTATIONAL COMPLEXITY

QR Decomposition is a well-known technique that finds application in sphere decoding and SIC. As explained in Section 5.2.2, the number of QR

decompositions to be performed in the proposed DESM is given by $\left[\binom{N'_t}{N'_a} \right]_{2^P}$. This is not a computational overhead since in each decomposition, \mathbf{Q}_k will be the same and it is to be computed only once. In \mathbf{R}_k s, only the last N'_a columns differ and for that only we have to compute r_{ij} . The reason for these peculiarities is explained now.

The structure of each of the \mathbf{H}_k matrices is given in Equation (5.9). In that we have to retain only $N_r + N_a - 2$ all zero columns which will ensure the same \mathbf{Q}_k and hence the detection uses

$$\mathbf{H}_k = [\mathbf{h}_1 \quad \mathbf{h}_2 \quad \mathbf{0}_{N_r \times N_r - 2} \quad \mathbf{h}_{C_k}] \quad (5.24)$$

where \mathbf{h}_{C_k} is the $N_r \times N'_a$ matrix formed by k^{th} permitted combination of non-fixed antenna responses.

Now we show why this structure of \mathbf{H}_k will guarantee the same \mathbf{Q}_k . We use the Modified Gram Schmidt (MGS) orthogonalisation method for QR decomposition which is computationally more stable (Singh *et al.*, 2006). The algorithm for the same for an $m \times m$ matrix is given in Figure.5.3. From this, we can see that the columns of \mathbf{Q} are orthogonalised in lines 10 and 11. Considering the structure of \mathbf{H}_k s here, since \mathbf{h}_1 and \mathbf{h}_2 are same for all \mathbf{H}_k s, the corresponding orthogonalised columns of \mathbf{Q}_k will be the same. If $\mathbf{v}_j = \mathbf{0}$ in any step, as in the case of $\mathbf{0}_{N_r \times N_r - 2}$ columns of \mathbf{H}_k , the algorithm proceeds by taking an arbitrary orthogonal vector and all the following columns corresponding to zero columns will be arbitrary. For an $m \times n$ matrix, if $m < n$, \mathbf{Q} matrix is of size $m \times m$. When the number of columns $N_t \geq N_r + N_a - 2$, this makes \mathbf{Q}_k the same in all decompositions. So, there is no extra computation required in finding all \mathbf{Q}_k s, compared to the sphere decoding or QRD-M algorithm.

Algorithm 1 : MGS-QR Decomposition

```

1: procedure INPUT(matrix  $H$  for QR decomposition)
2:   take size of  $H$  as  $(m, m)$  and elements as  $a_{ij}$ 
3:   for  $i = 1 : m$  do   - > iteration with columns of  $H$ 
4:      $\bar{v}_i = \bar{a}_i$        - > initialise columns of  $Q$ 
5:   end for
6:   for  $i = 1 : m$  do   - > iteration with columns of  $H$ 
7:      $r_{ii} = \|\bar{v}_i\|$    - > find norm of columns of  $Q$ 
8:      $\bar{q}_i = \frac{\bar{v}_i}{r_{ii}}$  - > normalise columns of  $Q$ 
9:     for  $j = i + 1 : m$  do
10:       $r_{ij} = \bar{q}_i^H * \bar{v}_i$  - > find elements of  $R$ 
11:       $\bar{v}_j = \bar{v}_j - r_{ij} * \bar{q}_i$  - > re-orthogonalise  $Q$ 
12:    end for
13:   end for
14:   return  $Q$  and  $R$ 
15: end procedure

```

Fig. 5.3. Algorithm for MGS QR decomposition

The computation required for finding one column of \mathbf{R} is $4N_r + 4N_r$ real multiplications, where the first factor is for calculating each r_{ij} , and the second factor is for calculating each v_j , as can be seen from the eighth and ninth rows of the algorithm in Figure.5.3. The total computation required is only $8N_r(N_t - N_a + 1)$ real multiplications due to the fact that considering all the \mathbf{H}_k s, only $(N_t - N_a + 1)$ columns at each position will be different and for that only r_{ij} and v_j are to be calculated.

Now, consider the computations required for finding the ML solution of $\|\tilde{\mathbf{y}} - \mathbf{R}\mathbf{x}\|^2$. The ML decoding rule when applied to the last two rows of the \mathbf{R} matrix is,

$$\hat{\mathbf{x}}_k = \arg \min_k \sum_{i=N_r-1}^{N_r} |\tilde{y}_i - \sum_{j=j1}^{j2} r_{ij} x_j|^2 \quad (5.25)$$

where $j1 = N_r + 1$ and $j2 = N_r + N'_a$

This amounts to $2(4KN'_a + 2)$ real multiplications for one matrix, where $4N'_a$ is the term that gives multiplications for calculating $r_{ij} x_j$ for the

last N'_a terms and the added 2 for squaring operation and K is the size of the constellation. Since this is done for two rows for increased reliability, the multiplicative factor 2 comes. As illustrated before, only $(N_t - N_a + 1)$ values of r_{ij} will be different and hence the total computation required is $2((N_t - N_a + 1)4K + 2N'_c)$. Finally, for finding the solution for the Alamouti code sent, only $2(4 + 2)K$ real multiplications are required, since the antenna indices are known (Kim *et al.*, 2010).

The computational complexity again reduces for a slow fading channel, since \mathbf{Q} is to be calculated only once and the term $\sum_{j=j_1}^{j_2} r_{ij} x_j$ for all i, j combinations can be computed and stored, for a frame. Simulation results given in section 5.4.2 illustrate how different parameters affect the complexity.

5.4 SIMULATION RESULTS

In this section, simulation results are presented to compare the performance of the proposed method with STBC-SM and ML detection in GSM-MIMO. The channel is assumed to be flat and block fading. For all the above systems, perfect CSI at the receiver is considered and for DESM, we assume a feedback channel that requires only $2 \log_2 N_t$ bits which transmit the indices of two antennas with largest SNR. The bit error rate and computational complexity of the systems are compared.

5.4.1 Performance

First we compare the BER vs. SNR performance for the proposed DESM system, STBC-SM and GSM for $N_t = N_r = 4$. We take $N_a < N_t$ and the possible active antennas in DESM are three – two for the diversity stream transmission and the third for low priority data. Even though any number of active antennas is possible for GSM, we take it as three for having a

fair comparison. Since STBC codes are transmitted in STBC-SM, the active antennas possible are two. We define the transmission tuple as (the antenna selection bits, the diversity stream bits, non- diversity stream bits). Figure 5.4 illustrates the BER vs. SNR performance of DESM and STBC-SM for different transmission tuples.

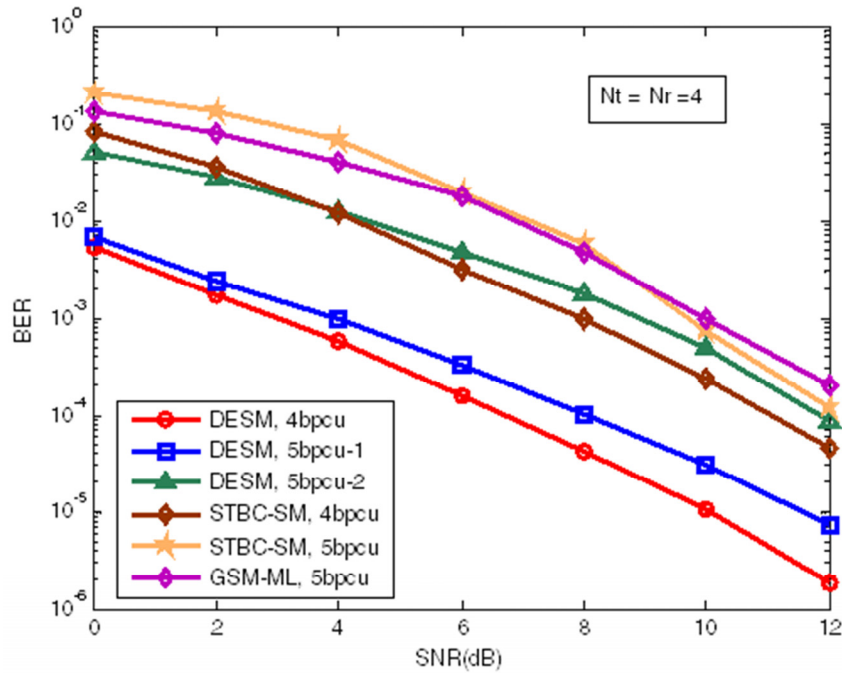


Fig. 5.4. BER vs. SNR curves for DESM, STBC-SM and GSM-ML for $N_t = N_r = 4, N_a = 3$

GSM with three active antennas have the minimum rate of 5 bpcu and its optimum ML detection performance is taken as a reference in all cases. For an overall rate of 4 bpcu, the transmission tuple in STBC-SM and DESM are (2, 6, 0) and (2, 4, 2) respectively. For 5 bpcu rate, DESM can have two transmission tuples, (2, 4, 4) and (2, 6, 2), which shows that the system can be configured adaptively for different diversity/non-diversity stream rates. For

STBC-SM the only possibility is to increase the diversity stream rate with the transmission tuple (2, 8, 0). Simulation results in Figure 5.4 illustrate that for the same overall rate, DESM performs better and for the same diversity stream rate also, the performance is comparable (see DESM- 5bpcu-2 and STBC-SM-4bpcu curves with diversity stream bits 6). The reason for the better performance of DESM is the use of fixed antennas for diversity stream transmission. In, GSM, there is uncertainty in the case of all the three active antennas and hence the BER will be high.

DESM system can be configured in many ways for the same rate of transmission and different performance. As stated, this is due to the possibility of varying the rate of diversity and non- diversity streams independently. Figure 5.5 illustrates the performance of DESM for various configurations, compared to STBC-SM. We consider $N_t = N_r = 6$ for both the systems and $N_a = 3$ for DESM, whereas $N_a = 2$ is assumed in STBC-SM, due to the restriction that the active antennas has to be a power of two. Note that with six transmit antennas, the antenna selection bits in STBC-SM is 3 whereas in DESM it is 4, two bits in each time slot. Figure 5.5 shows the performance curves of DESM for rates 5, 6 and 7 bpcu with corresponding transmission tuples (4, 4, 2), (4, 4, 4) and (4, 8, 2) and that for STBC-SM for rates 4.5 and 5.5 bpcu with transmission tuple (3,6,0) and (3,8,0) respectively. In DESM, compared to 5 bpcu curve, 6 bpcu curve is obtained by increasing the rate of the non-diversity stream, which still shows a better performance compared to both STBC-SM curves. Increasing the diversity stream rate in DESM (7 bpcu curve) shows a comparable performance with 5.5 bpcu in STBC-SM, which has the same diversity transmission rate. Hence, the diversity stream rate can be adjusted with performance or the overall rate.

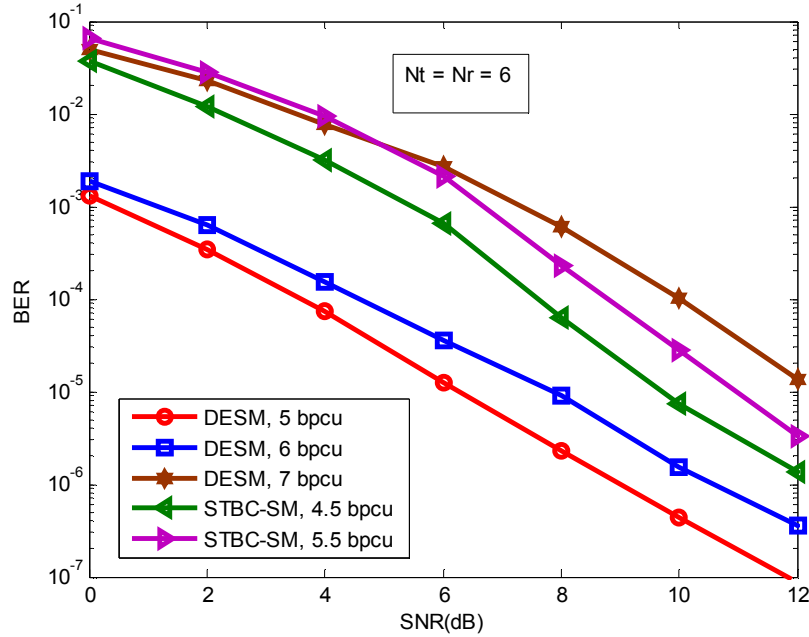


Fig. 5.5 BER vs. SNR curves of DESM and STBC-SM for $N_t = N_r = 6, N_a = 3$

As mentioned in the introduction of this chapter, DESM performs well even if the number of receive antennas is less than the transmit antennas. The performance of DESM for 4, 6, 10 transmit antennas with transmission tuples (2, 4, 2), (4, 4, 2), (6, 4, 2) and $N_r = 4$ is illustrated in Figure 5.6. Compared to the curve of $N_t = N_r = 4$, the performance curves of $N_t = 6$ and 10 are satisfactory, considering the increased rate due to the antenna selection bits. This has to be compared with the performance of STBC-SM curves shown, which is having a low rate. Here, again it is shown that the diversity stream rate can be compromised with performance and overall rate, if the rate of the system is varied by varying the diversity stream rate, as is clear from the DESM - $N_t = 6, 6$ bpcu curve.

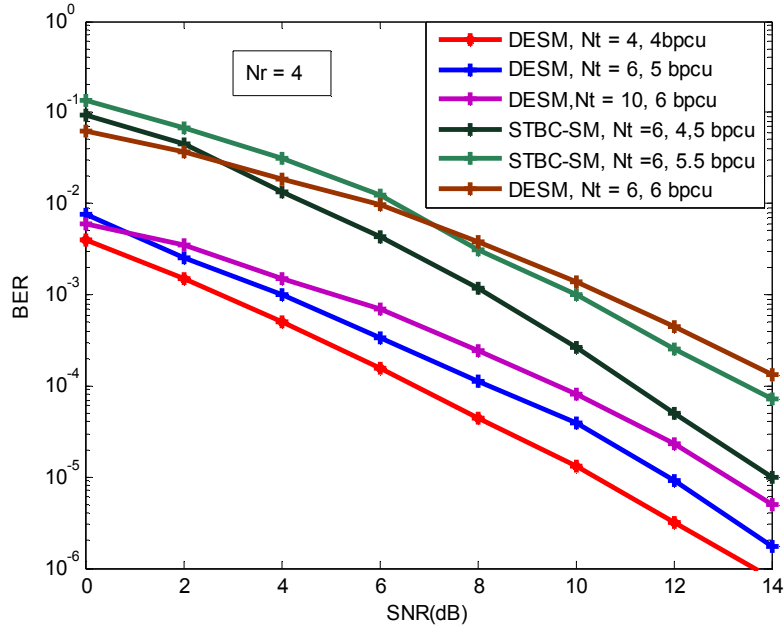


Fig. 5.6 BER vs. SNR curves of DESM for $N_t = 4, 6, 10$, $N_r = 4$, $N_a = 3$ and for STBC-SM

The diversity order achievable for the diversity stream in DESM is two in all the cases. The performance shown is the overall performance as rate is compared considering the overall rate. Also, the performance is affected by the number of receiving antennas, which will introduce receive diversity.

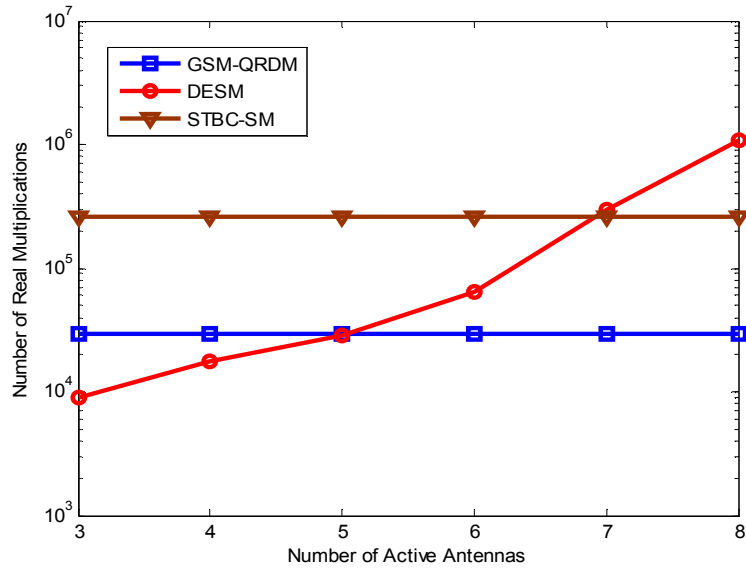
5.4.2 Computational Complexity

Simulations of the computational complexity in Figure 5.7 show that receiver complexity is less for reasonable number of active antennas in DESM. For GSM, the complexity of detection methods like sphere decoding and OB-MMSE is very high compared to the proposed system (of the order of 10^7) and is dependent on SNR (Wang *et al.*, 2012). Hence, comparison is made with the fixed complexity QRD-M detection (Kim and Yue, 2002; Kim *et al.*, 2010), in which we assumed $M = K/2$, where M is the number of candidates retained at

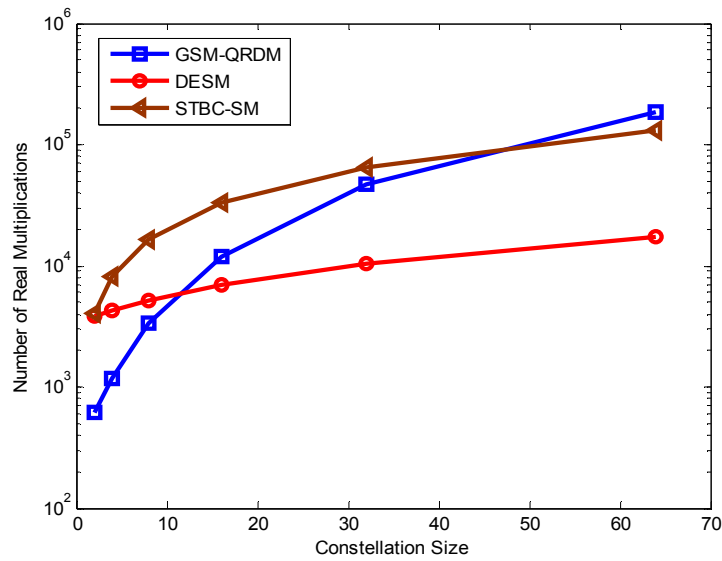
each level and K is the constellation size. For STBC-SM, two active antennas and the low complexity detection in (Basar *et al.*, 2011) are taken for simulation.

Figure 5.7(a) compares the complexity as the number of active antennas increases, for fixed constellation size of 16 and 24 transmit antennas. Also, there are four receive antennas for DESM and STBC-SM, whereas for GSM-QRD-M, there should be the same number of transmit and receive antennas. Figure 5.7(a) reveals that for DESM, the required computations are small up to five active antennas and only when the active antennas increases beyond seven, it exceeds the other two detection methods. So, there exists a possibility to trade off with complexity, power and rate in our proposed system. Since the active antennas are fixed in STBC-SM and GSM-QRD-M detection does not depend on the active antennas, the detection complexity is constant in those two methods. In Figure 5.7(b), for fixed transmit and active antennas (16, 4 respectively), the complexity as the constellation size increases is compared. The complexity of QRD-M and STBC-SM are much dependent on the constellation size. The proposed DESM is not much affected by the increase of constellation size, and hence rate can be increased without increasing complexity, when the channel conditions are favourable.

We further analyse how the rate of the system is affected when two of the antennas are earmarked for high priority data in Figure 5.8. Two separate comparisons are given in Figure 5.8(a) and 5.8(b), for low and high values of transmit and active antennas and QPSK constellation. Both the figures show that the percentage rate loss in DESM is not prominent as the rate of transmission is considered, and it decreases as the active antennas are increased. Also, fig 5.8(a) shows that increasing the number of transmit antennas without increasing the active antennas not makes much change in rate of transmission.



(a)



(b)

Fig.5.7. Comparison of computational complexity of DESM, STBC-SM and GSM-QRD-M (a) For fixed transmit antennas and constellation size (b) For fixed transmit and active antennas

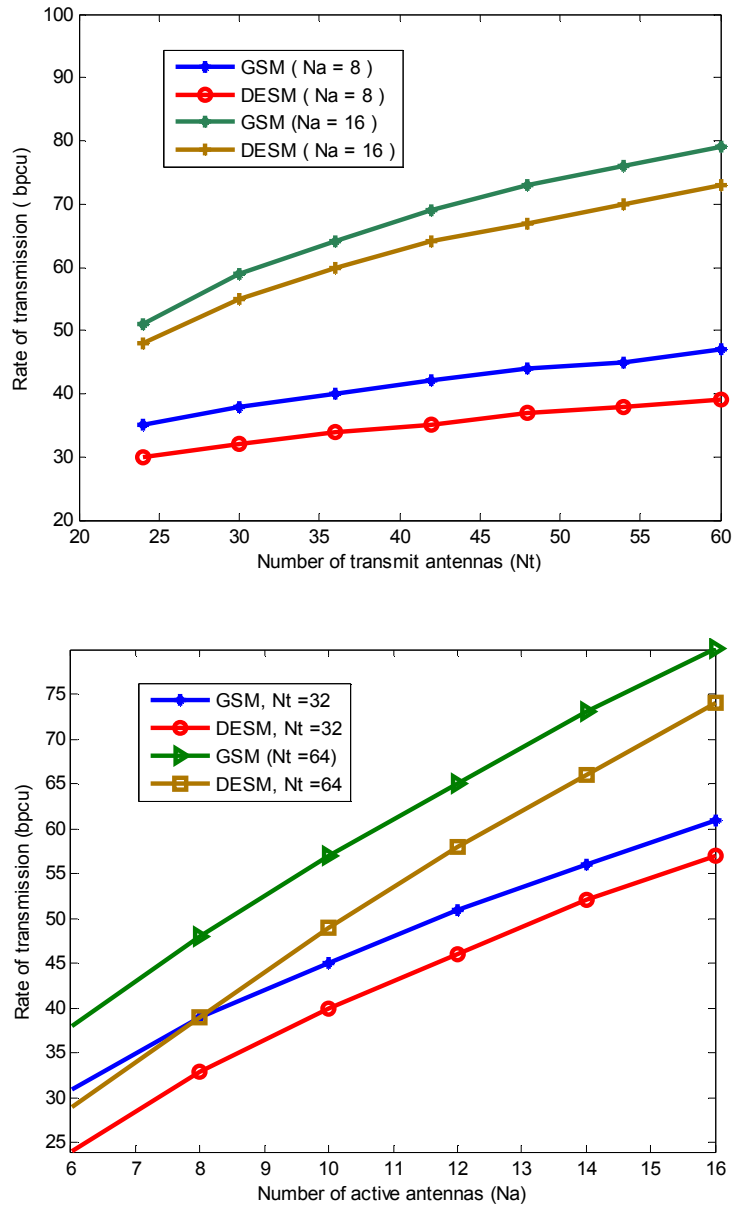


Fig. 5.8. Comparison of rate of DESM and GSM for (a) for fixed N_a
(b) fixed N_t

5.5 CONCLUSIONS

This chapter presented the performance of a system that combines the space time coding and spatial multiplexing with GSM. The proposed DESM does not impose any restriction on the number of active antennas, and only limited feedback is required to get good performance. Applying QR decomposition based detection with $N_r < N_t$, the system is shown to have very good performance. The BER vs. SNR performance compared to STBC-SM and GSM are better for the same overall rate. For the same diversity stream rate also the performance is comparable with that of STBC-SM. This is achieved without much increase in computational complexity, for reasonable number of transmit and active antennas and with the added advantage that the minimum number of receive antennas required is only four. The system can be configured in various ways by changing the diversity and non-diversity bits transmitted during each time slot, maintaining the same overall rate but with a performance trade off. The rate of the system compared with that of GSM is analysed and is found that the percentage rate loss is negligible, considering the performance improvement.

Chapter

6

RATE ADAPTATION IN GSM USING RCPC CODES

Generalised spatial modulation achieves both spectral and energy efficiency at fair transmission rates and allows trade off among these factors. But, inter channel interference affects the bit error rate performance, especially when the channel conditions are poor. The performance of GSM can further be improved by adjusting transmission parameters such as modulation order and coding rate dynamically according to channel conditions. This technique, in general called link adaptation, utilizes the channel state information fed back from the receiver to the transmitter to transmit at high rates when the channel condition is good and to reduce the rate if the channel turns poor. Though well-established in single antenna systems, designing adaptation schemes for MIMO systems is challenging. Along with the conventional modulation order/coding scheme change, different spatial signaling techniques can also be utilized in MIMO for adaptation. This results in large number of adaptation modes and to effectively utilize all these, complex circuits and high adaptive control overhead are required. As an alternative, code puncturing can be employed to make the system rate adaptive. In this chapter, we present an adaptive transmission technique in GSM MIMO using rate compatible punctured convolutional (RCPC) codes. An antenna grouping method based on limited CSI feedback is used to select the puncturing matrices and active antennas in GSM. The system throughput and BER performance are analyzed for various channel selection and puncturing schemes.

6.1 INTRODUCTION

MIMO technology provides significant capacity gain through multiplexing and increases link robustness through diversity techniques. But there exists a tradeoff among these (Zheng and Tse, 2003; Di Renzo and Haas, 2011 a) and to reap the full benefits of MIMO irrespective of varying channel conditions, adaptation is often required. MIMO systems that exploit time and frequency parameter changes for adaptation are well explored (Keller and Hanzo, 2000). Though complex, schemes that exploit spatial selectivity of the channel for adaptation are also available. Some of these schemes increase the throughput for a fixed error rate and the others reduce the error rate for a fixed transmission rate (Chae *et al.*, 2010). Throughput based techniques utilize robust modulation and coding schemes (MCS) when the channel condition is poor and as the channel quality improves, switches to higher order MCSs. Diversity based methods improve the error performance by selecting the MIMO transmission modes that offer higher robustness to fading. Several methods in these two categories are proposed for adaptation in MIMO (Chae *et al.*, 2004; Heath and Paulraj, 2005; Forenza *et al.*, 2005). Most of these methods need to resend information repeatedly as per automatic repeat request (ARQ), and is not suitable for wireless communications where ARQ is typically not implemented (Sari *et al.*, 2009). Also, adaptation with different MCS makes the system complex with the associated coding and decoding circuits and switching. Code puncturing is another method that allows an encoder/decoder pair to change code rates, which can be utilized for adaptation without the above said disadvantages. For example, in the case of convolutional coding, puncturing changes the rate simply by deleting specific code bits of the original low rate mother code as per a predefined rule. This bit deletion (puncturing) rule can be changed to generate codes of different rates.

At the receiver side, a Viterbi decoder based on the original (mother) code and with the same puncturing rule is used for decoding.

RCPC codes are punctured codes with some conditions on the general puncturing rule. Having nearly equivalent performance of convolutional codes and simplicity in decoding, RCPC code is a good candidate for adaptation in MIMO systems. The performance of RCPC codes in V-BLAST spatial multiplexing systems is well studied (Sari *et al.*, 2009; 2010), and is shown to increase the robustness of the system and bandwidth efficiency without much degradation in performance. But, BLAST systems are not energy efficient and the focus of today's research is in maximizing the energy efficiency along with spectral efficiency. GSM, in which only a limited number of antennas are activated during a time slot is a suitable solution for this. Rate adaptation can be utilized to further improve the GSM system performance, knowing the channel conditions. Here, we analyze the performance of a GSM MIMO system in which link adaptation is done using RCPC codes.

6.2 PROPOSED RCPC ENCODED GSM SYSTEM

In this section, the proposed method in which RCPC codes are used as a means of varying the rate of the GSM system according to the channel conditions is explained. Section 6.2.1 is an overview of RCPC coding and parameters involved. The adaptive GSM system is explained in Section 6.2.2.

6.2.1 RCPC Codes

RCPC codes are formed by imposing some conditions on the general puncturing rule of convolutional codes to ensure rate-compatibility. These conditions, as will be explained, ensure that if the channel errors are so high and efficient decoding is impossible, the previously punctured bits only have to be transmitted for upgrading the code. Besides, the compatibility of the codes

makes it possible to vary the rate within a data frame for achieving unequal error protection (Hagenauer, 1988).

Here we give an overview of RCPC code parameters. An example of coding with four puncturing tables ensuring rate-compatibility is shown in Figure 6.1. The boxes ‘M’ represent the memory elements/shift register stages and the ‘+’ symbol indicates logical XOR operation. The mother code is a half rate convolutional code with memory $M = 2$, specified by the code generator matrix $\begin{bmatrix} 1 & 1 & 0 \\ 1 & 0 & 1 \end{bmatrix}$, which is punctured periodically with a period $P = 4$. A zero in the puncturing table means that the particular symbol is not to be transmitted. For example, as indicated by the first rows of the tables in Figure 6.1, the puncturing matrix $P(1) = \begin{bmatrix} 1 & 0 & 0 & 1 \\ 1 & 1 & 1 & 0 \end{bmatrix}$, which means the second and third bit of the upper branch and the fourth bit of the lower branch are not transmitted.

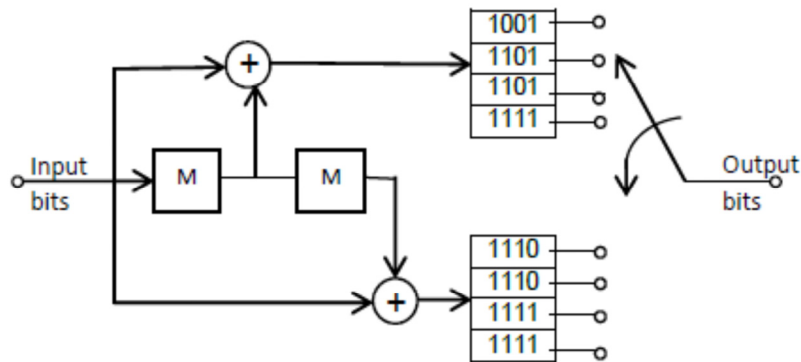


Fig. 6.1 Example of RCPC encoding

So, instead of transmitting $2 * P = 2 * 4 = 8$ bits, $P + l = P + 1 = 5$ bits are transmitted per $P = 4$ data bits and the rate of the code $R = P/(P + l) = 4/5$. Suppose with this code rate, it is not possible to correct the channel

errors, rate is lowered to 4/6, 4/7, or 4/8, to increase the redundancy. Here, instead of using a completely different low rate code, the already transmitted bits are utilized and only the additional bits required for increasing the redundancy are transmitted. So, additional ‘1’s can only be placed in places where the higher rate codes have zeros. The resulting puncturing matrices $P(l)$ would be $P(2)$, $P(3)$ and $P(4)$ as given below.

$$P(2) = \begin{bmatrix} 1 & 1 & 0 & 1 \\ 1 & 1 & 1 & 0 \end{bmatrix} \quad P(3) = \begin{bmatrix} 1 & 1 & 0 & 1 \\ 1 & 1 & 1 & 1 \end{bmatrix}$$

$$P(4) = \begin{bmatrix} 1 & 1 & 1 & 1 \\ 1 & 1 & 1 & 1 \end{bmatrix}$$

So, the following parameters and conditions specify a family of RCPC codes. The generator matrix is of size $N \times (M + 1)$ with elements $(g_{ik}) \in (0,1)$ where a ‘1’ denotes a connection from the k^{th} shift register stage of convolutional encoder to its i^{th} output. $R = 1/N$ is the original code rate and M is the number of memory elements. The rates of codes are determined by N and the puncturing period P as

$$R = P/(P + l) ; l = 1, 2 \dots (N - 1)P \quad (6.1)$$

The puncturing matrices $P(l)$ are of size $N \times P$ with elements $(a_{ij}) \in (0,1)$ where a ‘0’ represents a bit puncturing with the following conditions for rate compatibility.

$$\text{If } a_{ij}(l_0) = 1, \text{ then } a_{ij}(l) = 1 \text{ for all } l \geq l_0 \geq 1$$

$$\text{If } a_{ij}(l_0) = 0, \text{ then } a_{ij}(l) = 0 \text{ for all } l \leq l_0 \leq P(N - 1) - 1$$

Next we present the adaptive GSM system in which the transmission rate is varied as per the channel condition using different puncturing matrices.

6.2.2 Adaptive GSM system

We consider the GSM MIMO system model presented in 5.2.1 having N_t transmit antennas in which only N_a antennas are active at a time and N_r receiving antennas, represented by (N_t, N_a, N_r) . It is assumed that only two antennas are activated at a time out of the available antennas ($N_a = 2$).

As shown in Figure 6.2, the input bit stream is demultiplexed to form two streams that are to be separately encoded using convolutional codes. Based on the channel state information from the receiver, the antennas are grouped in such a way that the better channels come within a group. There is no limitation on the number of antennas in a group, except that at least two antennas should be there in group, so that there is a possibility for antenna selection within a group.

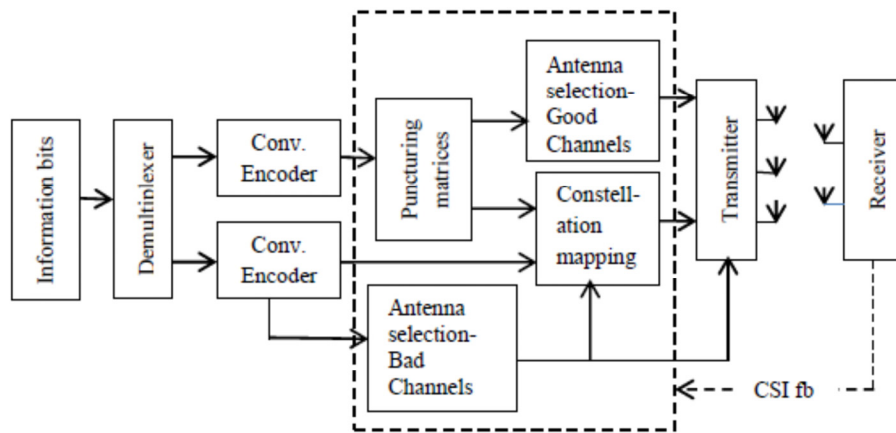


Fig. 6.2 GSM system with rate adaptation

For example, if there are twelve transmit antennas, in the two antenna activated system, they can be grouped as illustrated in Table.6.1. In case -1, the antenna selection bits are found assuming one antenna is selected from the group of good channels (G) and one from the poor channel group (B), as per

$\lfloor N_\alpha \rfloor_{2^p}$ where N_α is the number of antennas in a group. One advantage of this selection method is that this will increase the antenna selection bits when good channels are less (see column 1 in Table.6.1). Considering the correlation effects of antennas also, this may be advantageous in some cases. The other case (case-2) is applicable when both the active antennas are selected from G group and the antenna selection bits are given by $\left\lfloor \binom{N_g}{2} \right\rfloor_{2^p}$, where N_g is the number of antennas in group G.

Table. 6.1 Antenna selection in the adaptive GSM system

| | | | |
|--------------------------------------|-------|-------|--------|
| Grouping(G,B) | (4,8) | (6,6) | (10,2) |
| Antenna selection bits(g,b) - case 1 | (2,3) | (2,2) | (3,1) |
| Antenna selection bits(g) - case 2 | 2 | 3 | 5 |

G – good channels, B- bad channels; (g,b) corresponding antenna selection bits

The adaptive coding process is as follows. In case-1, the antenna selection (from group G) and constellation mapping is done after puncturing. The puncturing matrix can be selected as per the CSI feedback. The B group antenna transmission is without puncturing, as the channel condition is poor. If the channel condition permits, puncturing for a lower rate code can also be done. So, two code rates and throughputs are possible, for a particular error performance. Also, the code rate in the punctured stream can be changed according to channel condition feedback, while maintaining the same error performance. In case -2, both the antennas are selected from group G, and puncturing can be applied to both the streams. (This scenario is not shown in Figure.6.2) The same or different puncturing matrices can be used, as per the required Quality of Service (QoS) of the two streams, which can also be changed adaptively.

The following adaptation modes are possible in this system. The fixed rate mode and fixed modulation mode. In the fixed rate mode, transmission

uses different modulation schemes. When designed for a particular modulation scheme, for example QPSK, the transmission rate is varied depending on the antenna selection bits. Both the schemes can be optimized for given BER performance or throughput. In both the cases, according to the puncturing matrices used, the actual data rate varies.

For decoding, hard input Viterbi convolutional decoder is assumed. For providing hard input bits to Viterbi decoder, any of the GSM decoders can be utilized, which estimates the transmitted symbol as

$$\hat{\mathbf{x}} = \arg.\min_{\mathbf{x} \in \mathcal{C}} \|\mathbf{y} - \mathbf{H}\mathbf{x}\|^2 \quad (6.2)$$

where \mathcal{C} is the constellation assumed. After symbol estimation and demapping, the bit stream enters the decoder, where the same puncturing matrices and mother decoder are used to obtain the original source data.

6.3 SIMULATION RESULTS

Next we present the performance of the proposed system in terms of BER and average throughput. Here we assumed an (8, 2, 4) MIMO system with ML detection. However, these results can be extended to different numbers of transmit and active antennas and different transmission schemes.

Figure 6.3 compares the BER vs. SNR performance of our adaptive algorithm with that of fixed GSM transmission scheme. The mother code used is a rate 1/2 convolutional code. The puncturing period (P) used is three, and $l = 1, 2$ which will give a rate of $P/(P + l) = 3/4$ and $3/5$ respectively. Four different transmission scenarios with different rates are shown. The performance of the system without any channel grouping and punctuation and at 8 bpcu transmission rate with QPSK modulation (Figure.6.3, NCP-8bpcu) is taken as a reference. In the punctured case, a rate 3/5 code is transmitted using only good channel selection in GSM (GC, 3/5, 6bpcu). Since only good

channels are utilized, antenna selection bits ($\log_2 N_c$) are reduced from 4 to 2 and hence the overall rate is only 6 bpcu. Compared to non-punctured code, the performance is better because only good channels are selected and transmission rate is low. The performance is almost comparable even if the rate is increased to 3/4 as per GC, 3/4, 6bpcu curve shown. In the other scenario, the channels are divided into G and B groups consisting of four antennas each as explained in section 6.2.2. High rate code is transmitted through good channels, and low rate code is transmitted through poor channels, each with channel selection (G, 3/4, 4bpcu and B, 3/5, 4bpcu respectively). So the overall rate achieved is 8bpcu, with the performance shown as OGB. It is seen that when both good and poor channels are utilized, the performance degrades, giving only the high rate advantage.

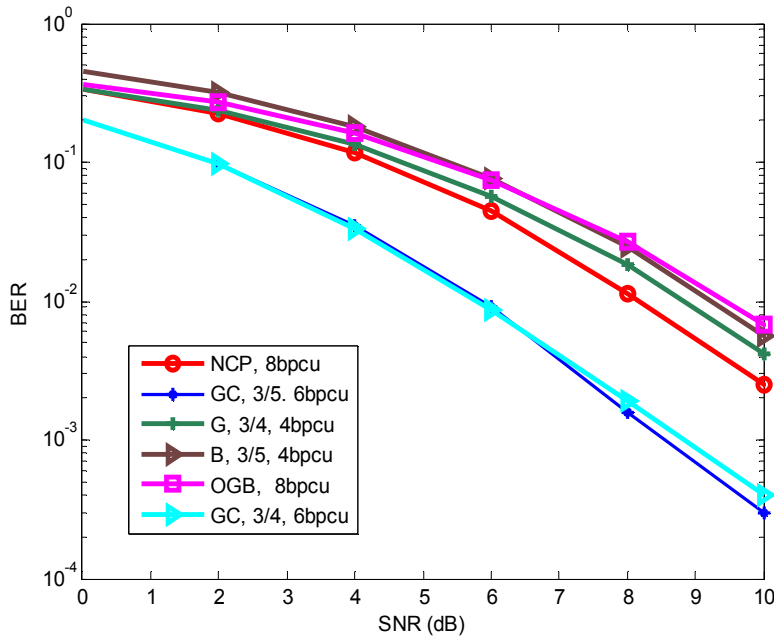


Fig.6.3 BER Vs. SNR curves for puncturing period $P=3$

The simulations for a higher puncturing period ($P = 8$) is shown in Figure 6.4. The rates used are 8/12 and 8/14 for $l = 4, 6$ respectively. The same transmission scenarios as in Figure 6.3 is assumed, but the comparison is with $P = 3$ curve. The better performance of higher puncturing period is clear in good channel selection case as well as antenna grouping case.

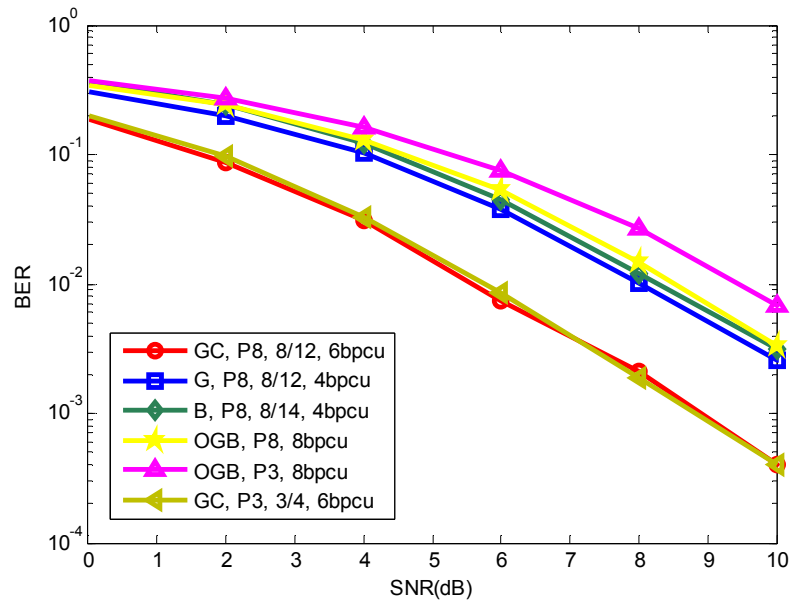


Fig. 6.4 Comparison of BER Vs. SNR curves for $P=3$ and $P=8$

Next we show the performance for a fixed transmission rate of 8bpcu for $P = 3$ in Figure 6.5. Here, the modulation scheme is selected as QPSK or 8QAM so as to maintain the same transmission rate. With antenna selection from both the group, antenna selection bits are four and QPSK modulation achieves 8bpcu rate. When the active antennas are selected only from group G, the antenna selection bits are reduced to two and to get the fixed transmission rate of 8bpcu, a higher modulation scheme, ie. 8QAM is opted. Here also, combined channel selection degrades the performance.

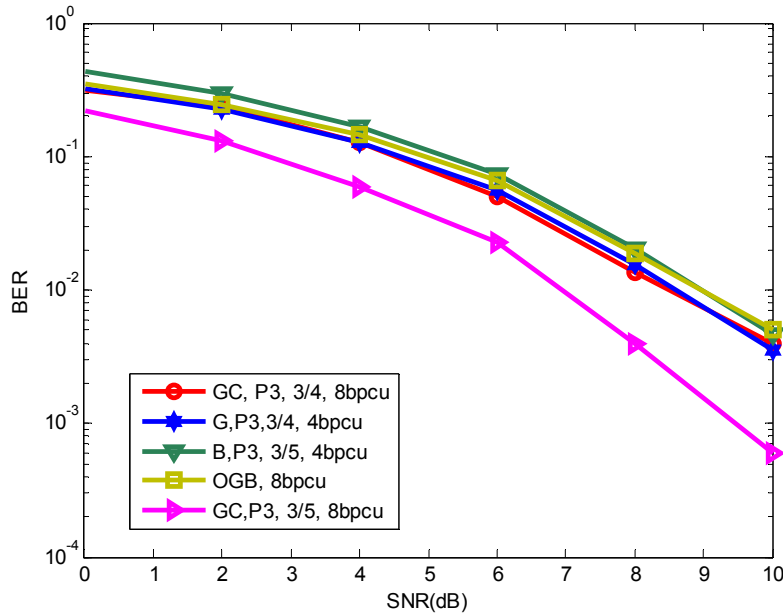


Fig. 6.5 BER Vs. SNR curves for fixed 8bpcu rate

Throughput of the system at a rate R and a specified SNR ρ as defined by $T_\rho = \sup(R(1 - P(\epsilon)))$ where $P(\epsilon)$ is the outage probability. This is simulated for 10% outage with various puncturing lengths and rates and compared with the throughput achieved without puncturing in Figure 6.6. The GC, P3 and GC, P8 curves are for the case of channel selection from group G only, whereas the OGB, P3 and OGB, P8 curves are for channel selection from both group G and group B. NP curve is the throughput achieved without puncturing. It is seen that increasing the puncturing length increases the throughput for both the channel selection methods. Also, utilizing full channel selection with grouping reduces the throughput, as seen from the two OGB curves. But, as the rate is higher, the time taken for transmission of same frame length will be reduced much by grouping.

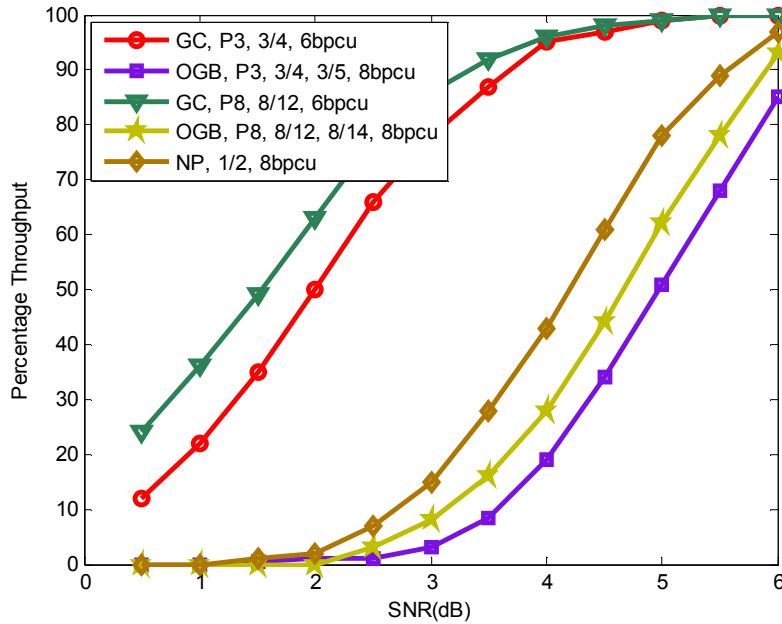


Fig.6.6 Throughput Vs. SNR curves for $P=3$ and $P=8$

6.4 CONCLUSIONS

In this chapter, we presented an adaptive transmission technique in GSM system using RCPC codes. An antenna grouping method based on the CSI feedback from the receiver is used to improve the transmission rate. The system is analyzed with half rate convolutional mother code and for puncturing lengths 3 and 8. It is seen that puncturing can be effected even with a performance improvement with channel selection. Also, increasing the puncturing length improves the BER performance as well as the throughput.

The objective of this research was to develop coding schemes for MIMO systems, having acceptable rate, reliability and low complexity of decoding. MIMO systems such as spatial multiplexing, spatial modulation and generalised spatial modulation are considered for this, and the work done is based on the shortfalls of the systems in literature. Here, we summarize the work we carried out in these areas so as to achieve the goals presented in chapter1, drawbacks of them and possible extensions.

7.1 THESIS CONTRIBUTION

7.1.1 Spatial Multiplexing

Spatial multiplexing achieves high data rates at the cost of poor detection performance. So, we proposed a method that improves the detection performance of SMX-MIMO using the parity information of transmitted symbols. The proposed method named as QRD-P achieves better BER performance than the traditional QRD-M method, even at low values of SNR, with much less computational complexity. Even though the actual data rate is reduced, it is seen that the percentage of correctly received bits to the sent information bits is higher compared to traditional QRD-M.

7.1.2 Spatial Modulation

In Spatial Modulation, the performance improvement through diversity is considered. An encoding scheme based on Weyl Group matrices is proposed that achieves second order transmit diversity. It is a single antenna activated

system and offers the simplicity of single stream ML decoding. The rate is higher than SM-STBC and CIOD based diversity schemes and the BER performance also is better. The computational complexity variation as the number of antenna elements is increased is found to be very less.

7.1.3 Generalized Spatial Modulation

Robustness against channel impairments is provided for a particular data stream and at the same time a fair data rate is maintained in the GSM system. The method proposed named as diversity embedded SM (DESM), have no restriction on the number of active antennas and the system shows very good performance even when the number of receive antennas is less than the transmit antennas. The system is configurable in various ways by changing the diversity and non- diversity bits transmitted during each time slot, maintaining the same overall rate but with a performance trade off.

7.1.4 Rate Adaptation in GSM

A rate adaptive transmission technique using RCPC codes for the GSM system is proposed. Based on the channel state information, different puncturing matrices are employed to vary the transmission rate. The system is analyzed with half rate convolutional mother code and for different puncturing lengths. It is seen that puncturing can be effected even with a performance improvement utilizing the channel selection possibility in GSM. Also, increasing the puncturing length improves the BER performance as well as the throughput.

7.2 DRAWBACKS

The constraints of our methods are mentioned here. The parity aided detection for spatial multiplexing reduces the information rate. As the number of transmit antennas increases, either more symbols are to be utilized for encoding

the parity information or more points in the constellation are to be used to represent the parity encoded symbol. In the first case, the effective throughput will be reduced whereas the second solution will increase the computational complexity slightly. This drawback is compensated with improved performance at low values of SNR, but not in the high SNR region.

Regarding Weyl Group Encoding, the disadvantage is that for encoding more than four bits at a time, the Kronecker product of the matrices are to be used, which will increase the complexity. The alternative method of bit padding reduces the rate.

In the DESM system, the rate reduction compared to GSM and the increase in computational complexity for large number of transmit / active antennas are the main issues.

The rate adaptation in GSM is based on an antenna grouping strategy that requires the indices of good channels/ bad channels as feedback information. For large number of antennas, the feedback overhead will be high.

7.3 FUTURE WORK

In our work related to spatial multiplexing, we assumed that CSI is available only at the receiver side, which is the general scenario. However, if CSI is feedback from the receiver to the transmitter, most favorable channels can be utilized to transmit parity information. In such a situation, parity encoding can be extended to large antenna system with antenna grouping so that required constellation size is not increased.

To achieve transmit diversity in SM, we have suggested the Weyl group encoding, in which only four bits can be encoded at a time. This scheme can be extended to encode more than four bits at a time using the Kronecker

product of the matrices. This requires more number of time slots and a different coding, since all the matrices in the Kronecker product are not unique.

Our proposed DESM provides diversity in GSM with acceptable rate, but the detection complexity is high for large number of active antennas. To reduce this, an alternative coding scheme that permits detection based on block QR decomposition can be developed.

In the link adaptation method proposed for GSM, we assumed that switching is done over frames only, based on CSI feedback available at transmitter side. The switching can be performed within the frame duration based on the instantaneous / threshold SINR information fed back from the receiver side, which is a possible extension.

APPENDIX-A

WEYL GROUP

Weyl group is a Unitary Matrix group. The multiplicative Weyl Group G_w is generated by two matrices, $\frac{1}{\sqrt{2}} \begin{bmatrix} 1 & 1 \\ 1 & -1 \end{bmatrix}$ and $\begin{bmatrix} 1 & 0 \\ 0 & i \end{bmatrix}$. As these matrices are unitary, all the matrices generated by them are also unitary. The group is divided into 12 cosets and each coset contains 16 invertible matrices. The first coset, which is a sub group of Weyl group given by

$$C_0 = \left\{ \alpha \begin{bmatrix} 1 & 0 \\ 0 & \pm 1 \end{bmatrix}, \alpha \begin{bmatrix} 0 & 1 \\ \pm 1 & 0 \end{bmatrix} \right\} \quad (\text{A1.1})$$

with $\alpha \in \{+1, -1, +i, -i\}$.

The 12 cosets of G_w are derived from C_0 as follows

$$C_k = A_k C_0, \text{ for } k = 0, 1, \dots, 11.$$

The matrices A_k for $k = 0, 1, \dots, 5$ are respectively

$$\begin{aligned} A_0 &= \begin{bmatrix} 1 & 0 \\ 0 & 1 \end{bmatrix}, \quad A_1 = \begin{bmatrix} 1 & 0 \\ 0 & i \end{bmatrix}, \quad A_2 = \frac{1}{\sqrt{2}} \begin{bmatrix} 1 & 1 \\ 1 & -1 \end{bmatrix}, \\ A_3 &= \frac{1}{\sqrt{2}} \begin{bmatrix} 1 & 1 \\ i & -i \end{bmatrix}, \quad A_4 = \frac{1}{\sqrt{2}} \begin{bmatrix} 1 & i \\ 1 & -i \end{bmatrix}, \quad A_5 = \frac{1}{\sqrt{2}} \begin{bmatrix} 1 & i \\ i & 1 \end{bmatrix} \end{aligned} \quad (\text{A1.2})$$

And the matrices A_k for $k = 6, 7, \dots, 11$ are given by

$$A_{k+6} = \eta A_k, \text{ with } \eta = (1 + i)/\sqrt{2}; \quad k = 0, 1, \dots, 5 \quad (\text{A1.3})$$

There are 192 matrices in this group.

The Kronecker product of two arbitrary matrices A and B is defined as:

$$A \otimes B = \begin{bmatrix} a_{11}B & \dots & a_{1n}B \\ \vdots & \ddots & \vdots \\ a_{m1}B & \dots & a_{mn}B \end{bmatrix} \quad (\text{A1.4})$$

where A is an $m \times n$ matrix, B is a $p \times q$ matrix and the resulting matrix is an $mp \times nq$ matrix.

The Kronecker product has the properties.

- The Kronecker product is not commutative ie. $A \otimes B \neq B \otimes A$
- $A \otimes B$ is invertible if and only if A and B are invertible, and

$$(A \otimes B)^{-1} = A^{-1} \otimes B^{-1}$$

- The operation of transposition is distributive over the Kronecker product:

$$(A \otimes B)^T = A^T \otimes B^T$$

- The Kronecker product is associative

$$(A \otimes B) \otimes C = A \otimes (B \otimes C)$$

Computing the Kronecker product between each couple of 2×2 matrices of the Weyl group, a 4×4 matrices set is obtained. There are $192 \times 192 = 36864$ matrices in this set among which only 4608 matrices are distinct. The set of these matrices is also a group denoted as G_{w4} .

APPENDIX-B

ALGORITHMS FOR THE SCHEMES

B.1. QRD-P Encoding

Algorithm 1 : Encoding in QRD-P in a 4 x 4 SMX system with 16QAM

```

1: procedure INPUT(framelength, input bits, channel matrix H) ▷
2:   while framelength do
3:     take a block of 12 bits
4:     demultiplex to group of 4 bits
5:     - >  $B(1)$  - >  $b_0 : b_3$ ,  $B(2)$  - >  $b_4 : b_7$ ,  $B(3)$  - >  $b_8 : b_{11}$ 
6:     for 2:3 do
7:       XOR the bits of  $B(i)$  - > get parity bits  $P_0, P_1$ 
8:     end for
9:     if  $P_0 P_1 = (00)$  then
10:      encode parity bits  $b_{12} : b_{15}$  as  $(0 \ 0 \ P_0 \ P_1)$ 
11:     else
12:      encode parity bits  $b_{12} : b_{15}$  as  $(0 \ 0 \ \overline{P_0} \ \overline{P_1})$ 
13:     end if
14:     modulate  $b_0 : b_{15}$  using 16 QAM - > get input symbols  $x_1 : x_4$ 
15:     form  $\bar{x} = [x_1 : x_4]^T$ 
16:     pre-multiply with channel matrix  $H$ 
17:     add Noise - >  $\bar{n}$ 
18:     return  $\bar{y} = H\bar{x} + \bar{n}$ 
19:   end while
20: end procedure

```

B.2. QRD-P Decoding

Algorithm 2 : Decoding in QRD-P in a 4 x 4 SMX system with 16 QAM

```

1: procedure INPUT(framelength, y vectors, channel matrix H, 16 QAM symbols)
2:   form symbol table ST1 with even parity symbols of QAM
3:   form symbol table ST2 with odd parity symbols of QAM ▷
4:   while framelength do ▷
5:     take input vector  $\bar{y}$ 
6:     do QR decomposition of H - > get Q and R
7:     premultiply y with  $Q^H$  - > get  $y_t$  - >  $y_{tilda}$ 
8:     for  $k = 1:4$  do - > with four parity symbols
9:       find norm( $y_t4 - r_{44}x_k$ ) - > find norm with fourth row of R
10:    end for
11:    find minimum norm
12:    take corresponding  $x_k$  as  $x_4$ 
13:    decode to binary - > get parity bits >  $b_{12} : b_{15}$ 
14:    if  $b_{12} : b_{13} = (0\ 0)$  then
15:      parity bits =  $b_{14} : b_{15}$ 
16:    else
17:      parity bits =  $\overline{b_{14} b_{15}}$  - > extract parity information of  $x_3$  and  $x_2$ 
18:    end if
19:    for  $k = 3:-1:2$  do
20:      select symbol table ST1/ST2 that satisfy parity
21:      for  $l = 1 : 8$  do
22:        find norm ( $y_tk - r_{kk}x_l - r_{kk+1}x_{k+1}..$ ) - > find norm
23:          with third/second rows of R and selected symbols
24:      end for
25:      find minimum norm
26:      take corresponding  $x_l$  as  $x_k$ 
27:      decode to binary - > get  $b_4 : b_7/b_8 : b_{11}$ 
28:    end for
29:    for  $l = 1:16$  do
30:      find norm ( $y_t1 - r_{11}x_l - r_{12}x_2 - r_{13}x_3 - r_{14}x_4$ ) - > find norm with
31:        first row of R and 16 QAM symbols to find  $x_1$ 
32:    end for
33:    find minimum norm
34:    take corresponding  $x_l$  as  $x_1$ 
35:    decode to binary get  $b_0 : b_3$ 
36:    append  $b_0:b_{15}$  to output bits
37:  end while
38:  compare with input bits
39:  return BER (bit error rate) ▷
40: end procedure

```

B.3. WET-SM Encoding

Algorithm 3 : Encoding in WET-SM in a 4 x 1 SM system with QPSK

```

1: procedure INPUT(framelength, Weyl matrices, stream1, stream2 bits, ch. matrix H)
2:   group the antennas to two - >  $A_\phi$  and  $A_\psi$ 
3:     - > two antennas in each group
4:   group the first column of the Weyl matrices to two - >  $B_\phi$  and  $B_\psi$ 
5:     - >  $B_\phi$  - > with positive elements;  $B_\psi$  - > others
6:   if  $B_\psi = \text{inverted } B_\phi$  then
7:     matrix group =  $B_\xi$ 
8:   else
9:     matrix group =  $B_\eta$ 
10:  end if
11:  while framelength do
12:    take input bits  $b_0 : b_4$  from stream1
13:    encode to Weyl matrix  $W$  - > using look up table
14:    decide the group of matrix  $W$  - >  $B_\xi$  or  $B_\eta$ 
15:    take the first bit of stream2 - > stream2 :  $b_0$ 
16:    if  $b_0 = 0$  then
17:      select antenna group  $A_\phi$ 
18:    else
19:      select antenna group  $A_\psi$ 
20:    end if
21:    take column 1 of  $W$ ;  $C_1$ 
22:    QPSK modulate  $C_1$  - > get  $x_1$ , transmit symbol during time slot T1
23:    if  $C_1 \in B_\phi$  then
24:      select first antenna of group selected
25:    else
26:      select second antenna of group selected - > for time slot T1
27:    end if
28:    take the second bit of stream2 - > stream2 :  $b_1$ 
29:    if  $b_1 = 0$  then
30:      select first antenna of other group
31:    else
32:      select second antenna of other group - > for time slot T2
33:    end if
34:    take next two bits of stream2 - >  $b_2 : b_3$ 
35:    QPSK modulate  $b_2 : b_3$ 
36:      - > get  $x_2$ , transmit symbol for time slot T2
37:    do constellation rotation - > rotation angle  $\phi$  to ensure diversity
38:    form the codebook
39:    if  $W$  belongs to  $B_\xi$  then
40:      do codebook rotation with  $\theta_1/\theta_3$  > for diversity
41:    else
42:      do codebook rotation with  $\theta_2/\theta_4$  > implicit information of C2
43:    end if
44:    multiply  $x_1$  and  $x_2$  with corresponding channel gain
45:    add noise
46:    return ( $y_1, y_2$  transmit symbols during time slots 1 and 2)
47:  end while
48: end procedure

```

B.4. WET-SM Decoding

Algorithm 4 : Decoding in WET-SM in a 4 x 1 SM system with QPSK

```

1: procedure INPUT(framelength, y vectors, ch. matrix H, QPSK symbols, Weyl group W)
  ▷
2:   while framelength do
3:     take  $y_1$ , receive symbol in time slot T1
4:     for  $k = 1:4$  do
5:       for  $l = 1:16$  do > with 16 rotated constellation points
6:         find norm ( $y_1 - h_k x_l$ )
7:       end for
8:     end for
9:     find minimum norm - > ML rule
10:    take corresponding  $k$  as antenna index
11:    find the antenna group of  $k$ 
12:    if group is  $A_\phi$  then
13:       $b_0$  of stream2 = 0
14:    else
15:       $b_0$  of stream2 = 1
16:    end if
17:    take corresponding  $l$  as constellation index
18:    decode  $l$  to binary - > bits of column C1 of W
19:    find the codebook - > from  $k$  and  $l$ 
20:    take  $y_2$ , receive symbol in time slot T2
21:    for  $k = 1:2$  do - > antennas corresponding to other group
22:      for  $l = 1:8$  do - > 8 rotated constellation points that satisfy codebooks
23:        find norm ( $y_2 - h_k x_l$ )
24:      end for
25:    end for
26:    find minimum norm
27:    take corresponding  $k$  as antenna index
28:    take corresponding  $l$  as constellation index
29:    decode  $k$  to binary - > bit  $b_1$  of stream2
30:    decode  $l$  to binary - > bits  $b_2$  and  $b_3$  of stream2
31:    if codebook is 1 or 3 then
32:      column C2 - > inverted C1 of W
33:    else
34:      column C2 - > -1(inverted C1 of W)
35:    end if
36:    form the matrix W
37:    decode to corresponding binary - > using look up table
38:    - > bits  $d_0 : d_3$  of stream1
39:    append  $b_0 : b_3$  to output bits stream2
40:    append  $d_0 : d_3$  to output bits stream1
41:  end while
42:  compare with input bits
43:  return BER1 and BER2 (bit error rate of stream1 and stream2) ▷
44: end procedure

```

B.5. DESM Encoding

Algorithm 5 : Encoding in DESM in a GSM system with QPSK

$N_t = N_r = 4, N_a = 3$

```

1: procedure INPUT(framelength, input bits(DS and NDS) ch. matrix H, QPSK symbols)
2:   while framelength do
3:     take 4 input bits of DS,  $b_0 : b_4$  of diversity stream
4:     modulate  $b_0 : b_1$  and  $b_2 : b_3$  using QPSK,
5:      $b_0 : b_1 \rightarrow x_1, b_2 : b_3 \rightarrow x_2$ 
6:     select two antennas with best channel gain  $\rightarrow \bar{h}_1$  and  $\bar{h}_2$ )
7:     multiply  $\bar{h}_1$  with  $x_1$ 
8:     multiply  $\bar{h}_2$  with  $(x_2) \rightarrow$  Alamouti coding
9:     take first input bit of NDS  $\rightarrow n_0$  of non-diversity stream
10:    if  $n_0 = 0$  then
11:      select antenna 3 channel gain  $\rightarrow \bar{h}_3$ 
12:    else
13:      select antenna 4 channel gain  $\rightarrow \bar{h}_4$ 
14:    end if
15:    take next two bits of NDS  $\rightarrow n_1 : n_2$ 
16:    modulate  $n_0 : n_1$  using QPSK,  $n_0 : n_1 \rightarrow x_3/x_4$ 
17:    multiply  $\bar{h}_3/\bar{h}_4$  selected with  $x_3/x_4$ 
18:    transmit vector  $\bar{y}_1$  during time slot T1 is
19:     $\bar{y}_1 = \bar{h}_1 x_1 + \bar{h}_2 x_2 + \bar{h}_3 x_3$ 
20:     $\rightarrow$  assuming third antenna is selected
21:    multiply  $\bar{h}_1$  with  $-\text{conj}(x_2)$ 
22:    multiply  $\bar{h}_2$  with  $\text{conj}(x_1) \rightarrow$  Alamouti coding
23:    take fourth input bit of NDS  $\rightarrow n_3$  of non-diversity stream
24:    if  $n_3 = 0$  then
25:      select antenna 3
26:    else
27:      select antenna 4
28:    end if
29:    take next two bits of NDS  $\rightarrow n_4 : n_5$ 
30:    modulate  $n_4 : n_5$  using QPSK,  $n_4 : n_5 \rightarrow x_3/x_4$ 
31:    multiply  $\bar{h}_3/\bar{h}_4$  selected with  $x_3/x_4$ 
32:    transmit vector  $\bar{y}_2$  during time slot T2 is
33:     $\bar{y}_2 = -\bar{h}_1 \text{conj}(x_2) + \bar{h}_2 \text{conj}(x_1) + \bar{h}_4 x_4$ 
34:    if fourth antenna is selected
35:    return transmit vector  $\bar{y}_1$  and  $\bar{y}_2$ 
36:  end while
37: end procedure

```

B.6. DESM Decoding

Algorithm 6 : Decoding in DESM in a GSM system with QPSK
 $N_t = N_r = 4, N_a = 3$

```

1: procedure INPUT(framelength, y vectors, channel matrix H, QPSK symbols)
2:   while framelength do
3:     take receive vector  $\bar{y}_{t1}$  - > of time slot T1
4:     form H1 from H - > third column zeros; fourth column  $\bar{h}_4$ 
5:     do QR decomposition of H1 - > get Q1 and R1
6:     premultiply  $\bar{y}_{t1}$  with Q1 Hermitian; - > get  $\hat{y}_{t1}$  - >  $y_{t1}$ tilda
7:     for  $k = 1:4$  do - > with QPSK symbols
8:       find norm( $\hat{y}_{t1}4 - r_{144}x_k$ ) - > with fourth row of R1
9:     end for
10:    find minimum norm N1
11:    form H2 from H - > third column zeros; fourth column  $\bar{h}_3$ 
12:    do QR decomposition of H2 - > get Q2 and R2
13:    premultiply  $\hat{y}_{t1}$  with Q2 hermitian; - > get  $\hat{y}_{t1}$  - >  $y_{t1}$ hat
14:    for  $k = 1:4$  do - > with QPSK symbols
15:      find norm( $\hat{y}_{t1}4 - r_{244}x_k$ ) - > with fourth row of R2
16:    end for
17:    find minimum norm N2
18:    if  $N1 < N2$  then
19:      take corresponding  $x_k$  as  $x_4$ 
20:      NDS bit  $n0 = 1$ 
21:       $\bar{y}_{1a} = \bar{y}_{t1} - \bar{h}_4x_4$ 
22:    else
23:      take corresponding  $x_k$  as  $x_3$ 
24:      NDS bit  $n0 = 0$ 
25:       $\bar{y}_{1a} = \bar{y}_{t1} - \bar{h}_3x_3$  - > form first part of Alamouti coded matrix
26:    end if
27:    decode  $x_3/ x_4$  to binary - > get NDS bits  $n1 : n2$ 
28:    repeat steps 3 to 27 with  $\bar{y}_{t2}$  to get NDS  $n3 : n5$ , and
29:    second part of Alamouti coded matrix  $\bar{y}_{2a}$ 
30:    form Alamouti equations  $\bar{y}_a = H_a\bar{x} + \bar{n}_a$ 
31:    multiply  $\bar{y}_a$  with  $H_a^H$  to get  $\bar{y}_{an}$  - > independently detect  $x_1$  and  $x_2$ 
32:    for  $k = 1:4$  do
33:      find norm ( $y_{1an} - h_Nx_k$ )
34:      find norm with  $x_1$  - >  $h_N$  - > diagonal element of  $H_a^H H_a$ 
35:    end for
36:    find minimum norm
37:    take corresponding  $x_k$  as  $x_1$ 
38:    decode to binary - > get  $b0 : b1$  of DS
39:    for  $k = 1:4$  do
40:      find norm ( $y_{2an} - h_Nx_k$ ) - > find norm with  $x_2$ 
41:    end for
42:    find minimum norm
43:    take corresponding  $x_k$  as  $x_2$ 
44:    decode to binary - > get  $b2 : b3$  of DS
45:    append  $b0 : b3$  to output bits DS
46:    append  $n0 : n5$  to output bits NDS
47:  end while
48:  compare with input bits
49:  return BER (bit error rate)
50: end procedure

```

B.7. GSM-RCPC Encoding

Algorithm 7 : Encoding with RCPC codes in a GSM system

$N_t = 8, N_r = 4, N_a = 2$

```

1: procedure INPUT(framelength, input bits ch. matrix H, QPSK symbols)
2:   form group G and group B of antennas ; 4 antennas in a group
3:     - > G - > good channel group, B - > bad channel group
4:   demultiplex input stream to two : stream1; stream2
5:   convolutional encode stream1 with puncturing
6:   convolutional encode stream2 without puncturing
7:   while framelength do ▷
8:     take 4 input bits of stream1, - >  $g0 : g4$ 
9:     select antenna from group G using  $g0 : g1$ 
10:    modulate  $g2 : g3$  using QPSK, - >  $x1$ 
11:    multiply with selected channel gain - >  $\bar{h}_1$ 
12:    take 4 input bits of stream2, - >  $n0 : n4$ 
13:    select antenna from group B using  $n0 : n1$ 
14:    modulate  $n2 : n3$  using QPSK, - >  $x2$ 
15:    multiply with selected channel gain - >  $\bar{h}_2$ 
16:    return  $\bar{y} = \bar{h}_1 x_1 + \bar{h}_2 x_2$ 
17:   end while
18: end procedure

```

B.8. GSM-RCPC Decoding

Algorithm 8 : Decoding with RCPC codes in a GSM system

 $N_t = 8, N_r = 4, N_a = 2$

```

1: procedure INPUT(framelength, y vectors ch. matrix H, QPSK symbols)
2:   form group G and group B of antennas ; 4 antennas in a group
3:   - > G - > good channel group, B - > bad channel group
4:   while framelength do
5:     take input vector  $\bar{y}$ 
6:     for  $k_1 = 1 : 4$  do
7:       for  $k_2 = 1 : 4$  do
8:         for  $l_1 = 1 : 4$  do
9:           for  $l_2 = 1 : 4$  do
10:            find norm  $(\bar{y} - \bar{h}_{k_1}x_{l_1} - \bar{h}_{k_2}x_{l_2})$ 
11:          end for
12:        end for
13:      end for
14:    end for
15:    find minimum norm - > ML rule
16:    take corresponding  $k_1, k_2$  and  $l_1, l_2$ 
17:    decode to binary
18:    - >  $k_1$  - >  $b0 : b1$ ;  $k_2$  - >  $n0 : n1$ 
19:    - >  $l_1$  - >  $b2 : b3$ ;  $l_2$  - >  $n2 : n3$ 
20:    append  $b0 : b3$  to output bits S1
21:    append  $n0 : n3$  to output bits S2
22:  end while
23:  Apply Viterbi decoding to S1 and S2
24:  - > S1 : on decoding > stream1 bits
25:  - > S2 : on decoding > stream2 bits
26:  compare with input stream1, stream2 bits
27:  return BER1, BER2
28: end procedure

```

REFERENCES

1. **Akyildiz, I. F., D. M. Gutierrez-Estevez, R. Balakrishnan and E.C.Reyes** (2014) LTE Advanced and the evolution to beyond 4G (B4G) Systems, *Physical communication-* **10**, 31-60
2. **Alamouti, S.** (1998) A simple transmitter diversity technique for wireless communications, *IEEE Journal of Selected Areas of Communication*, **16**, 1451–1458.
3. **Arab, A. E., J.C. Carlach and M. Hélar** (2011) A new non-coherent MIMO scheme: Matrix Coded Modulation “MCM”, Proceedings of *International Symposium on Communications and Information Technologies*, October, 120-125.
4. **Azzam, L. and E. Ayanoglu** (2007) Reduced Complexity Sphere Decoding for Square QAM via New Lattice Representation, *IEEE Global Telecommunications Conference*, Washington, November, 4242-4246.
5. **Barbero, L. G. and J. H. Thompson** (2006) A fixed complexity MIMO detector based on Complex Sphere Decoder, Proceedings of *IEEE Workshop on Signal Processing Advances in Wireless Communications*, Cannes, France, July.
6. **Basar, E., U. Aygolu, E. Panayirci and H. V. Poor** (2011) Space-time block coded spatial modulation, *IEEE Transactions on Communication*, **59**, 823–832.
7. **Biglieri, E., R. Calderbank, A. Constantinides, A. Goldsmith, A. Paulraj and H. Vincent Poor** MIMO Wireless Communications, *Cambridge university press*, Cambridge, New York, 2007
8. **Böhnke, R., Wübber D, Kühn V, and Kammeyer K. D.** (2003). Reduced complexity MMSE detection for BLAST architectures, Proceedings of *IEEE Global Telecommunications Conference*, San Francisco, CA, USA, December, 2258–2262.

9. **Cal-Braz, J.A., and R. Sampaio-Neto** (2014) Low Complexity Sphere decoding Detector for Generalised Spatial Modulation Systems, *IEEE Communication Letters*, **18**, 949-952.
10. **Cal-Braz, J.A., and R. Sampaio-Neto** (2015) Projection Based List Detection in Generalised Spatial Modulation System, *IEEE Communication letters*, **19**, 1145-1148.
11. **Cal-Braz, J.A., C.A. Medina and R. Sampaio-Neto** (2013) Group Maximum Likelihood Detection in Generalised Spatial Modulation, Proceedings of *International symposium on Wireless Communication Systems*, Ilmenau, Germany, August, 293-296.
12. **Castillo Leon, J. F., U. P. Rico and E. Stevens- Navarro** (2012) Complexity improved Sphere Decoder for MIMO systems using PSK Modulation, *Procedia Technology* , **3**, 52 – 60.
13. **Chae, C.B., A. Forenza, R. Robert W. Heath, M. R. McKay and I. B. Collings** (2010) Adaptive MIMO Transmission Techniques for Broadband Wireless Communication Systems, *IEEE Communications Magazine* , May, 112-118.
14. **Chae, C.B., M. Katz , C. Suh and H. Jeong** (2004) Adaptive Spatial Modulation for MIMO-OFDM, Proceedings of *IEEE Wireless Communications and Networking Conference*, GA,USA, March, 87–92
15. **Chan, A. M. and I. Lee** (2002) A new reduced-complexity sphere decoder for multiple antenna systems, Proceedings of *International Conference on Communication*, New York, April , 460–464
16. **Chau, Y. A. and S.H. Yu** (2001) Space modulation on wireless fading channels, Proceedings of *IEEE Vehicular Technology Conference*, Atlantic City, NJ, USA, October, 1668-1671.
17. **Chen, C., C.H. Li, and Y.H. Huang** (2015) An Improved Ordered-Block MMSE Detector for Generalized Spatial Modulation, *IEEE Communication Letters*, **19**, 707 – 710.
18. **Cho, Y. S., J. Kim, W. Y. Yang and C. G. Kang** MIMO-OFDM wireless communications with MATLAB, *John Wiley & Sons*, New Jersey, United States, 2010

19. **Choi, J. W., B. Shim, A. C. Singer** and **N. I. Cho** (2010) Low-Complexity Decoding via Reduced Dimension Maximum-Likelihood Search, *IEEE Transactions on Signal Processing*, **58**, 1780-1793.
20. **Damen, O., A. Chkeif, and J.C. Belfiore** (2000) Lattice code decoder for space-time codes, *IEEE Communication Letters*, **4**, 161-163.
21. **Di Renzo, M. and H. Haas** (2011a) Space shift keying (SSK) modulation: On transmit-diversity/multiplexing trade-off, Proceedings of *IEEE International Conference on Communication*, Kyoto, Japan, June.
22. **Di Renzo, M. and H. Haas** (2011b) Space shift keying (SSK-) MIMO over correlated Rician fading channels: Performance analysis and a new method for transmit-diversity, *IEEE Transactions on Communication*, **59**, 116-129.
23. **Di Renzo, M. and H. Haas** (2013) On transmit-diversity for spatial modulation MIMO: Impact of spatial-constellation diagram and shaping filters at the transmitter, *IEEE Transactions on Vehicular Technology*, **62**, 2507-2531.
24. **Di Renzo, M., H. Haas, A. Ghayeb, S. Sugiura, and L. Hanzo** (2014) Spatial Modulation for Generalized MIMO: Challenges, Opportunities, and Implementation, Proceedings of the IEEE , **102**, 56-103.
25. **Diggavi, S.N., A. R. Calderbank, S. Dusad and N. Al-Dhahir** (2008) Diversity Embedded Space Time codes, *IEEE Transactions on Information Theory*, 33-50
26. **Ditert, T** (2007) An efficient fixed complexity QRD-M algorithm for MIMO-OFDM using Per-Survivor Slicing, Proceedings of *International Symposium on Wireless Communication Systems*, Trondheim, Norway, October,
27. **Duman, T.M. and A. Ghayeb** Coding for MIMO communication systems, *John Wiley & Sons Ltd* , New Jersey, United States, 2007.
28. **Fincke, U. and M. Pohst** (1985) Improved methods for calculating vectors of short length in a lattice, including a complexity analysis, *Mathematics of Computation*, **44**, 463-471.

29. **Forenza, A., A. Pandharipande, Hojin Kim and Robert W. Heath** (2005) Adaptive MIMO Transmission Scheme: Exploiting the Spatial Selectivity of Wireless Channels, Proceedings of *IEEE Vehicular Technology Conference*, Stockholm, Sweden, June.
30. **Foschini, G. J. and M. J. Gans** (1998) On limits of wireless communication in a fading environment when using multiple antennas, *Wireless Personal Communications*, **6**, 311–335.
31. **Foschini, G. J.** (1996) Layered space–time architecture for wireless communication in a fading environment when using multi element antennas, *Bell Labs Technical Journal*, **1**, 41–59.
32. **Gavrilovska, L., V. Rakovic and V. Atanasovski** (2016) Visions Towards 5G: Technical Requirements and Potential Enablers, *Wireless Personal Communication*, **87**, 731-757.
33. **Golden, G. D., G. J. Foschini, R. A. Valenzuela and P. W. Wolniansky** (1999), Detection algorithm and initial laboratory results using V-BLAST space-time communication architecture, *Electronic Letters*, **35**, 14–16.
34. **Guo, Z. and P. Nilsson** (2006) Algorithm and implementation of the K-best sphere decoding for MIMO detection, *IEEE Journal on Selected Areas of Communication*, **24**, 491–503.
35. **Haas, H., E. Costa and E. Schultz** (2002) Increasing spectral efficiency by data multiplexing using antennas arrays, Proceedings of *IEEE International Symposium on Personal, Indoor and Mobile Radio Communication*, Pavilhao Atlantico, Portugal, September, 610–613.
36. **Hagenauer. J** (1988) Rate-Compatible Punctured Convolutional Codes (RCPC Codes) and Their Applications, *IEEE Transactions on Communications*, **36**, 389-400.
37. **Handte, T., A. Muller and J. Speidel** (2009) BER analysis and optimization of generalized spatial modulation in correlated fading channels, Proceedings of *IEEE Vehicular Technology Conference*, Anchorage, AK, USA, September.

38. **Heath, R. W. and A. Paulraj** (2005) Switching between Spatial Multiplexing and Transmit Diversity Based on Constellation Distance, *IEEE Transactions on Communication*, **53**, 962–68.
39. **Hochwald, B. M. and S. Brink** (2003) Achieving near-capacity on a multiple antenna channel *IEEE Transactions on Communication*, **51**, 389–399.
40. **Hui, B., M. Mohaisen, D. Han, K. Chang, Y. Back and B. Koo** (2012) MIMO Detection Techniques Based on Low Complexity Adaptive QR-Decomposition with M-Algorithm for 3GPP LTE Systems, *Wireless Personal Communications*, **67**, 505–523
41. **Jang, H., S.Nooshabadi, K. Kim and H. Lee** (2017) Circular Sphere Decoding: A Low Complexity Detection for MIMO Systems With General Two-dimensional Signal Constellations, *IEEE Transactions on Vehicular Technology*, **66**, 2085-2098.
42. **Jeganathan, J., A. Ghrayeb and L. Szczecinski** (2008) Generalized space shift keying modulation for MIMO channels, Proceedings of *IEEE International Symposium on Personal, Indoor and Mobile Radio Communication*, Cannes, France, September.
43. **Jeganathan, J., A. Ghrayeb, L. Szczecinski and A. Ceron** (2009) Space shift keying modulation for MIMO channels, *IEEE Transactions on Wireless Communication*, **8**, 3692–3703.
44. **Jeganathan, J., A. Ghrayeb and L. Szczecinski** (2008) Spatial modulation: Optimal detection and performance analysis, *IEEE Communication Letters*, **12**, 545–547.
45. **Jeon, K., H. Kim and H. Par** (2006) An Efficient QRD-M Algorithm Using Partial Decision Feedback Detection, Proceedings of *Asilomar Conference on Signals, Systems and Computers*, Pacific Grove, CA, USA, November, 1658-1661.
46. **Kang, H. G., Ickho Song, J. Oh, J. Lee and S. Yoon** (2008) Breadth-first signal decoder: A novel maximum likelihood scheme for multi-input multi-output systems, *IEEE Transactions on Vehicular Technology*, **57**, 1576-1584.

47. **Keller, T., and L. Hanzo** (2000) Adaptive Multicarrier Modulation: A Convenient Framework for Time-Frequency Processing in Wireless Communications, *Proceedings of the IEEE* , **88**, 611–640.
48. **Kim, J.S., S. H. Moon and I. Lee** (2010) A New Reduced Complexity ML Detection Scheme for MIMO Systems, *IEEE Transactions on communications*, **58**, 1302-1310.
49. **Kim, K. J. and Iltis R. A.**(2002) Joint Detection and Channel Estimation Algorithms for QS-CDMA Signals Over Time-Varying Channels, *IEEE Transactions on Communications*, **50**, 845-855.
50. **Kim, K. J. and J. Yue** (2002) Joint channel estimation and data detection algorithms for MIMO-OFDM systems, *Proceedings of Asilomar Conference on Signals, Systems and Computers*, Pacific Grove, CA, USA, November, 1857–1861.
51. **Kim, T.K., H.M. Kim and G.H. Im** (2012) Enhanced QRD-M Algorithm for Soft-Output MIMO Detection , *Proceedings of IEEE Global Communications Conference*, Anaheim, CA, USA, December.
52. **Lai, K.C., J.J. Jia and L.W. Lin** (2011) Maximum Likelihood MIMO Detection Using Adaptive Hybrid Tree Search, *Proceedings of IEEE International Symposium on Personal, Indoor and Mobile Radio Communications*, Toronto, ON, Canada, September, 1506-1510.
53. **Le, L. B., V. Lau, E. Jorswieck, N.Dao, A. Haghghat, D. In Kim and T.Ngoc** (2015) Enabling 5G mobile wireless technologies, *EURASIP Journal on Wireless Communications and Networking*.
54. **Liu, T. H. and Y.L. Y. Liu** (2008) Modified fast recursive algorithm for efficient MMSE-SIC detection of the V-BLAST system, *IEEE Transactions on Wireless Communication*, **7**, 3713–3717.
55. **Ma, N., A. Wang, C. Han and Y. Ji** (2012) Adaptive joint mapping generalised spatial modulation, *Proceedings of IEEE International Conference on Communication*, China, Aug, 579–582.
56. **MacWilliams, F.J. and N.J.A. Sloane** *The Theory of Error-Correcting Codes*, *Elsevier North-Holland Mathematical Library series*, North-Holland, 1977.

57. **Mandloi, M., M. A. Hussain and V. Bhatia** (2017) Improved Multiple Feedback Successive Interference Cancellation Algorithms for near - optimal MIMO Detection, *IET Communications*, **11**, 150-159.
58. **Mesleh, R. Y., H. Haas, C. W. Ahn and S. Yun** (2005) Inter channel interference avoidance in MIMO transmission by exploiting spatial information, Proceedings of *IEEE International Symposium on Personal, Indoor and Mobile Radio Communication*, Berlin, Germany, September, 141–145.
59. **Mesleh, R. Y., H. Haas, S. Sinanovic, C. W. Ahn and S. Yun** (2008) Spatial modulation, *IEEE Transactions on Vehicular Technology*, **57**, 2228–2241.
60. **Meslesh, R., H. Hass, C. W. Ahn and S. Yun** (2006) Spatial Modulation - A new low complexity spectral efficiency enhancing Technique, Proceedings of *Conference on Communications and Networking in China*, Beijing, China, October.
61. **Mietzner, J., R. Schober and L. Lampe** (2009) Multiple-antenna techniques for wireless communications – A comprehensive literature survey, *IEEE communications surveys & tutorials*, **11**, 87-105.
62. **Mthethwa, B. M. and H. Xu** (2012) Adaptive M quadrature amplitude spatial modulation, *IET Communications*, **6**, 3098–3108.
63. **Narasimhan, T. L., and A. Chockalingam** (2016) On the Capacity and Performance of Generalized Spatial Modulation, *IEEE communications letters*, **20**, 252-255.
64. **Ntontin, K., M. Di Renzo, A. Perez-Neira and C.Verikoukis** (2013) Adaptive generalized space shift keying, *EURASIP Journal on Wireless Communications and Networking*, **43**, February.
65. **Paulraj, A.J. and T. Kailath** (1992) Increasing capacity in wireless broadcast systems using distributed transmission/directional reception, Patent: US5345599 A.
66. **Proakis, J. G.** Digital Communications, *McGraw Hill, New York*, 2008.

67. **Qu, Q., A. Wang, Z. Nie and J. Zheng** (2011) Block mapping spatial modulation scheme for MIMO systems, *Journal of China University of Posts and Telecommunications*, **18**, 30–36.
68. **Rachid, M., and B. Daneshrad** (2009) A low complexity iterative MIMO sphere decoding algorithm, Proceedings of *European Signal Processing Conference*, Glasgow, Scotland, August, 456-460.
69. **Rajashekar, R. and K. V. S. Hari** (2012a) Low complexity maximum likelihood detection in spatial modulation systems, arXiv : 1206.6190[cs.IT]
70. **Rajashekar, R. and K. V. S. Hari** (2012b) Modulation diversity for spatial modulation using complex interleaved orthogonal design, Proceedings of *IEEE Region 10 Conference*, Cebu, Philippines, November.
71. **Sari, L., G. Wibisono and D. Gunawan** (2009) Design of RCPC Encoded V-BLAST MIMO System, *Journal of ICT Research and Applications*, **3**, 67-88.
72. **Sari, L., G. Wibisono and D. Gunawan** (2010) Performance of RCPC-Encoded V-BLAST MIMO In Nakagami- m Fading Channel, *Journal of Telecommunications*, **2**, 49-57.
73. **Schnorr, C. P., and M. Euchner** (1994) Lattice basis reduction: Improved practical algorithms and solving subset sum problems, *Mathematical Programming*, **66**, 181–191.
74. **Serafimovski, N., M. Di Renzo, S. Sinanovic, R. Y. Mesleh and H. Haas** (2010) Fractional bit encoded spatial modulation (FBE-SM), *IEEE Communication Letters*, **14**, 429–431.
75. **Shen, C.A. and A. M. Eltawil** (2010) An Adaptive Reduced Complexity K-Best Decoding Algorithm with Early Termination, Proceedings of *IEEE Consumer Communications and Networking Conference*, Las Vegas, NV, USA, January.

76. **Shen, C.A., A. M. Eltawil, S. Mondal and K. N. Salama** (2010) A Best-First Tree-Searching Approach for ML Decoding in MIMO System, Proceedings of *IEEE International Symposium on Circuits and Systems*, Paris, France, May, 3533 – 3536.
77. **Shim, B. and I. Kang** (2008) Sphere decoding with a probabilistic tree pruning, *IEEE Transactions on Signal Processing*, **56**, 4867–4878.
78. **Singh, C.K., S. H. Prasad and P. T. Balsara** (2006) A Fixed-Point Implementation for QR Decomposition, Proceedings of IEEE Workshop on Design, Applications, Integration and Software, Richardson, TX, USA, October.
79. **Song, S., Y. L. Yang, Q. Xiong, K. Xie, B.J. Jeong and B. L. Jiao** (2004) A channel hopping technique I: Theoretical studies on band efficiency and capacity, Proceedings of *IEEE International Conference on Communication, Circuits and Systems*, Chengdu, China, June, 229–233.
80. **Sugiura, S., S. Chen and L. Hanzo** (2010a) Coherent and differential space-time shift keying: A dispersion matrix approach, *IEEE Transactions on Communication*, **58**, 3219–3230.
81. **Sugiura, S., S. Chen and L. Hanzo** (2011b) Generalized space-time shift keying designed for flexible diversity, multiplexing and complexity tradeoffs, *IEEE Transactions on Wireless Communication*, **10**, 1144–1153.
82. **Sun, S., Y. Dai, Z. Lei, K. Higuchi and H. Kawai** (2006) Pseudo-inverse MMSE based QRD-M Algorithm for MIMO OFDM, Proceedings of *IEEE Vehicular Technology Conference*, Melbourne, Vic., Australia, May, 1545-1549.
83. **Tarokh, V., H. Jafarkhani and A. R. Calderbank** (1999) Space-time block codes from orthogonal designs, *IEEE Transactions on Information Theory*, **45**, 1456–1467.
84. **Tarokh, V., N. Seshadri and A. R. Calderbank** (1998) Space-time codes for high data rate wireless communication: Performance criterion and code construction, *IEEE Transactions on Information Theory*, **44**, 744–765.

85. **Teletar, E.** (1999) Capacity of Multi antenna Gaussian Channels, *European Transactions on Telecommunication*, **10**, 585-595
86. **Tse,D., and P.Viswanath**, Fundamentals of Wireless Communication, Cambridge Univ. Press, Cambridge, U.K , 2005.
87. **Van Nee, R., Zelst A. V. and Awater G.** (2000) Maximum Likelihood Decoding in a Space Division Multiplexing System, Proceedings of *IEEE Vehicular Technology Conference*, Tokyo, Japan, 6-10.
88. **Viterbo, E., and J. Boutros** (1999) A universal lattice code decoder for fading channels, *IEEE Transactions on Information Theory*, **45**, 1639–1642.
89. **Wang,J., Jia. S and Song.J** (2012a) Signal Vector based detection scheme for spatial modulation, *IEEE Communication Letters*,**16**, 19-21.
90. **Wang, C.X., F. Haider, X.Gao, X.H. You, Y.Yang, D. Yuan, H.Aggoune, H. Haas , S. Fletcher and E. Hepsaydir** (2014) Cellular Architecture and Key Technologies for 5G Wireless Communication Networks, *IEEE Communications Magazine*, **51**, February, 122-130.
91. **Wang, J., S. Jia, and J. Song** (2012b) Generalised spatial modulation system with multiple active transmit antennas and low complexity detection scheme, *IEEE Transactions on Wireless Communication*, **11**, 1605–1615.
92. **Wittneben, A.** (1993) A new bandwidth efficient transmit antenna modulation diversity scheme for linear digital modulation, Proceedings of *International Conference on Communication*, Geneva, 1630–1634.
93. **Wolniansky P. W., Foschini G. J., Golden G. D. and Valenzuela R. A.** (1998) V-BLAST: an Architecture for Realizing very High Data Rates over the Rich-scattering Wireless Channel, Proceedings of *URSI International Symposium on Signals, Systems, and Electronics*, Pisa, Italy, October, 295-300.

94. **Wong, K., C.Y. Tsui, R.S. Cheng and W.Mow** (2002) A VLSI Architecture of a K-Best lattice decoding algorithm for MIMO channels, *IEEE International Symposium on Circuits and Systems*, Phoenix-Scottsdale, AZ, USA, August, 273-276.
95. **Xian, L. and H. Liu** (2005) Optimal rotation angles for Quasi Orthogonal Space Time Block Codes with PSK Modulation, *IEEE Communications Letters*, **9**, 676-678.
96. **Xiao, Y., Q.Tang, L. Gong, P. Yang and Z. Yang** (2013) Power Scaling for Spatial Modulation with Limited Feedback, *International Journal of Antennas and Propagation*, **2013**, 1-5.
97. **Xiao, Y., Z. Yang, L. Dan, P. Yang, L. Yin and W. Xiang** (2014) Low complexity signal detection for generalized spatial modulation, *IEEE Communication Letters*, **18**, 403-406.
98. **Xu, C., S. Sugiura, S. X. Ng, and L. Hanzo** (2013) Spatial modulation and space-time shift keying: Optimal performance at a reduced detection complexity, *IEEE Transactions on Communication*, **61**, 206-216.
99. **Xu, H.** (2012) Simple Low Complexity Detection Schemes for M-ary Quadrature Amplitude Modulation Spatial Modulation, *IET Communications*, **6**, 2840-2847.
100. **Yang, D., C. Xu, L.L. Yang, and L. Hanzo** (2011) Transmit-diversity-assisted space-shift keying for colocated and distributed/cooperative MIMO elements, *IEEE Transactions on Vehicular Technology*, **60**, 2864-2869.
101. **Yang, P., Y. Xiao, L. Li, Q. Tang, Y. Yu and S. Li** (2012) Link Adaptation for Spatial Modulation with Limited Feedback, *IEEE transactions on vehicular technology*, **61**, 3808-3813.
102. **Yang, P., Y. Xiao, Y. Yi and S. Li** (2011) Adaptive spatial modulation for wireless MIMO transmission systems, *IEEE Communication Letters*, **15**, 602-604.
103. **Yang, Y. and B. Jiao** (2008) Information-guided channel-hopping for high data rate wireless communication, *IEEE Communication Letters*, **12**, 225-227.

104. **Yang, Y. and S. Aissa** (2011) Bit-padding information guided channel hopping, *IEEE Communication Letters*, **15**, 163–165.
105. **Younis, A., N. Serafimovski, R. Mesleh and H. Haas** (2010) Generalised spatial modulation, Proceedings of *IEEE Asilomar Conference on Signals Systems and Computers*, CA, USA, 1498–1502.
106. **Younis, A., S. Sinanovic, M. Di Renzo, R. Y. Mesleh and H. Haas** (2013) Generalised sphere decoding for spatial modulation, *IEEE Transactions on Communication*, **61**, 2805–2815.
107. **Yu, C. M., S.H. Hsieh, H.W. Liang, C.S. Lu, W.H. Chung, S.Y. Kuo and S.C. Pei**, (2012) Compressed sensing detector design for space shift keying in MIMO systems, *IEEE Communication Letters*, **16**, 1556–1559.
108. **Zhang, J. K., Kavcic. A and Wong. K.M** (2005) Equal-Diagonal QR Decomposition and its Application to Precoder Design for Successive-Cancellation Detection, *IEEE Transacions on Information Theory*. **51**, 154 - 172.
109. **Zheng, B., M. Wen, F.Chen, N. Huang, Fei Ji, and H. Yu** (2017) The K-Best Sphere Decoding for Soft Detection of Generalized Spatial Modulation Accepted for *IEEE Transactions on Communications*.
110. **Zheng, L. and D. Tse** (2003) Diversity and multiplexing: a fundamental tradeoff in multiple-antenna channels, *IEEE Transactions on Information Theory*, **49**, 1073–1096.

LIST OF PAPERS SUBMITTED ON THE BASIS OF THIS THESIS

I REFEREED JOURNALS

1. **Bindu. P (Palakkal) and Jibukumar. M. G** (2017) Transmit diversity and high rate in SM - MIMO with Weyl Group Encoding. *Wireless Personal Communications*, **97**, 5439-5454.
2. **Bindu. P (Palakkal) and Jibukumar. M. G** (2018) Diversity Embedded Rate Configurable GSM and Low Complexity Detection, *International Journal of Electronics and Communications-AEU*, **88**, 166-173

II PRESENTATIONS IN CONFERENCES

1. **Bindu. P (Palakkal) and Jibukumar. M. G** Parity Aided Detection of SM- MIMO Systems *IEEE Region 10 conference - TENCON*, Bangkok, Thailand, October, 2014
2. **Bindu. P (Palakkal) and Jibukumar. M. G** Rate adaptation in GSM with RCPC Codes *IEEE International conference on Wireless Networks and Embedded Systems - WECON*, Chandigarh, India, November, 2018

CURRICULUM VITAE

1. NAME : BINDU. P(PALAKKAL)

2. DATE OF BIRTH : 02 February 1971

3. EDUCATIONAL QUALIFICATION

1992 Bachelor of Technology. (B. Tech.)

Institution : Government Engineering
College, Thrissur.

Branch : Electronics and Communication
Engineering.

2008 Master of Technology (M. Tech.)

Institution : National Institute of Technology,
Calicut.

Branch : Electronics and Communication
Engineering.

Specialization : Digital Systems and
Communication Engineering

Doctor of Philosophy (Ph. D)

Institution : Cochin University of Science &
Technology

Registration date : 25.11.2011 (Part-time)
